Projected Changes in Ventura County Climate

RESOURCES LEGACY FUND®
CREATIVE SOLUTIONS. LASTING RESULTS.

DRI
Desert Research Institute

CNAP
California-Nevada Climate Applications Program
A NOAA RISA team

OJAI VALLEY LAND CONSERVANCY

Watersheds Coalition of Ventura County

Oakley, N.S., Hatchett, B.J., McEvoy, D., Rodriguez, L., 2019. Projected Changes in Ventura County Climate. Western Regional Climate Center, Desert Research Institute, Reno, Nevada. Available at: wrcc.dri.edu/Climate/reports.php.

All images courtesy N. Oakley and B. Hatchett unless otherwise noted.
Title page bottom photo by ©John Carman, United Water.
Table of contents page bottom photo by ©Tony Webster, Wikimedia Commons.
Publication designed by Kunder Design Studio.

Projected Changes in Ventura County Climate

June 2019

Nina S. Oakley, Ph.D.[1]
Benjamin J. Hatchett, Ph.D.[1]
Daniel McEvoy, Ph.D.[1]
Lynn Rodriguez[2]

[1]Western Regional Climate Center, Desert Research Institute
Reno, Nevada
[2]Watersheds Coalition of Ventura County

This research supported by:

RESOURCES LEGACY FUND®
CREATIVE SOLUTIONS. LASTING RESULTS.

In partnership with:

DRI Desert Research Institute
CNAP California-Nevada Climate Applications Program A NOAA RISA team
OJAI VALLEY LAND CONSERVANCY

Targeted Stakeholder Groups Involved in Development of this Report

Watersheds Coalition of Ventura County including the three watershed committees: Ventura River Watershed Council, Calleguas Creek Steering Committee, Santa Clara River Watershed Committee

Wholesale Water Agencies: Casitas Municipal Water District, United Water Conservation District, Calleguas Municipal Water District

California Department of Water Resources Climate Change Program

Groundwater Sustainability Agencies

Ventura County Watershed Protection District

Environmental Organizations: The Nature Conservancy, Santa Clara River Conservancy, Ojai Valley Land Conservancy

Agricultural Organizations: Resource Conservation District, Farm Bureau, UC Cooperative Extension

Ventura County Watershed Protection District

Project Motivation and Goals

Integrated Regional Water Management (IRWM) is a paradigm for managing water and related resources on a regional scale that was established with the passage of Senate Bill 1672 in 2002. The act encourages local and regional agencies to work together to establish a strong foundation for IRWM. Three voter-approved state bond measures followed the IRWM Planning Act: Proposition 50 (2002), Proposition 84 (2006), and Proposition 1 (2014). Each bond measure allocated state funds to help support IRWM planning and implementation efforts by regional water management groups (RWMGs). For additional information, please see: https://water.ca.gov/Work-With-Us/Grants-And-Loans/IRWM-Grant-Programs/Proposition-1/Implementation-Grants.

State guidance on the IRWM process requires consideration of water resources vulnerabilities with respect to climate change. Previous work on climate change in Southern California (e.g., California 4th Climate Change Assessment: Los Angeles Region) provides information at scales too broad to fit the specific needs of the IRWM process in Ventura County. The information presented herein addresses climate change in Ventura County at scales relevant to the County's watersheds. Additionally, this report results from an iterative process of information sharing between climate scientists and stakeholders in Ventura County. The Watersheds Coalition of Ventura County had an opportunity to partner with Drs. Nina Oakley and Benjamin Hatchett of the Western Regional Climate Center at the Desert Research Institute in Reno, Nevada, to conduct analyses using existing climate data and knowledge in support of the IRWM planning process. The analyses presented here were supported by the Resources Legacy Fund (https://resourceslegacyfund.org/) as part of a grant administered by the Ojai Valley Land Conservancy (https://ovlc.org/).

The goal of this project and report is to "paint a picture" of future climate in Ventura County to support decision making and prioritization of vulnerabilities related to climate during the IRWM planning process. This has been a stakeholder-driven effort, in which the scientists and representatives of the Watersheds Coalition of Ventura County (WCVC) have discussed challenges. This process included meetings with a large stakeholder group (General Membership) as well as meetings with targeted groups of interested agencies (see title page) resulting in tailored analyses to address their specific needs. The analyses and interpretation act as a bridge between the climate model output and decisions to be made by various stakeholders with water-related needs. Outcomes from this project will ultimately support water management and planning agencies in Ventura County in satisfying IRWM, the Sustainable Groundwater Management Act (SGMA) and land use planning requirements to improve the resiliency of Ventura County to projected changes in climate over the next two decades (2021–2040; relevant for the IRWM planning process) and beyond.

Table of Contents

Executive Summary

This report analyzes output from 32 Global Climate Models that have been statistically downscaled using the Localized Constructed Analogs (LOCA) method to examine projected changes in temperature, precipitation, and evapotranspiration using the "business as usual" emissions pathway for the **2021–2040 period as compared to a 1950–2005 baseline.** Potential changes in hourly precipitation characteristics in a warming climate are also examined.

There is good agreement across models that inland areas will see an air temperature increase of at least 3–5°F (depending on specific location) while coastal areas will observe an increase of at least 2–3°F on average. Models agree on an increase in the number of days exceeding various extreme or impactful temperature thresholds. However, there is considerable spread across models as to the number of days. Evapotranspiration is projected to increase as well with the greatest changes, on the order of 5–10%, in the upper Santa Clara River watershed during the spring and fall seasons.

Climate models disagree on whether average annual precipitation will increase or decrease in Ventura County and adjacent areas, though changes are generally relatively small. There is greater model consensus that the number of dry days will increase, such that there are approximately 7% fewer days experiencing precipitation in winter, 11% fewer in spring, and 20% fewer in fall. If annual precipitation does not change substantially, this implies precipitation will intensify on wet days. Rainfall at hourly durations is also projected to intensify, such that historic thresholds for extremes are more frequently exceeded. The winter season is projected to become slightly wetter, with little change during summer and slight decreases in spring and fall average precipitation. Changes in precipitation, temperature, and evapotranspiration presented here for 2021–2040 generally intensify by mid-century (2041–2070).

Potential impacts of the changing climate include:

- *Changes in precipitation characteristics* (intensification and concentration into winter season) may have implications for groundwater recharge and how surface water is conveyed, captured, and stored.
- *Increased potential for post-fire flash flooding and/or debris flows* due to more frequent short-duration, high intensity rainfall.
- *Increased evaporative demand* may affect what crops can be grown economically, alter ecosystem function, and/or increase drought susceptibility.
- *Increasing temperatures* and *more frequent extreme* (hot) temperatures may have negative impacts on plants and worker health.
- *Increases in maximum temperatures* and *overnight minimum temperatures* as well as frequency of extreme temperatures will likely have negative impacts on human health and ecosystems, disproportionately affecting disadvantaged communities and impacting species extent and abundance.
- *Wildfire season will likely extend* earlier into the spring and early summer and later into the fall and early winter due to drying in these seasons, increased temperature, and greater evaporative demand. There is still *considerable uncertainty* in predicting the future frequency, size and intensity of wildfires.

Introduction

1.1 Climate of Ventura County

Ventura County features a Mediterranean climate with cool, dry summers at the coast and warm, dry summers inland. Winters are mild and wet; nearly all precipitation falls between October and April. The mountainous terrain is a major factor in the region's climate. Elevations range from sea level in the south to 8847 ft at the top of Mt. Pinos in the Transverse Ranges at the County's northern edge (Fig. 1.1).

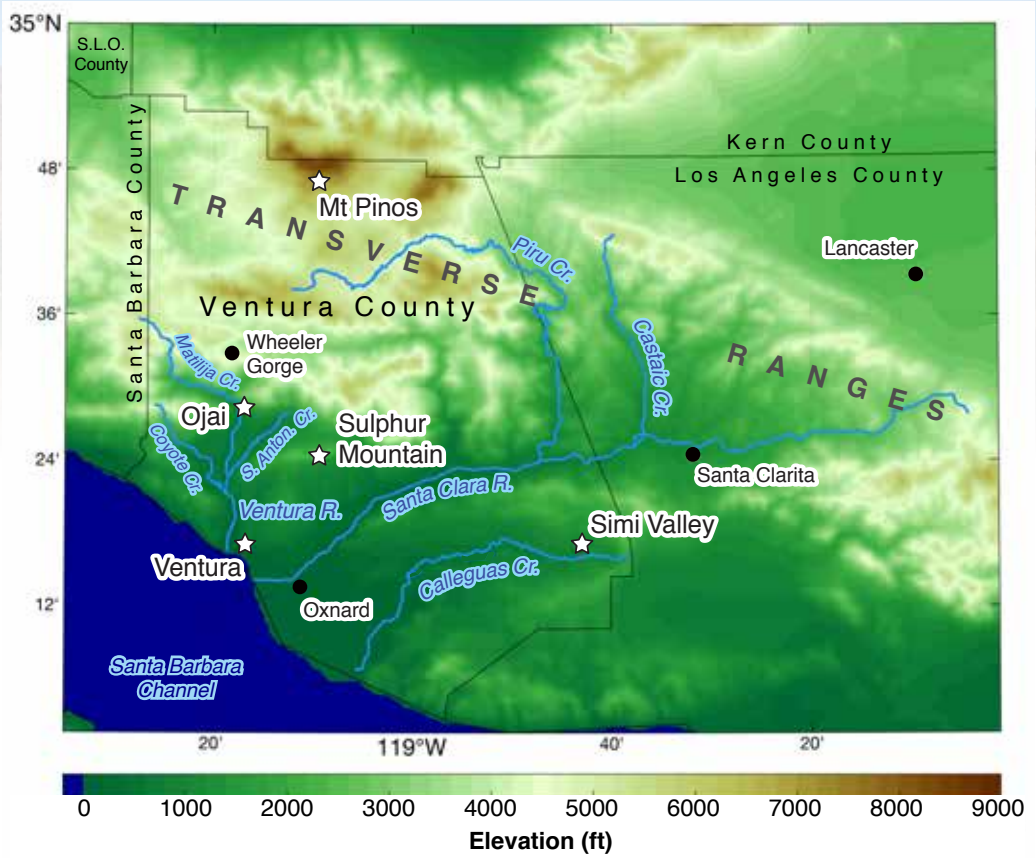

FIGURE 1.1: Map of Ventura County and vicinity. Terrain is shaded with key waterways noted. Stars represent the locations of grid points used to provide specific location-based ranges of downscaled climate projections. Black dots show other points of reference.

Coastal temperatures are moderated year-round by the Pacific Ocean and especially during summer as cold water upwelled near Pt. Conception and Pt. Arguello by prevailing northwesterly winds flows into the Santa Barbara Channel (Hendershott and Winant 1996). Marine stratus, commonly referred to as "fog," also plays an important role in regulating temperatures and evaporative demand in the region. In Oxnard, three miles from the coast, temperatures are generally warmer during the winter and cooler during the summer than inland areas, such as Ojai, situated 13 miles inland from the coast (Table 1.1).

Due to the complex, mountainous terrain, average precipitation is highly variable across the region and varies dramatically with elevation as well as distance from the coast and rain shadow effects of upstream terrain (Table 1.1). Southern California observes high interannual precipitation variability (Oakley et al. 2018b; Dettinger 2011), such that years with well above or below normal precipitation are not uncommon; an "average" year is the exception and not the rule.

	OXNARD (36 FT)	OJAI (745 FT)	MATILIJA CANYON (1400 FT)
Normal December Max. Temperature	66.1°F	66.3°F	
Normal December Min. Temperature	44.5°F	35.4°F	
Normal August Max. Temperature	75.9°F	90.5°F	
Normal August Min. Temperature	58.8°F	55.1°F	
Record High Temperature	105°F (Sept. 26 2016)	119°F (Jun. 16 1917)	
Record Low Temperature	26°F (Jan. 22 1937)	13°F (Jan. 7 1913)	
Normal Annual Precipitation	15.33 in	21.26 in	34.27 in

TABLE 1.1: Climatological characteristics for a few Ventura County locations. Oxnard and Ojai values are based on National Centers for Environmental Information 1981–2010 normals and uses the Oxnard ThreadEx record. Records for Oxnard began in 1923 and Ojai in 1905. Precipitation values for Matilija Canyon are based on Ventura County Watershed Protection District normals (1957–1992 average).

1.2 Natural and Human Landscapes of Ventura County

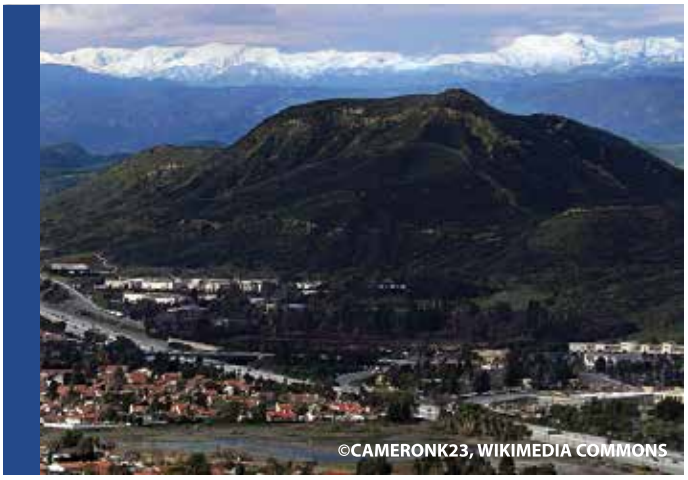

LANDSCAPE AND ECOSYSTEMS

The diverse topography and climate in Ventura County creates a broad range of vegetation communities. These communities support a diversity of wildlife, including rodents, insectivores, hares, fox, coyotes, raptors (such as hawks, falcons, owls, and eagles) and numerous perching birds, from hummingbirds to ravens. The upland plant communities, such as the oak woodlands, pinyon-juniper, and mixed-conifer, provide habitat for larger animals as well, and include populations of bobcat and mountain lion, mule deer, and black bear, in addition to a game population of quail, rabbit, tree squirrel, band-tailed pigeon, dove, and turkey. Reptiles are commonly found throughout the county. *Adapted from the Ventura County General Plan Update (2018).*

The Southern California steelhead distinct population segment was listed as endangered by National Marine Fisheries Service (NMFS) in 1997 (62 FR 43937), with listing of Critical Habitat in 2005 (70 FR 52488) and reaffirmation of listing status in 2006 (71 FR 834). The Santa Clara River watershed (1625 sq. mi.) is one of the largest basins in Southern California that supports anadromous runs of steelhead, and has been identified as a Salmonid Stronghold by the Wild Salmon Center (one of six in the state - https://www.wildsalmoncenter.org/stronghold-approach/), part of a wild salmonid conservation strategy that recognizes watersheds that support "wild, diverse, and abundant" salmonid populations as critical to steelhead recovery in California. According to South Coast Wildlands (2006), over 117 threatened, endangered or sensitive plant and wildlife species or communities have been recorded. This includes 18 mammals, 27 birds, 10 reptiles, six amphibians, five fish, three invertebrates, 29 plants, and 19 sensitive communities. Of these species, 18 are federally listed and 14 are state listed as endangered.

NATURAL HAZARDS

Ventura County is subject to various natural hazards. Wildfire is common in the area, and much of the County is rated as "very high" for fire hazard severity (CAL FIRE 2007). With a prolonged dry season lasting from late spring through the onset of fall rains, the area is susceptible to wildfires most years (Keeley and Syphard 2017). Strong, dry, and persistent northerly to northeasterly winds, known as Santa Anas, can create hazardous fire weather conditions from roughly November-April, with northerly Sundowner Winds also influencing fire weather in the Santa Ynez Mountains in the western portion of the County during spring (Hatchett et al. 2018). If Santa Ana or Sundowner winds coincide with a dry period (such as the delayed onset of fall precipitation), hazardous wildfire conditions result. The 2017 Thomas Fire, ignited in December under strong Santa Ana winds and following an extremely dry fall, represents a prime example of this scenario (Nauslar et al. 2018).

Wildfire has profound effects on storm runoff, erosion, and sedimentation in the complex terrain within Ventura County. For several years following a fire, runoff rates can more than double due to fire-driven changes in soil properties that render it water-repellant and reduce infiltration rates (USGS 2005; USGS 2019). Short-duration, high-intensity precipitation under these conditions increases surface runoff that can cause movement of

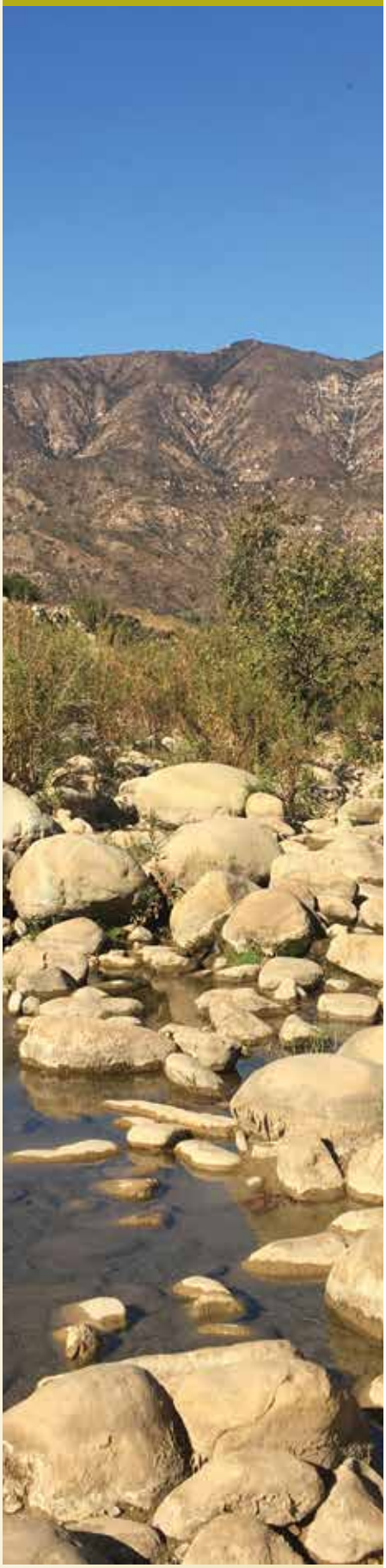

ash, burned vegetation, soil, rocks, and other debris. This material is scoured from steep channels and moved downslope where it may impact communities or infrastructure below as a debris flow. Numerous debris flow events have been noted historically in the area (Oakley et al. 2017; Keller et al. 1997) as well as recently in storms following the 2017 Thomas Fire.

Distinct from post-wildfire debris flows described above, the erodible soils and steep terrain found throughout Ventura County also create conditions favorable for shallow landslides (Campbell 1975). These events are often triggered by periods of intense precipitation following a period of sufficient antecedent precipitation to increase pore water pressures. Increased pore pressures cause the soil and weathered rock to rapidly lose strength and flow downslope (CGS 2018). Numerous landslide events have been observed across the region (Stock and Bellugi 2011; Wills et al. 2017; Oakley et al. 2018a).

Ventura County has a long history of damaging floods (Gruntfest and Taft 1992; Ventura County Flood Info 2019). Varved sedimentary cores from the Ocean Drilling Project and evidence of submarine landslides in the Santa Barbara Channel (Basin) indicate flooding has occurred long before humans inhabited the area (Behl and Kennett 1996; Greene et al. 2006). Following persistent precipitation, when soil becomes saturated and runoff production is most efficient, flooding can occur on rivers and creeks. Flash flooding is associated with short-duration, high-intensity precipitation. Flash flooding does not necessarily require antecedent precipitation and saturated soils to occur; it results when the rate of precipitation exceeds the infiltration rate of the soil (infiltration excess). Because of their ability to trigger flash floods and mass movements, short duration, high intensity precipitation events pose a major threat to life and property in Ventura County.

POPULATION

As of 2017, the population of Ventura County was estimated to be 854,223 (U.S. Census Bureau 2019). According to the County General Plan Update 2040 Draft Alternatives Report – Section 6, the County's population is expected to grow to at least 930,392 by 2040 and up to 1,096,023 (Ventura County, California 2018). Ventura County has experienced notable population growth in recent decades, increasing by more than 185,000 people since 1990 (U.S. Census Bureau 1995). Of particular concern is the rapid expansion of the Wildland Urban Interface (WUI) since 1990 (Radeloff et al. 2018). The WUI is the region where human construction or even general presence comes in contact with native landscapes such as chaparral. Expansion into the WUI creates areas of Ventura County communities that are susceptible to the impacts of various natural hazards including wildfire, post-wild fire debris flows, flash flooding, and shallow landslides. Most wildfires in Ventura County are ignited by humans (Balch et al. 2017). Expansion of the WUI increases the likelihood of ignitions due to both human activities and damages from wildfire.

1.3 Agriculture and Water Resources

AGRICULTURE

The estimated gross value of Ventura County's agriculture for calendar year 2017 was approximately $2.1 billion (Ventura County Agricultural Commission 2017). This represents a 0.4% decrease from 2016. For statewide and national perspective, in 2014, County agricultural crop values were ranked 10th in California and 11th nationally (Farm Bureau of Ventura County 2016). The largest gross revenue crops are strawberries, lemons, celery, nursery stock, raspberries, avocados, cut flowers, tomatoes, peppers, and cabbage.

WATER RESOURCES

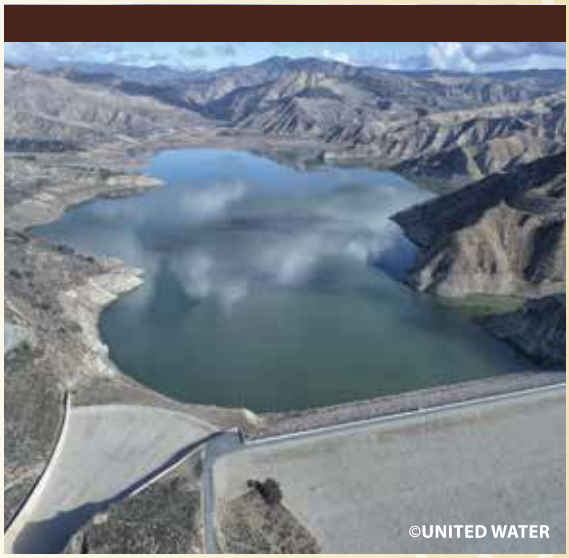

Ventura County relies primarily on local surface and groundwater, as well as imported State Water, for its water resources. The County's primary surface waterways are the Ventura River, Santa Clara River, Calleguas Creek, and Coyote Creek. Coyote Creek is dammed to create Lake Casitas. Groundwater provides about 67% of the county's water supply. Approximately 25% of the County's water demands are currently met with imported water from the State Water Project (SWP), brought into the county by the Calleguas Municipal Water District. In addition, the City of Ventura, United Water Conservation District and Casitas Municipal Water District collectively hold entitlement to 20,000 acre-feet per year from the SWP. There is currently no infrastructure available to deliver this allocation directly to all these entities, with the exception of the United Water Conservation District. Treated wastewater effluent provides a relatively small percentage of the directly piped landscape and agriculture irrigation demands. A significant portion of treated effluence discharge is currently supporting groundwater recharge as well as instream and estuarine uses. The City of Ventura recently completed a study of the potential for direct potable reuse through development of a small pilot recycling plant.

1.4. Temperature and Precipitation Over the Past Century

Data for the past 123 Water Years (October 1–September 30; 1896–2018) reveal variability and trends in precipitation and temperature in the broader South Coast climate region. For maximum temperature, the running mean suggests a tendency toward increasing values over the period of record, though appreciable variability exists (Fig. 1.2). Above-average maximum temperatures were observed in eight of the past 10 years. Minimum temperature (typically associated with overnight low temperatures) shows a steady upward trend (Fig. 1.3) as compared to maximum temperature. The increase in minimum temperatures reflects regional background warming associated with increased greenhouse gas concentrations. In contrast, maximum temperatures are influenced by local and regional weather conditions.

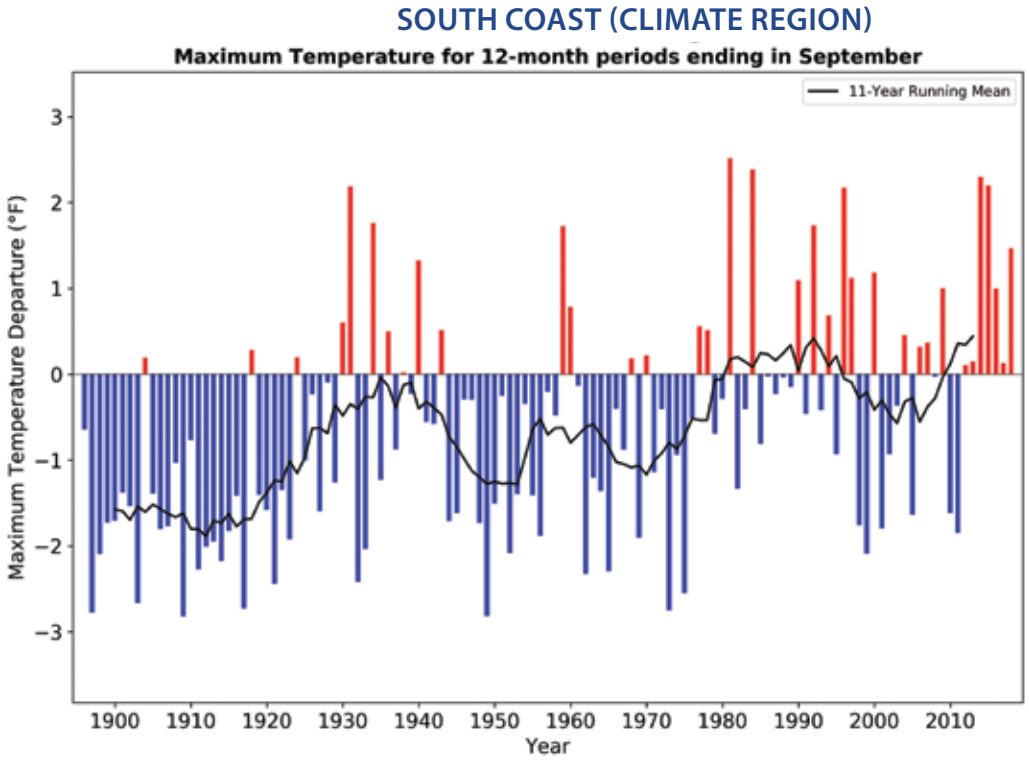

FIGURE 1.2: Maximum temperature departure from 1981–2010 average for 1 October–30 September (Water Year) periods for Water Years 1896 through 2018 for the South Coast climate region of California. Source: California Climate Tracker https://wrcc.dri.edu/Climate/Tracker/CA/

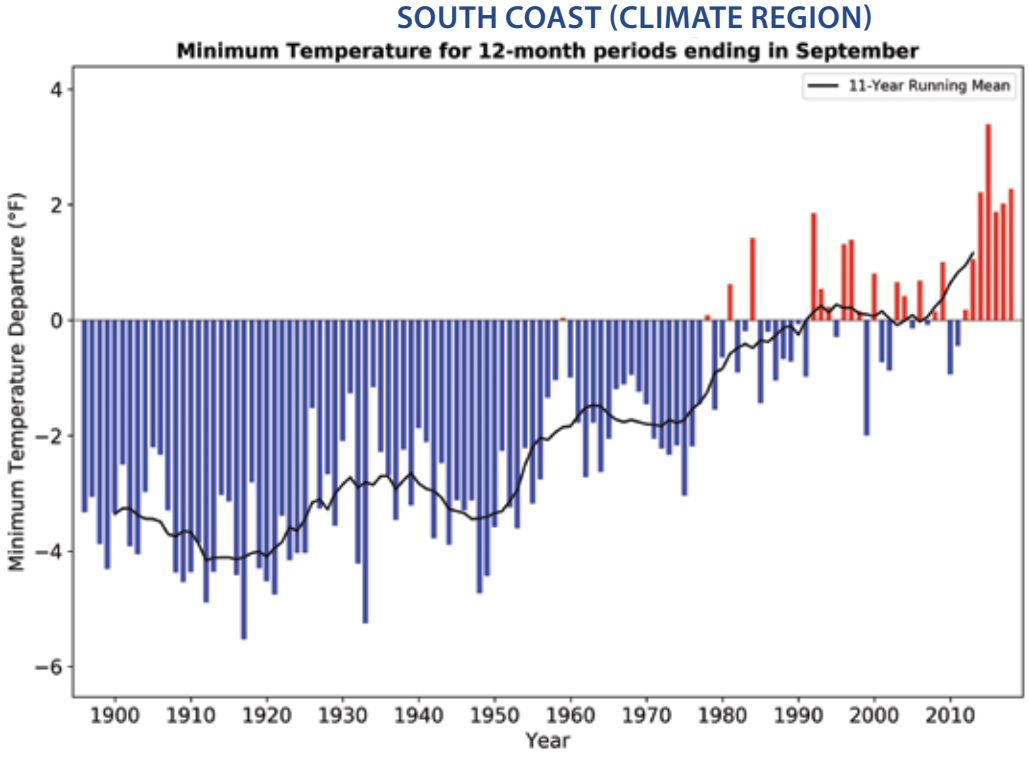

FIGURE 1.3: Minimum temperature departure from 1981–2010 average for 1 October–30 September (Water Year) periods for Water Years 1896 through 2018 for the South Coast climate region of California. Source: California Climate Tracker https://wrcc.dri.edu/Climate/Tracker/CA/

Precipitation in the South Coast region exhibits high interannual variability over the period examined. No notable long-term trends are observed (Fig. 1.4). Since approximately 2000, the 11-year running mean decreases, associated in part with the 2012–2019 drought. It is unclear whether this trend will continue in subsequent years.

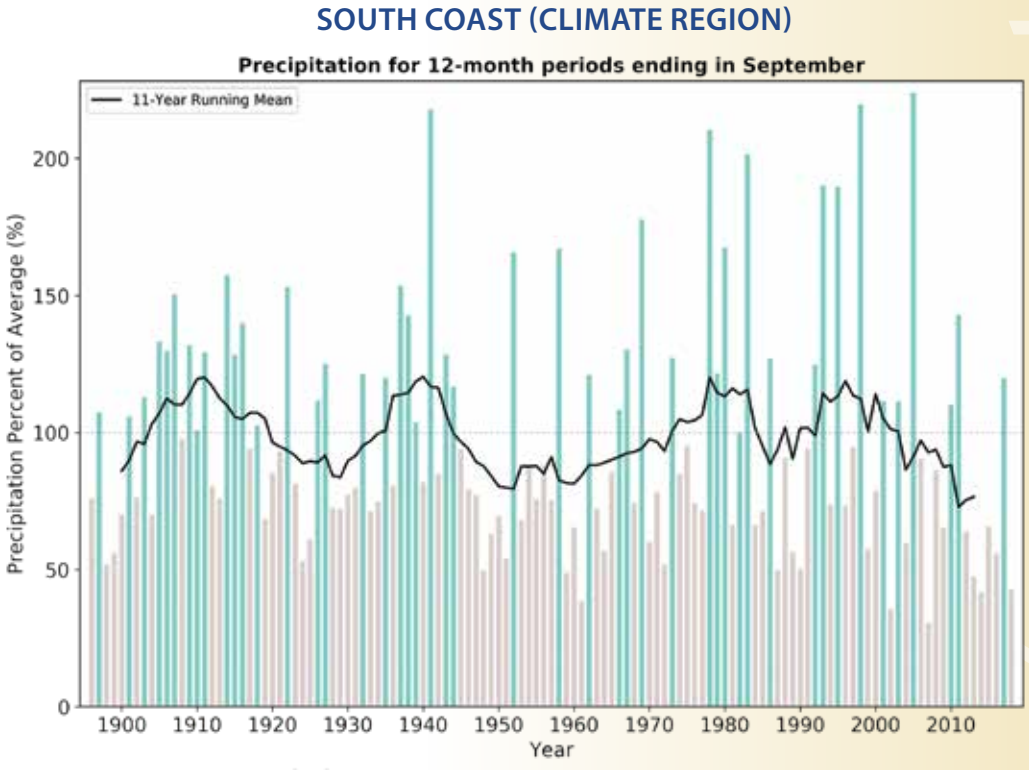

FIGURE 1.4: Precipitation percent of 1981–2010 average for 1 October–30 September (Water Year) periods for Water Years 1896 through 2018 for the South Coast climate region of California. Source: California Climate Tracker https://wrcc.dri.edu/Climate/Tracker/CA/

1.5. Looking Forward

The diverse ecosystems, population, and economy of Ventura County reflect its unique geography and natural resources. Ventura County has always experienced impactful weather and climate-related events. Recently, an extreme and persistent drought was followed by severe late-season wildfires, post-wildfire debris flows, and localized flash flooding. These events demonstrated the County's vulnerabilities to weather and climate extremes. Projected increases in temperature, temperature extremes, and changes in precipitation characteristics may further exacerbate extreme events and are likely to have serious impacts on Ventura County and its inhabitants.

The aim of this report is to evaluate projected changes in temperature and precipitation characteristics at scales relevant for decision-making based upon state-of-the-art climate projections. Such an evaluation will support the IRWM planning process and help the County achieve SGMA compliance. Through the process of examining projected changes in weather and climate extremes, this report will aid in the identification of potential vulnerabilities to climate extremes and facilitate prioritization of investments in adaptation measures. The implementation of adaptation strategies will make the people, economy, resources, and natural landscape of Ventura County more resilient to the negative outcomes of projected climate change.

SECTION 2

Data and Methods

2.1 Datasets Used

The analyses presented herein result from the processing and visualization of several existing datasets; no new datasets were created for this report. The Localized Constructed Analogs (LOCA) dataset (Pierce et al. 2014) was selected as the primary dataset due to its use in the 4th California Climate Assessment as well as demonstrated suitability in representing California climate (Pierce et al. 2016). The LOCA dataset is freely available online through Cal-Adapt at: https://cal-adapt.org/data/loca/

There are two greenhouse gas emissions scenarios established by the International Panel on Climate Change (IPCC) that are commonly used to describe probable future scenarios in terms of both greenhouse gas emissions and associated warming. The Representative Concentration Pathway (RCP) 4.5 represents a scenario where emissions peak around 2040 and then decline towards the end of the century. This is known as the "mitigation" scenario and assumes global agreement and implementation of greenhouse gas reductions. In the RCP 8.5 scenario, commonly known as the "business as usual" scenario, emissions continue to rise throughout the 21st Century (Meinshausen et al. 2011). Based on current worldwide social and political conditions, RCP 8.5 is the more likely emissions scenario, thus the analyses presented here reflect emissions and warming associated with the RCP 8.5 scenario.

DATASET NAME	TEMPORAL/ SPATIAL	PERIOD	VARIABLES	METHOD	REFERENCES
Localized Constructed Analogs (LOCA)	Daily at 6 km	1950–2099	Temperature, precipitation RCP 8.5	Statistically downscales output from 32 CMIP5 climate models using systematic historical effects of topography on local weather patterns.	Pierce et al. (2014) loca.ucsd.edu cal-adapt.org
Prein pseudo-global warming experiment	Hourly at 4 km	Oct 2000–Mar 2013	Precipitation	A pseudo-global warming experiment that uses the Weather Research and Forecasting model to dynamically downscale ERA-Interim data following the RCP 8.5 pathway.	Prein et al. (2017)
VCWPD gauge data	Hourly	2000–2013	Precipitation	Gauge data used as comparison to Prein output	vcwatershed.net/fws/
LOCA ET_0	Daily at 6 km	1950–2099	Reference evapo-transpiration (ET_0)	ET_0 derived from 7 CMIP5 models downscaled with the LOCA method that have temperature, wind speed, incoming solar radiation, and specific humidity.	N/A

TABLE 2.1: Datasets used in this analysis.

2.2 Methods

All 32 CMIP5 climate models available in LOCA are used for analyses of temperature and precipitation. The analyses focus on the period 2021–2040 or the immediate planning horizon relevant to the IRWM planning process. Analyses for the period 2041–2070 are available in Appendix A. The historical period spans 1950–2005. The beginning of the historical period is constrained by the availability of the historic gridded dataset developed by Livneh et al. (2015), which begins in 1950. This dataset is used to train the LOCA statistical model. The historic period for the CMIP5 models ends in 2005 and therefore is used as the end of the LOCA historic period as well (Pierce et al. 2016).

In each section, values plotted are the minimum change that 75% of models agree on (24 of 32 models), unless stated otherwise. For these other cases, the median and a measure of the range of outcomes (either top and bottom 10th or 25th percentile values) will be provided. These latter cases are predominantly related to changes in precipitation where a consistent change (increase or decrease) is not observed. Distribution across models for a given analysis is represented as a boxplot. Fig. 1 describes the interpretation of these figures.

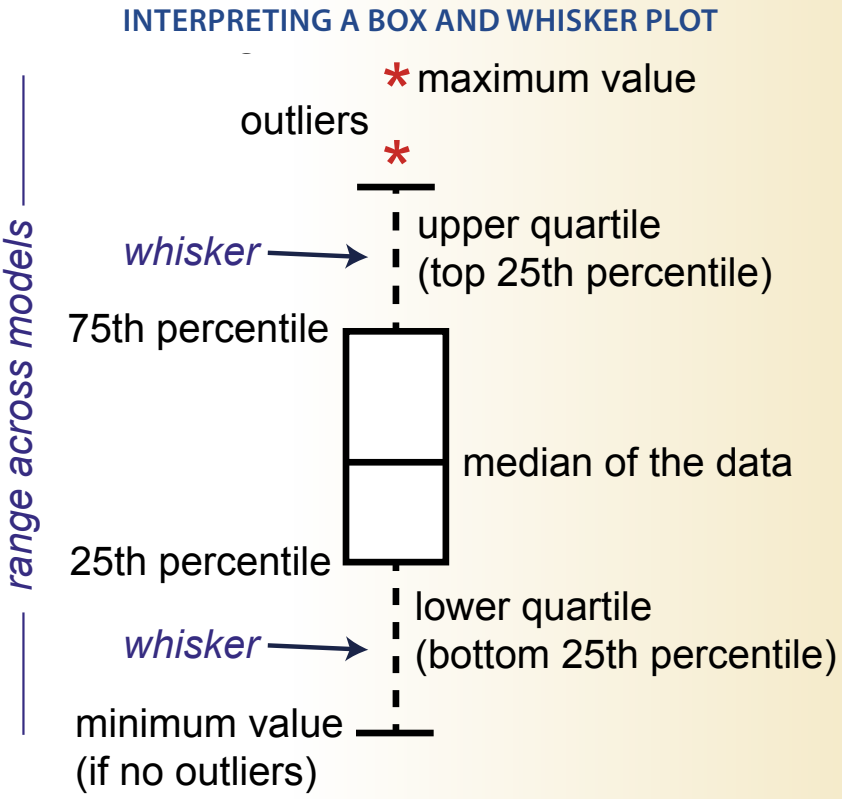

FIGURE 2.1: Features of a box and whisker plot. In the calculations performed herein, an outlier is defined as 1.5 times the interquartile range. For representation of model spread, the top and bottom whiskers or outliers (labeled maximum and minimum values here) represent the models with the most extreme projections for a given analysis. Each box and whisker plot represents the distribution of projected outcomes across a suite of 32 models, except for the reference evapotranspiration (ET_0) plots, where a distribution of outcomes across seven models is presented.

2.3 Calculations

Dry days are calculated as days with zero (0) inches of simulated precipitation. For each grid point, total annual dry days are calculated and divided by the duration of the period of interest (e.g., 2021–2040), giving the average annual number of dry days. **Changes in dry days** are calculated as the difference in average annual future dry days from average annual historical dry days, calculated for each grid point and each of the 32 models. We report the median change across all models and top 25th percentile and top 10th percentile changes. Grid points with at least 24 models indicating a positive change (increase) in future dry days are dotted.

Annual average (median) precipitation is calculated as the calendar year (January–December) average (median) precipitation. **Changes in annual average (median) precipitation** are calculated as the difference between the future and historical periods. Upper (top 25th percentile) and lower (bottom 25th percentile) quartiles of annual average (median) precipitation are provided.

Top 5% wettest days (Number of days exceeding 95th percentile daily precipitation) provide context for the role of extreme precipitation in contributing to the total annual precipitation (Dettinger and Cayan 2014). The wettest days are calculated as the top 5% daily precipitation values for each grid point and each model from the continuous period of record spanning 1950–2005. The contribution of wettest days to total precipitation is calculated for each grid point by summing up the total precipitation for each year contributed by days exceeding the top 5% threshold and dividing by the calendar year total precipitation. The value for each year is summed and divided by the total number of years to calculate the average annual contribution of wettest days to total precipitation. For the future period, the same calculation is performed using the historical estimate of the 95th (top 5th) percentile of daily precipitation. **Changes in contribution of the top 5% of wettest days to annual precipitation** are calculated by differencing the future and historical periods. The top 10th percentile and bottom 10th percentile quartiles of changes in contributions of the wettest days to annual precipitation are also provided.

Number of days exceeding 85th percentile daily precipitation provides context for the role of heavy precipitation in stormwater management. These days are calculated as the top 15% of daily precipitation values for each grid point and each model from the continuous period of record spanning 1950–2005. For the future period, the same calculation is performed using the historical estimate of the 85th (top 15th) percentile of daily precipitation. **Changes in number of 85th percentile precipitation days** are calculated by differencing the future and historical periods. The top 10th percentile and bottom 10th percentile quartiles of changes in number of 85th percentile precipitation days are also provided.

Seasonal changes in average minimum (maximum) temperature are calculated by differencing the average annual minimum (maximum) temperatures between the future and historical periods annually and for the meteorological seasons (Fall: September–November; Winter: December–February; Spring: March–May; Summer: June–August).

Annual changes in temperatures exceeding thresholds of interest. A variety of temperature thresholds are used for both maximum (T_{max}) and minimum (T_{min}) temperature to evaluate potential impacts on human and crop health. For each threshold, the average number of days in a calendar year that each grid point and model exceed the given threshold were calculated for both the historical and future periods. The resulting values are differenced to provide an estimate of the changes in each temperature threshold. The thresholds calculated include: T_{max} > 95°F, T_{max} > 88°F, T_{max} > 80°F, and T_{min} < 28°F. The motivation for each selected threshold is described in the temperature results, Section 3.

Annual changes in minimum or maximum temperature exceeding the 90th and 98th percentile. Cal-Adapt (https://cal-adapt.org/tools/extreme-heat/) uses a percentile-based threshold approach to estimate heat impacts on human health, defining heat days (nights) when T_{max} (T_{min}) exceeds the 98th percentile. By calculating both the 90th and 98th percentiles, we provide the range of commonly used thresholds for heat extremes. Thresholds were calculated over the historical period using a 10-day moving window centered on the Julian day of interest to remove seasonal effects and allow a more robust estimation of the changes in temperature extremes throughout the year. For example, the percentile estimated for the 10th of June utilizes the dates between June 5–15 over all historical years. The calculation is performed for each grid point and each GCM. The historical values were used to calculate the number of days exceeding this threshold over the future period. Differences between the future and historical periods of the average number of days exceeding each threshold are reported. These calculations were repeated for the more modest, but still representing the tail of the distribution, 90th percentile threshold as well.

Evaporative demand represents the 'thirst of the atmosphere'. It can be considered an idealized estimate of the maximum fluxes of water to the atmosphere through evaporation from bare soil, open water, and transpiration from vegetative surfaces (Hobbins and Huntington 2017). Evaporative demand provides a physical integration of the radiative (solar radiation) and advective (wind) forcings driving actual evapotranspiration and by virtue of partitioning land surface-atmosphere feedbacks into latent and sensible heat fluxes (Hobbins et al. 2016). Here, we estimate

©GREEKMATTHEW, WIKIMEDIA COMMONS

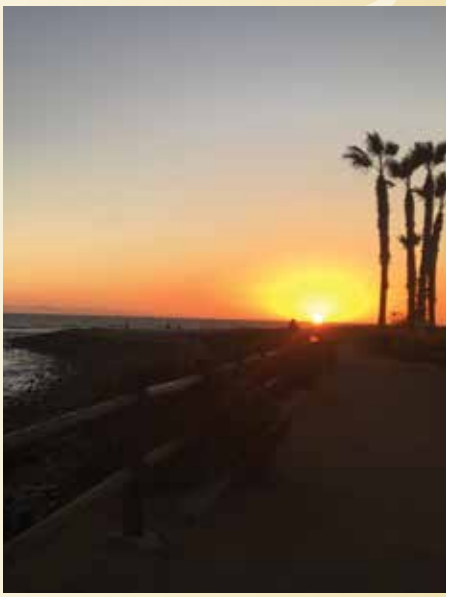

evaporative demand as reference evapotranspiration (ET_0), which uses a constant value to represent at hypothetical well-watered reference crop (in this case short grass) to cover all surfaces (Hobbins and Huntington 2017). The American Society for Civil Engineers Standardized ET_0, a form of the Penman-Monteith equation, was used following Allen et al. (2005) and calculations were performed using the open source Western States Water Use Program ET_0 functions (https://github.com/WSWUP). ET_0 was calculated at daily timesteps and summed over each year. Average annual ET_0 was calculated for both historical and future periods with differences reported as the future ET_0 subtracted from the historical ET_0. We also provide projected seasonal changes in ET_0 as well as projected seasonal percentage changes in ET_0 to provide context for the relative magnitudes of changes by season.

Prein dataset analysis (hourly precipitation): This report utilizes a 4-km hourly pseudo-global warming dataset developed by Prein et al. (2017). In their work, Prein et al. dynamically downscaled the ERA-INTERIM Reanalysis to 4 km for the period October 2000 to March 2013 using the Weather Research and Forecasting model as a "control" simulation. A "perturbed" pseudo-global warming simulation is also run, where the perturbation is the RCP 8.5 95-year ensemble monthly mean climate change signal from 19 CMIP5 models. The signal is derived from analysis of the period 2071 to 2100 as compared to 1976 to 2005. The benefit of this experiment is it demonstrates impact of thermodynamic changes associated with warming on hourly precipitation characteristics for the period studied. A primary limitation of this experiment is it does not account for large-scale circulation changes in the ocean and atmosphere occurring in a warmer climate. Additional limitations and uncertainties are described in Prein et al. (2017).

For the changes in count of precipitation events exceeding 10 mm h^{-1} and 25 mm h^{-1}, all events exceeding these thresholds are summed at each grid point over the period specified (e.g., all months of year or a selected season) for the October 2000–March 2013 period for both the control and perturbed simulation. The difference in count of these events (perturbed scenario minus control) is presented in the "difference" maps.

For the January 11–17, 2005 storm event, hourly precipitation is summed at all grid points for the duration of the event to present storm total precipitation for both the control and perturbed scenario. A difference between the two is also presented. The highest 1-hour precipitation value is extracted for the five-day period for both the control and perturbed scenarios, and the difference calculated.

SECTION 3

Projected Changes in Temperature

3.1 Summary

The 32 CMIP5 models agree that both annual average temperatures and the frequency of extreme temperatures will increase across Ventura County. This continues the upward trends in maximum and minimum temperature already demonstrated in historical climate data for the South Coast region (Section 1.4). For both maximum and minimum temperature, changes are greatest in the summer and fall seasons, where inland areas are most likely to see an increase of at least 3–5°F, depending on location. In other words, 75% of models agree on at least this magnitude of warming for the RCP 8.5 scenario. Coastal areas are likely to see an increase of at least 2–3°F. Inland low-to-moderate elevation areas see the greatest change in number of days exceeding extreme/impactful temperature thresholds (number of days >88°F, >95 °F, etc.). However, there is considerable spread across models regarding increases in the number of days over various thresholds. Projected warming of average minimum and maximum temperatures as well as more frequent temperature extremes may pose challenges to water and energy demand as well as public health, agriculture, and ecosystem function.

The warm (summer) season demonstrates the greatest uncertainty for changes in both maximum and minimum temperature. It should be noted that global and regional climate models have difficulty simulating marine stratus (coastal fog). The reader should consider that the range of temperature projections presented here may represent a minimum estimate as declines in marine stratus in a future climate may lead to greater changes. Limitations associated with marine stratus are discussed in more detail in Section 6.3.

3.2 Implications of Changes in Temperature

- Hard freeze days change little in the coastal plain, where they are already uncommon (Fig. 3.3). There are notable changes in decreased frequency in elevated terrain. The decrease in hard freeze days may permit plants to grow in these areas that were not previously viable.
- Models generally agree on an increase of more than 30 days >80°F at low elevations across the county and an increase of at least 15 days >95°F for inland valleys (Figs. 3.4, 3.5), thresholds pertinent to farmworker health (Cal/OSHA n.d.). More days exceeding these thresholds in agricultural areas may have implications for farmworker health, productivity and employer cost.
- Increases in the frequency of days with extreme minimum and maximum temperatures (>95°F, >90th and 98th percentile; Figs. 3.5-3.7-10) will likely have significant negative impacts on human health. Increased temperatures will enhance needs for air conditioning, increasing energy demand. Certain populations (e.g., low-income communities, homeless, and elderly) will be more vulnerable to the impacts of extreme heat (Hall et al. 2018 and references therein). Extreme heat impacts may be exacerbated in inland areas more prone to urban heat island effects, such as Thousand Oaks and Simi Valley, than coastal regions (Taha and Freed 2015).

- Higher temperatures may have yield benefits for citrus and avocado (Lobell et al. 2007); however, extreme temperatures have negative impacts. For inland areas, models agree on an additional 25–30 days exceeding 88°F, where avocado trees experience stomatal closure, and an additional 15–20 days >95°F, where avocado flowering is impacted (Liu et al. 2002, Figs. 3.5-3.6).
- Increased maximum and minimum temperatures are likely to increase pest and disease pressure on Ventura County crops, though impacts will vary by species (Hall et al. 2018 and references therein).
- Temperature, as well as precipitation changes, could drive changes in the range and abundance of native species (Loarie et al. 2008); restoration efforts may benefit from consideration of plant palates tolerant to the projected climatic changes.
- Juvenile steelhead display sensitivities to water temperature (Spina 2006). Air temperature increases will likely drive water temperature increases and may reduce the extent of suitable habitat for steelhead.

3.3 Temperature Analyses

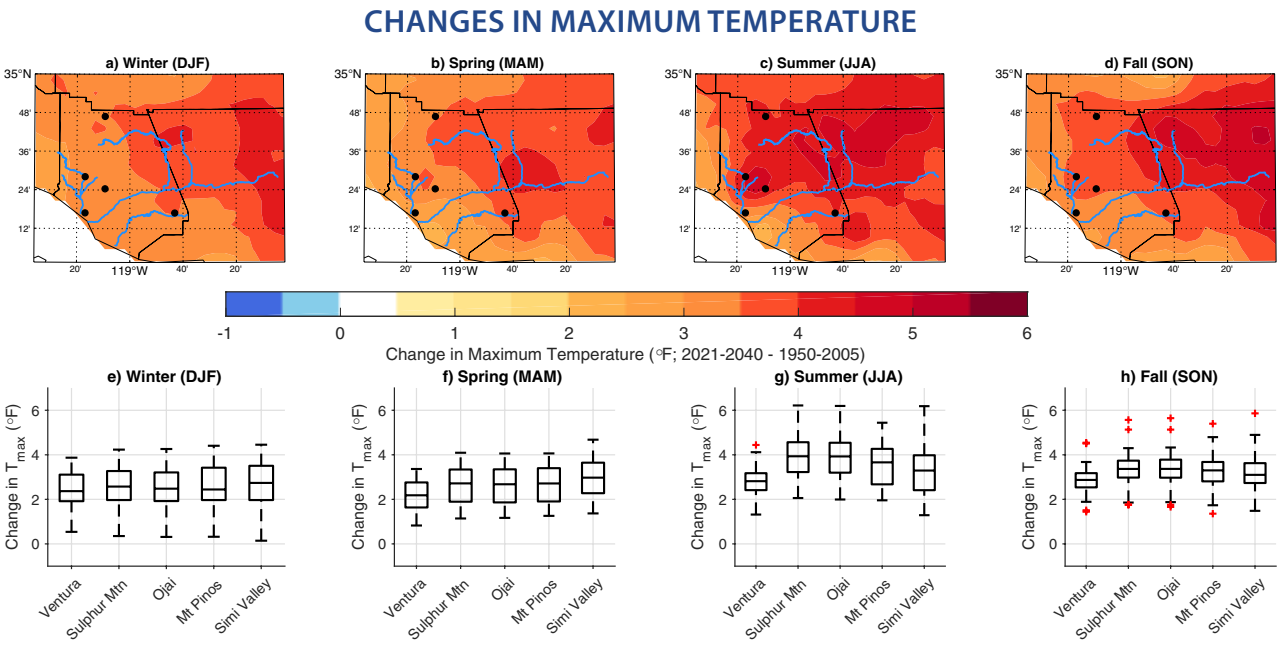

FIGURE 3.1: Change in maximum temperature by season, 2021–2040 mean minus 1950–2005 mean. The top row shows the minimum change that ≥75% of models (≥24 of 32) agree on. Bottom row depicts spread of average change in maximum temperatures across all 32 CMIP5 models for five selected locations within Ventura County (black dots on map). Rivers and creeks are shown as blue lines (Fig. 1.1).

All areas of the county are projected to see an increase in maximum temperatures across all seasons. Inland terrain sees the greatest increases, on the order of 3–5°F. The summer and fall seasons display greater spatial extent and more pronounced changes in maximum temperature than the winter and spring seasons.

Coastal areas are projected to see a 2–3°F change across all seasons (Fig. 3.1). However, the inability of these global climate models and the downscaling approach to accurately represent changes in the distribution of marine fog and onshore/offshore flow regimes introduces uncertainty (see Section 6.3). These changes are therefore minimum estimates of warming.

All 32 simulations agree on increasing average maximum temperatures for each season for selected points across the county, though the magnitude of the change varies with location and season (Fig. 3.1 e-h). During spring and fall, the spread across models, as indicated by length of whiskers, is relatively small (generally 2-3 °F) indicating greater certainty in model projections. During the winter, and especially summer, model spread is greater (3-5°F).

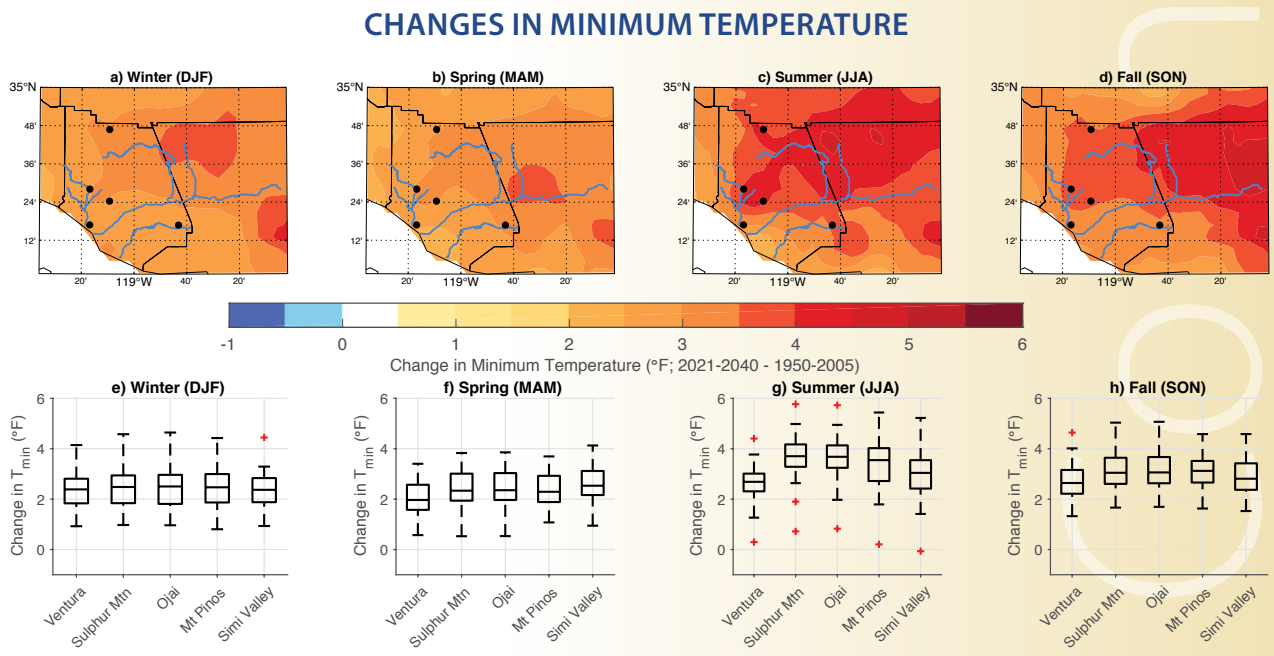

FIGURE 3.2: Change in minimum temperature by season, 2021–2040 mean minus 1950–2005 mean. The top row shows the minimum change that ≥75% of models (≥24 of 32) agree on. Bottom row depicts spread of average change in minimum temperatures across all 32 CMIP5 models for five selected locations within Ventura County (black dots on map).

All areas of the county see increasing minimum temperatures, typically realized as overnight lows, across all seasons (Fig. 3.2a-d). The greatest changes in minimum temperature are predicted in summer and fall. During these seasons, inland areas are anticipated to see increases on the order of 3–5°F on average (Fig. 3.2c-d). Inland areas display slightly less change, 2–4°F, on average during the winter and spring seasons. Coastal areas see an increase of 2–3°F on average across all seasons, associated with the moderating effect of the Pacific Ocean. As previously noted, the inability of these models to accurately represent changes in maritime fog and onshore/offshore flow introduces uncertainty.

Nearly all 32 simulations agree on increasing average minimum temperatures for each season for the selected points across the county, though they vary in the magnitude of the change (Fig. 3.2e-h). The spread across models (generally 1–3°F) is similar across locations. However, in spring and summer (Fig. 3.2f-g) there is more uncertainty, shown by greater whisker length, as to the magnitude of increase in average minimum temperature.

CHANGE IN NUMBER OF DAYS WITH MINIMUM TEMPERATURE ≤28°F

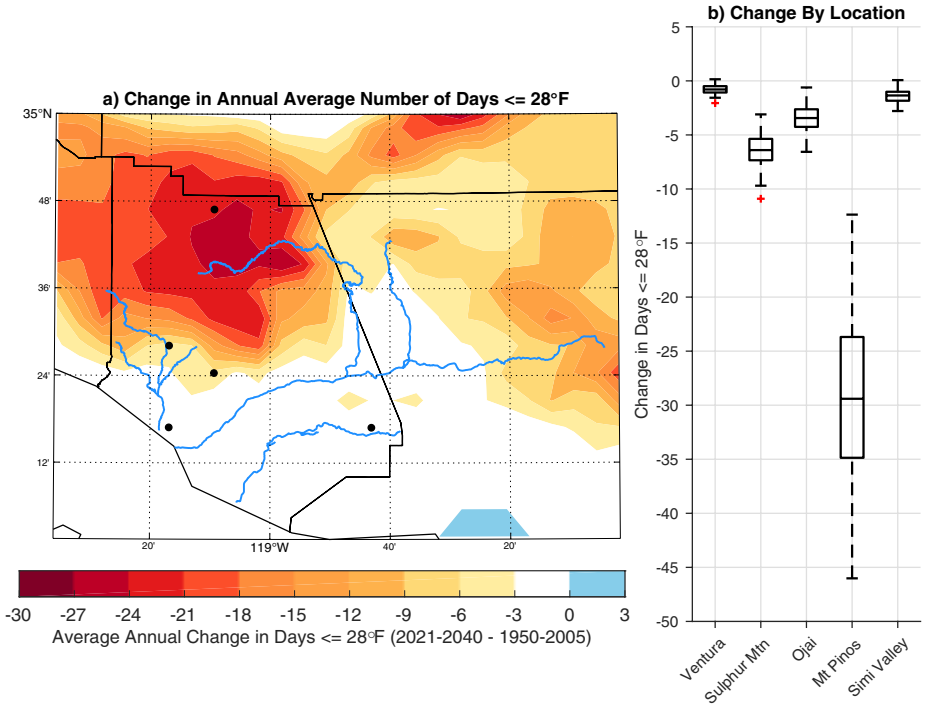

FIGURE 3.3: Change in average annual number of days with minimum temperature ≤28°F, 2021–2040 mean minus 1950–2005 mean. Panel a shows minimum change that ≥75% of models (≥24 of 32) agree on. Panel b depicts spread of change in average annual number of days with minimum temperature ≤28°F across all 32 CMIP5 models for five selected locations within Ventura County (black dots on map).

The National Weather Service (NWS) issues a hard freeze warning when forecast temperatures are ≤28°F during the locally defined growing season (NWS 2018). In the coastal areas, hard freezes are rare due to characteristically low elevations and the moderating oceanic influence. In high-elevation areas in the northern part of the county, models project a decrease ranging from 18 to 27 hard freeze days (Fig. 3.3). In the Ojai Valley, projections suggest 5–7 fewer days (Fig. 3.3). On average, the NWS Cooperative Observer weather station in Ojai measures nine hard freeze days per year over the station's historic record (1905–2018).

All 32 models agree the number of hard freeze days will not increase in Ventura County. Uncertainty across models increases with elevation. Sulphur Mountain and Ojai see a spread of approximately 5–7 days, while model spread at the Mt. Pinos location is over 20 days.

CHANGE IN NUMBER OF DAYS WITH MAXIMUM TEMPERATURE >80°F

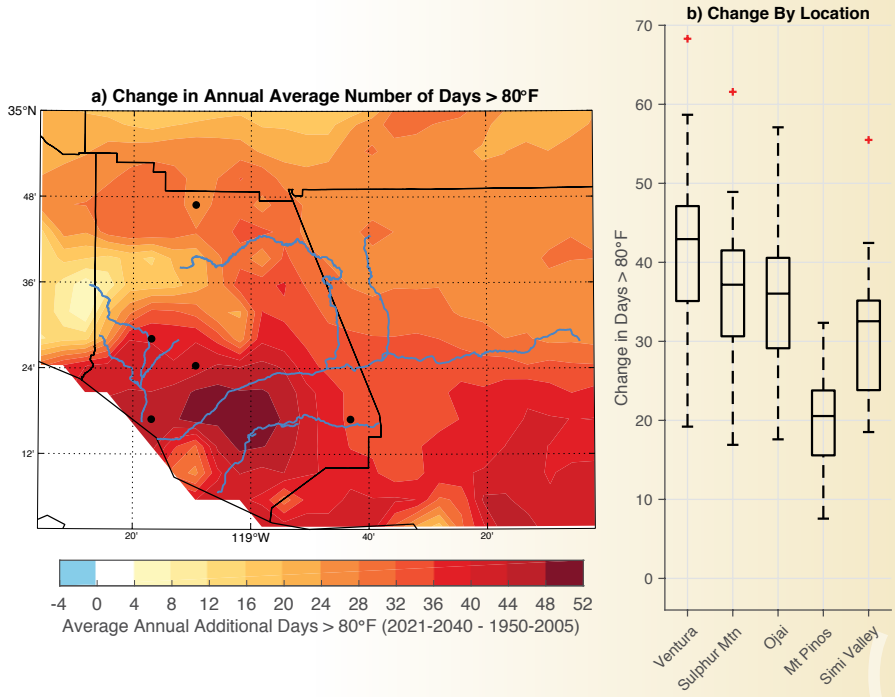

FIGURE 3.4: Change in average annual number of days with maximum temperature >80°F, 2021–2040 mean minus 1950–2005 mean. Panel a shows minimum change that ≥75% of models (≥24 of 32) agree on. Panel b depicts spread of change in average annual number of days with maximum temperature >80°F across all 32 CMIP5 models for five selected locations within Ventura County (black dots on map).

The threshold of >80°F is used by Cal/OSHA for determining when shade needs to be provided for farmworkers (Cal/OSHA n.d.). The greatest changes in >80°F days are observed in the Moorpark-Camarillo area at more than 50 additional days on average per year. In other low elevation areas in the southern part of the county, models suggest an increase of 35–45 days. In the higher elevations of the western part of the county, 4–20 more days >80°F are possible (Fig. 3.4a). The higher elevations experience infrequent >80°F days, so changes are smaller compared to lower elevation locations.

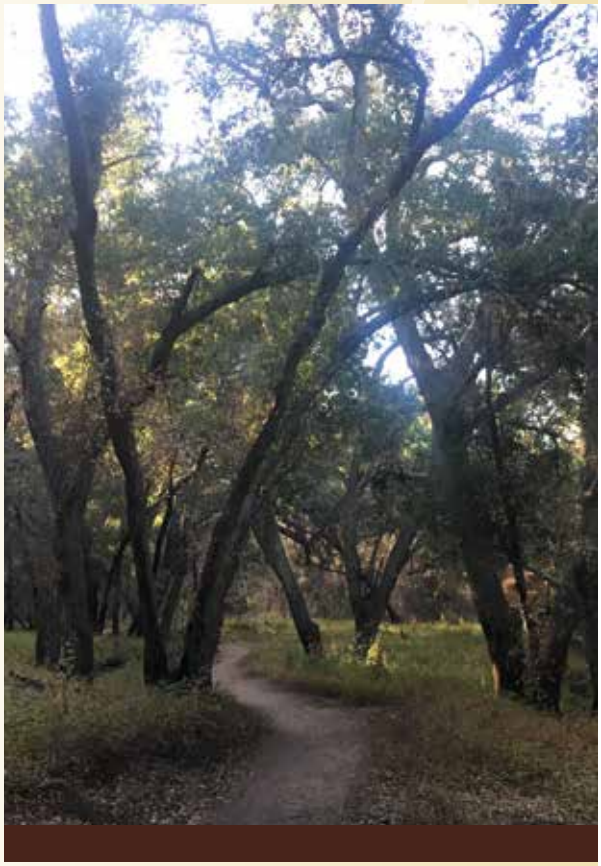

While all models agree on an increase in the annual number of >80°F days, there is uncertainty as to how many such days will occur. Depending on elevation and distance from the coast, there is a spread of approximately 20–40 days across models (Fig. 3.4b). Future changes in cloudiness and marine fog along the coast remain a source of uncertainty.

CHANGE IN NUMBER OF DAYS WITH MAXIMUM TEMPERATURE >95°F

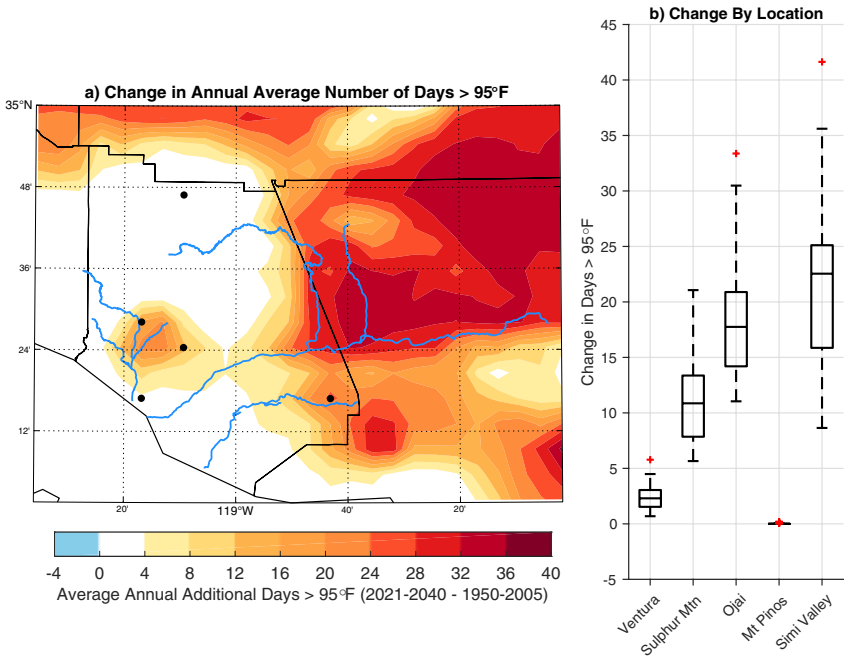

FIGURE 3.5: Change in average annual number of days with maximum temperature >95°F, 2021–2040 mean minus 1950–2005 mean. Panel a shows minimum change that ≥75% of models (≥24 of 32) agree on. Panel b depicts spread of change in average annual number of days with maximum temperature >95°F across all 32 CMIP5 models for five selected locations within Ventura County (black dots on map).

Above 95°F, employers must implement high-heat procedures for outdoor workers, which may impact labor costs and productivity (Cal/OSHA n.d.). Additionally, above 95°F, avocado trees experience flowering problems (Liu et al. 2002). Inland valleys that climatologically experience higher temperatures tend to see more frequent and/or more extreme hot temperatures. Climatologically cooler coastal areas do not see notable increases. Most models suggest at least a 16–20 day increase in the number of days exceeding 95°F for inland locations such as Ojai, Simi Valley, Santa Clarita and the headwaters of the Santa Clara River (Fig. 3.5a).

At the coast and high elevations (Ventura and Mt. Pinos, Fig. 3.5b), the spread across models is low, on the order of zero to five days. However, for inland and low-to-moderate elevation locations of Sulphur Mountain, Ojai, and Simi Valley, the range across models is much larger, with discrepancies of 15–25 days.

CHANGE IN NUMBER OF DAYS WITH MAXIMUM TEMPERATURE >88°F

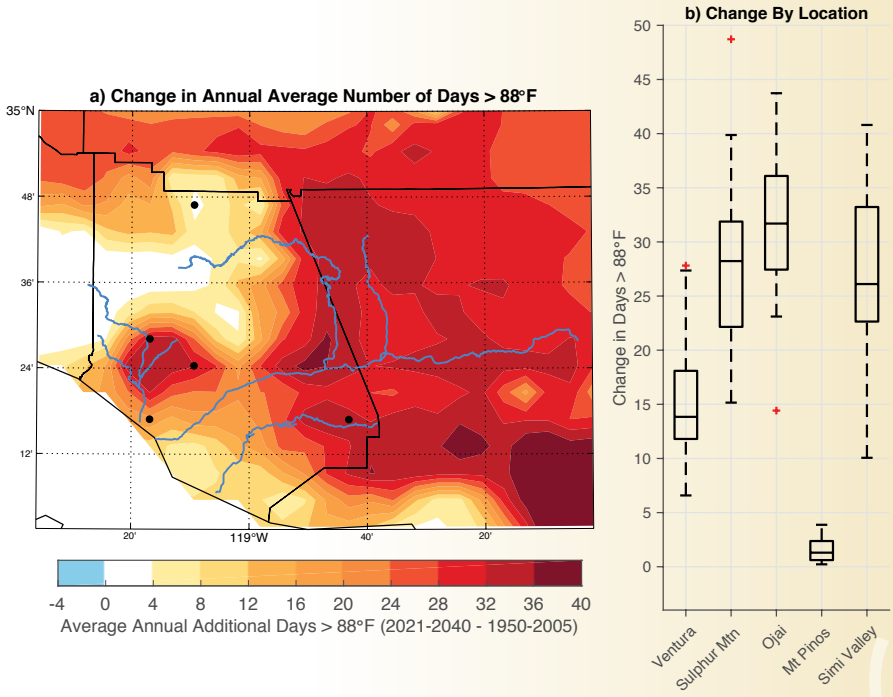

FIGURE 3.6: Change in average annual number of days with maximum temperature >88°F, 2021–2040 mean minus 1950–2005 mean. Panel a shows minimum change that ≥75% of models (≥24 of 32) agree on. Panel bdepicts spread of change in average annual number of days with maximum temperature >88°F across all 32 CMIP5 models for five selected locations within Ventura County (black dots on map).

Above 88°F, avocado trees experience stomatal closure, stressing the plant. This is a response to prevent both water loss and the development of embolisms in the xylem of the plant (Liu et al. 2002). Across the region, models agree on an increase in the average number of days per year with temperatures exceeding 88°F. Inland low-to-mid elevation areas (Simi Valley, Fillmore, Ojai) see the greatest change in number of days, with an increase of 25–30 days on average (Fig. 3.6a).

While models agree on the sign of the change (increasing), there is disagreement as to the magnitude of the change at all locations examined (Fig. 3.6b), with a spread of roughly 10-15 days at all selected locations.

90TH PERCENTILE TEMPERATURE THRESHOLD

The 90th percentile maximum temperature represents the top 10% hottest days, while 90th percentile minimum temperature represents the top 10% warmest overnight lows. In these analyses, the 1950–2005 90th percentile threshold is calculated for minimum and maximum temperature over an 11-day moving window, a method selected to account for seasonality of temperature distributions. The average number of days per year exceeding that threshold is determined. The average number of days per year exceeding the 1950–2005 period threshold is also calculated for the 2021–2040 period, and the values are differenced.

CHANGE IN FREQUENCY OF >90TH PERCENTILE MAXIMUM TEMPERATURE DAYS

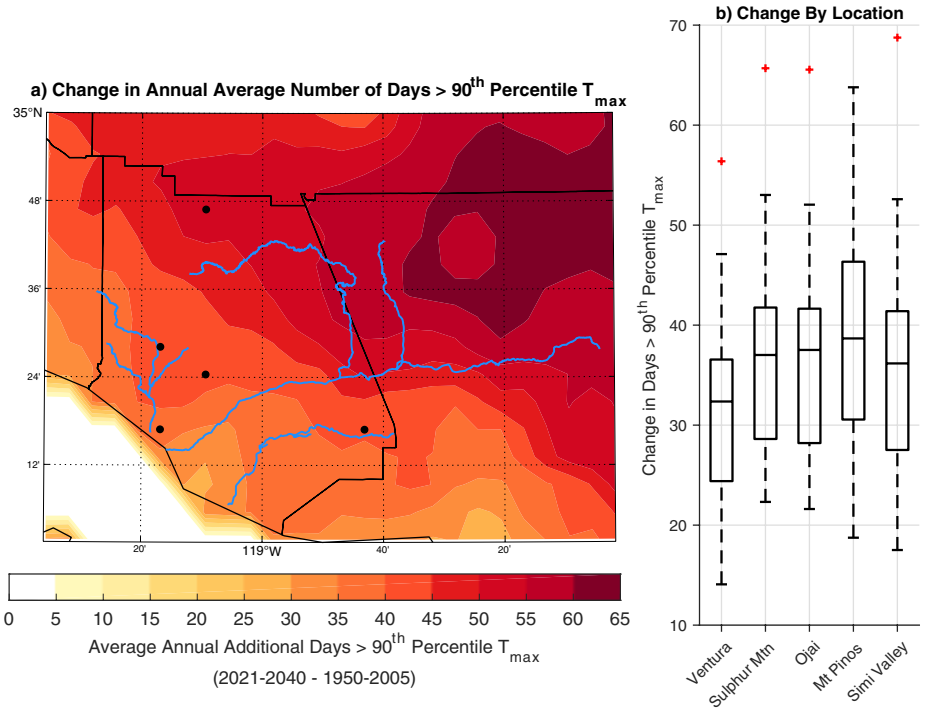

FIGURE 3.7: Change in average annual number of days with maximum temperature exceeding the historic 90th percentile maximum temperature. Panel a shows minimum change that ≥75% of models (≥24 of 32) agree on. Panel b depicts spread of change in average annual number of days with maximum temperature >90th percentile across all 32 CMIP5 models for five selected locations within Ventura County (black dots on map).

There is a ubiquitous increase in the number of days exceeding the historic 90th percentile maximum temperature threshold across the region. The number of days over this threshold increases moving inland from the coast. Some of the largest changes are seen in high elevation regions, notably the headwaters of the Santa Clara River and Mt. Pinos (Fig. 3.7b) where models generally agree on an increase of 45–60 days. Although the high elevation areas do not see changes in the number of days exceeding a specific absolute temperature threshold as large as those in the lower elevation areas (e.g., Fig. 3.4-6), the increases in percentile-based extremes (Fig. 3.7a) suggests that these regions will experience more frequent extremely hot days relative to the historic period.

There is disagreement among models as to number of days exceeding the historic 90th percentile maximum temperature. All locations (Fig. 3.7b) show a spread of at least 30 days across models as well as outliers at the high end. The median change in 90th percentile maximum temperature days across all locations and all models is at least 30 days (Fig. 3.7b).

CHANGE IN FREQUENCY OF >90TH PERCENTILE MINIMUM TEMPERATURE DAYS

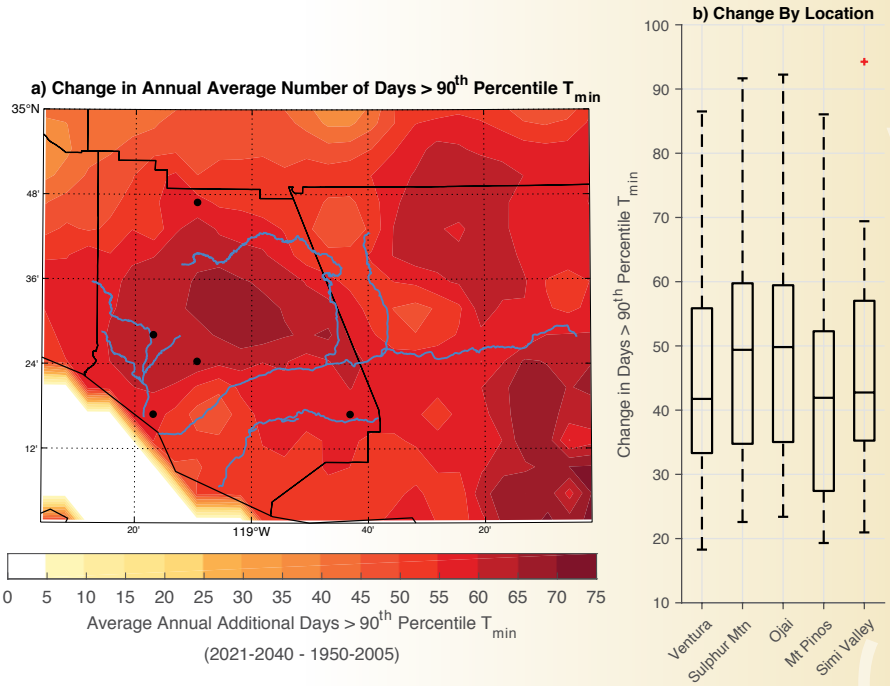

FIGURE 3.8: Change in average annual number of days with minimum temperature exceeding the historic 90th percentile minimum temperature. Panel a shows minimum change that ≥75% of models (≥24 of 32) agree on. Panel b depicts spread of change in average annual number of days with minimum temperature >90th percentile across 32 CMIP5 models for five selected locations within Ventura County (black dots on map).

Models agree on an increase in number of days exceeding the 90th percentile minimum temperature across the region. However, distinct from maximum temperature (Fig. 3.7), the increase is more uniform across the region rather than greater for inland areas. The study region sees an increase of 40–75 days, with some of the greatest increases in the high terrain of the central and northern parts of Ventura County (Fig. 3.8a). Changes in minimum temperature extremes are more widespread and generally greater than those associated with maximum temperature extremes. This reflects regional background warming associated with increased greenhouse gas concentrations. In contrast, maximum temperatures are influenced by local and regional weather conditions.

There is notable disagreement among models as to number of days, more than seen for >90th percentile maximum temperature (Fig. 3.7). All locations have a spread of at least 50 days with some up to 70 days. However, median change among models for all five locations is at least 40 days (Fig. 3.8b).

98TH PERCENTILE TEMPERATURE THRESHOLD

The 98th percentile maximum temperature represents the top 2% hottest days, while 98th percentile minimum temperature represents the top 2% warmest overnight lows. In these analyses, the 1950–2005 98th percentile threshold is calculated for minimum and maximum temperature over an 11-day moving window to account for seasonality effects. The average number of days per year exceeding that threshold is determined. The average number of days per year exceeding the 1950–2005 threshold is also calculated for the 2021–2040 period, and the values are differenced. Temperatures exceeding the 98th percentile are relatively rare as compared to the 90th percentile.

CHANGE IN FREQUENCY OF >98TH PERCENTILE MAXIMUM TEMPERATURE DAYS

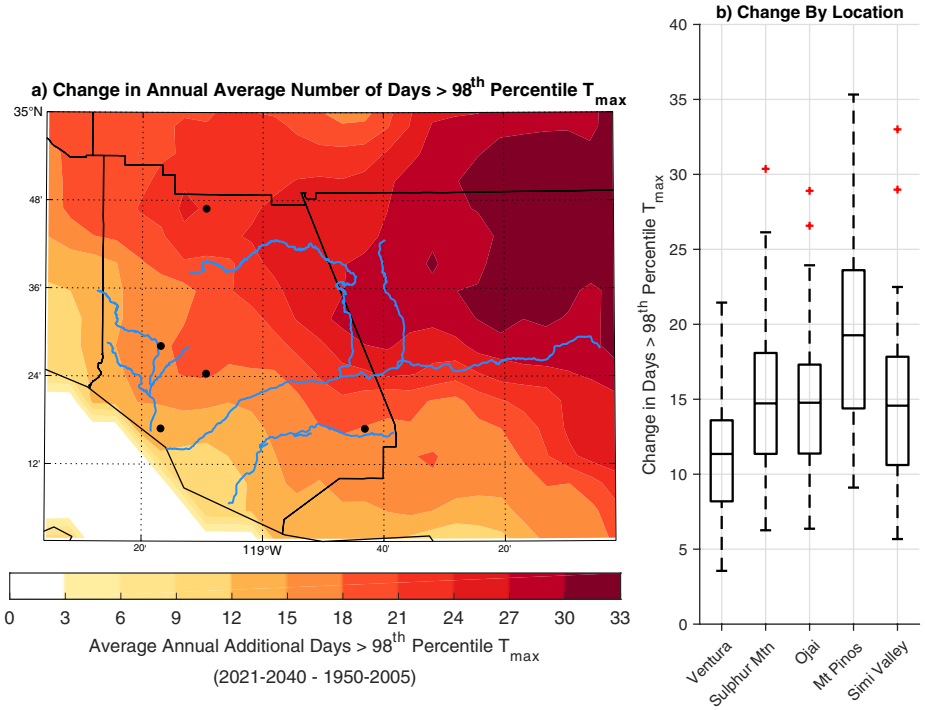

FIGURE 3.9: Change in average annual number of days with maximum temperature exceeding the historic 98th percentile maximum temperature. Panel a shows minimum change that ≥75% of models (≥24 of 32) agree on. Panel b depicts spread of change in average annual number of days with maximum temperature >98th percentile across all 32 CMIP5 models for five selected locations within Ventura County (black dots on map).

All models project an increase in the number of days exceeding the historic 98th percentile maximum temperature threshold across the region. The number of days over this threshold increases moving inland from the coast towards the Mojave Desert region of Los Angeles and Kern Counties. Some of the largest changes are seen in elevated and inland regions, notably the headwaters of the Santa Clara River, where models generally agree on an increase of 20–30 days (Fig. 3.9a). While the high elevation areas do not see changes in the number of days exceeding a specific absolute temperature threshold as large as those in the lower elevation areas (e.g., Fig. 3.4-6), the increases in percentile-based extremes (Fig. 3.9a) suggests that these regions will experience more frequent extremely hot days relative to the historic period.

There is some disagreement among models as to the change in number of days >98th percentile maximum temperature. All locations show a spread of at least 15 days across models. The median change in 98th percentile maximum temperature days among models across all locations is at least 12 days (Fig. 3.9b).

CHANGE IN FREQUENCY OF >98TH PERCENTILE MINIMUM TEMPERATURE DAYS

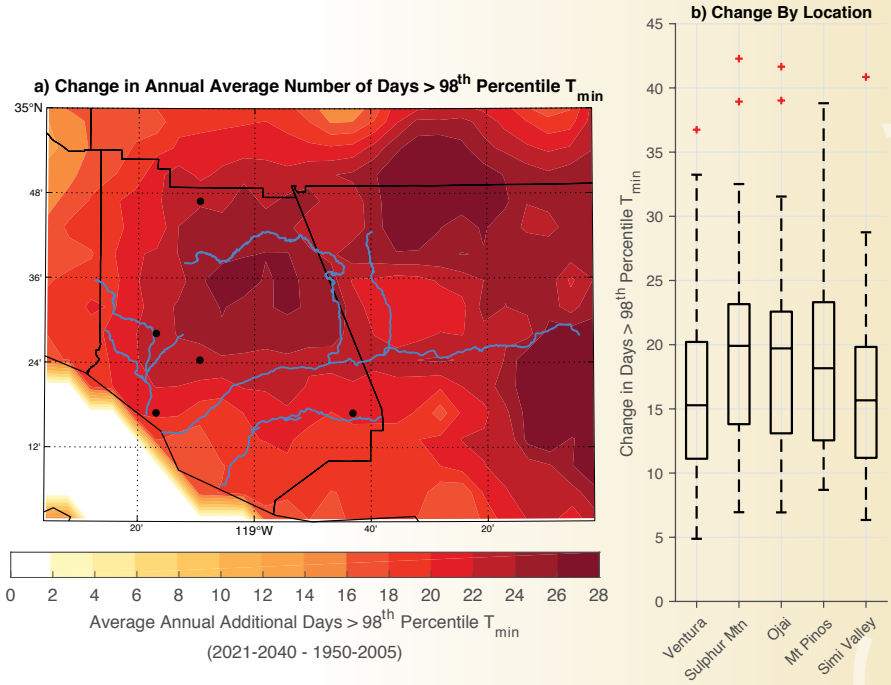

FIGURE 3.10: Change in average annual number of days with minimum temperature exceeding the historic 98th percentile minimum temperature. Panel a shows minimum change that ≥75% of models (≥24 of 32) agree on. Panel b depicts spread of change in average annual number of days with minimum temperature >98th percentile across all 32 CMIP5 models for five selected locations within Ventura County (black dots on map).

Models agree on an increase in number of days exceeding the 98th percentile minimum temperature across the region. However, distinct from maximum temperature (Fig. 3.9), the increase is somewhat more uniform across the region rather than greater for inland areas. Models generally agree on an increase of 14–26 days across the region (Fig. 3.10a).

There is some disagreement among models as to the change in the number of days >98th percentile minimum temperature. All locations (Fig. 3.10b) show a spread of at least 20 days across models. The median change in 98th percentile minimum temperature days across all locations and among all models is at least 15 days (Fig. 3.10b).

SECTION 4

Precipitation

4.1 Summary

Simulated future precipitation (inclusive of rain and snow) demonstrates considerable disagreement across the 32 CMIP5 models regarding whether the future will be wetter or drier. This is in contrast to the broad agreement among models projecting warming (Section 3) and increases in evaporative demand (Section 5). Model spread for precipitation is greatest during the winter season, when most precipitation occurs in Ventura County. On average, several models trend wetter, several trend drier, and others show little to no change (Fig. 4.1). Models do, however, show relatively good agreement on precipitation intensification. They consistently project increases in the annual number of dry days (Fig. 4.5), while there is little to no change in overall precipitation (Fig. 4.1). This suggests that the same amount of precipitation must fall in fewer days, requiring an intensification of daily precipitation. Projections suggest a 7% decrease in winter precipitation days, an 11% decrease in spring precipitation days, and a 20% decrease in fall precipitation days (Figs. 4.6-7) with little overall projected change in seasonal precipitation totals (Fig. 4.2).

The concept of intensification is further supported by a tendency toward an increase in the contribution to total precipitation from the 5% of wettest days (Fig. 4.4) and an increase in the frequency of days with precipitation exceeding the 85th percentile (Fig. 4.7). The median across LOCA data for 32 CMIP5 models indicates a slight increase in winter season precipitation (0.25-1.5 in. across the county, Fig. 4.2). In all other seasons, little to no change is projected; median changes range from -0.5 in. to +0.25 in. (see Section 7.1 on how this may change by mid-century).

A growing body of research depicts an intensification of precipitation at the sub-daily timescale in a warming climate. This intensification occurs at a greater rate than precipitation at the daily timescale (Westra et al. 2014). Using output from a pseudo-global warming experiment (Figs. 4.9-19), a shift in the distribution of hourly precipitation intensities towards more frequent high intensity events and more frequent events over a given threshold (e.g., 10 mm h^{-1}, 25 mm h^{-1}) is observed. These results are consistent with the analysis of downscaled global climate model projections discussed above. Additionally, changes can be seen in how a historic storm event, simulated under conditions of a warmer climate, can produce greater storm total precipitation and have higher maximum intensities (Fig. 4.18-19). Results do not suggest an increased influence of decaying tropical systems in the fall season in terms of adding to annual precipitation.

4.2 Implications of Changes in Precipitation

- The number of dry days increases in the spring and fall (Fig. 4.6); however, there is little change projected in precipitation totals for these seasons (Fig. 4.2), implying some intensification of precipitation in these seasons, although these increases grow with time (Appendix A). Prolonged dry periods are associated with wildfire activity (e.g., Nauslar et al. 2018). With more dry days there may be potential for a longer wildfire season due to additional opportunities for persistence of dry conditions.
- Groundwater recharge is projected to decrease in the Southwest in a warming climate (Niraula et al. 2017) and may in part be related to increasing rainfall intensities (Dettinger and Earman 2007). Precipitation intensification at the seasonal to sub-daily timescales may have implications for the methods by which groundwater recharge occurs or how surface water is conveyed, captured, and stored.
- Roughly half of models project more frequent days exceeding historic 85th percentile daily precipitation totals (Fig. 4.7), resulting in more days with storm water management concerns if these outcomes are realized.
- Intensification of sub-daily precipitation (Figs. 4.8-16) raises concerns for increased flash flooding (Modrick and Georgakakos 2015), landslides, and debris flows (e.g., Oakley et al. 2018a) in a warming climate. In addition to the potential for increased threats to life and property, this may have impacts on infrastructure design and water resource management.
- Precipitation intensification creates the potential for greater exposure to saturated conditions for crops grown in Ventura that are sensitive to these conditions, such as berries and vegetables (Hall et al. 2018)
- Potential for storms with similar atmospheric characteristics to historic events to produce greater event total precipitation due to warming and ability for greater amounts of water vapor to be present in the atmosphere (Figs. 4.17-18; Prein et al. 2017).
- With uncertainty in annual precipitation changes, potential for increasing dry days, and increased temperatures (Section 3) and evapotranspiration (Section 5), diversified water supply portfolios will likely allow for more resilient water management (Sterle et al. 2019).

4.3 Precipitation Analyses

Due to the spread across models seen in the LOCA data for precipitation, instead of looking at the minimum change that at least 75% of models agree on, the extremes (top 10th/bottom 10th percentile) and/or upper and lower quartiles of outcomes are examined. This is done to highlight the distribution of model output.

AVERAGE ANNUAL PRECIPITATION CHANGE

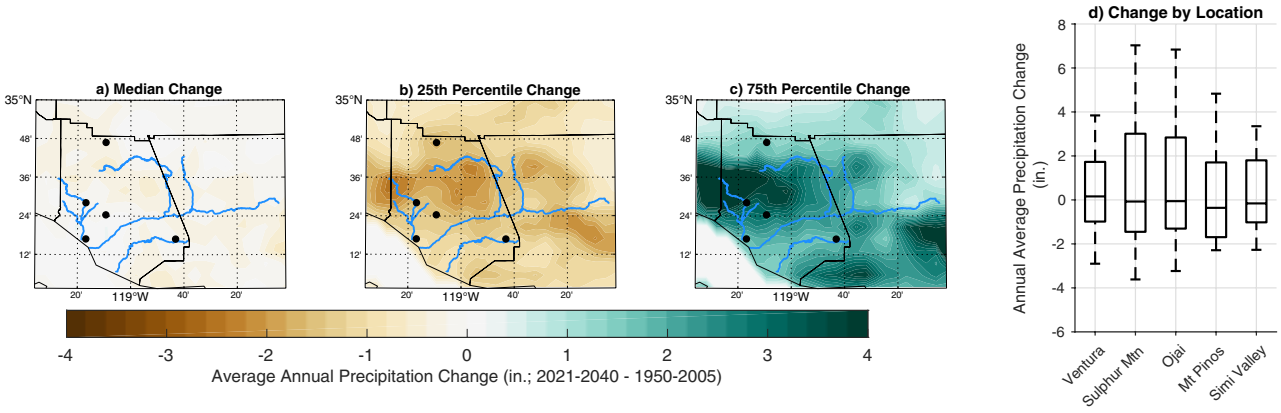

FIGURE 4.1: Changes in average annual precipitation (2021–2040 minus 1950–2005), shown as: a) The median change across all 32 models; b) The 25th percentile (driest quartile) change in a distribution fit to the model range of values; c) The 75th percentile (wettest quartile) change in a distribution fit to the model range of values; d) Spread in average annual precipitation change across all 32 CMIP5 models for five selected locations within Ventura County (black dots on map).

At the annual timescale, there is little to no change in the median average annual precipitation across models (Fig. 4.1a). Some models suggest drier conditions (Fig. 4.1b,d) by 0–3 in., while some suggest wetter conditions, by 0–4 in. or more (Fig. 4.1c,d). There is greater spread across models towards the wetter end (Fig. 4.1d), suggesting greater uncertainty as to how much precipitation increase might occur if that were the outcome.

AVERAGE SEASONAL PRECIPITATION CHANGE

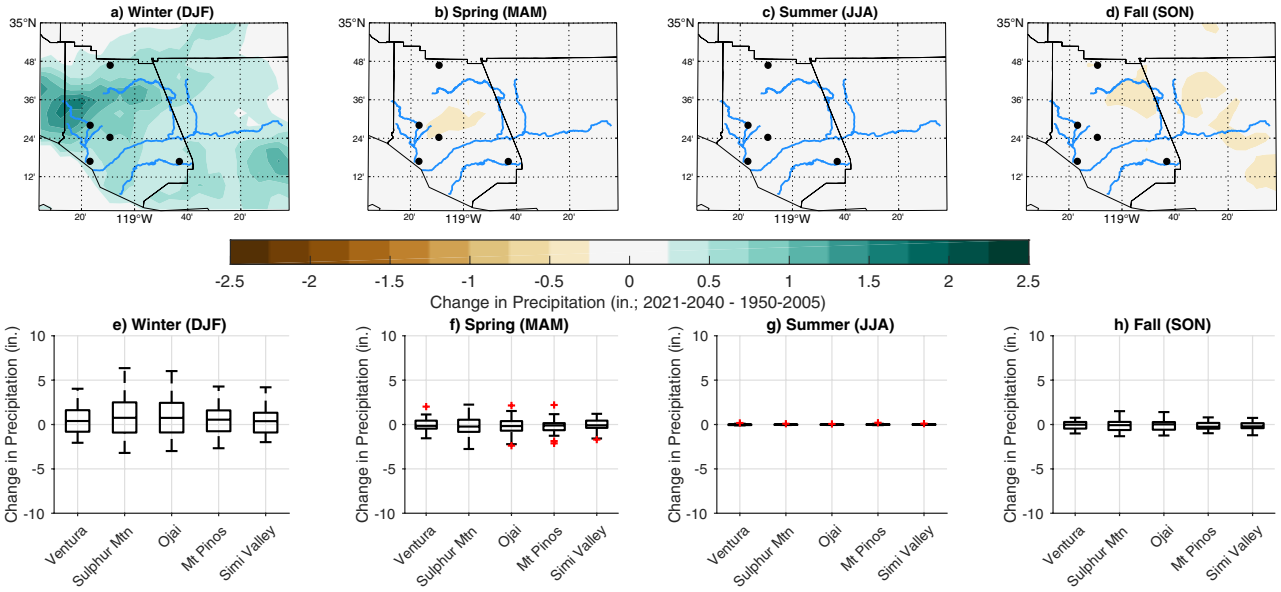

FIGURE 4.2: Changes in average seasonal precipitation (2021–2040 minus 1950–2005), shown as: a-d) Median average precipitation change across models for each season; e-h) Spread in average seasonal precipitation change across all 32 CMIP5 models for five selected locations within Ventura County (black dots on map).

The greatest projected changes in precipitation are observed in the winter season, where the median change across the 32 models is 0.25–0.75 in. at lower elevations and 0.75–1.5 in. at higher elevations in the western part of Ventura County (Fig. 4.2a). These changes, however, are small compared to average annual precipitation in these areas (Table 1.1). Little to no precipitation change is observed in the spring, summer, and fall seasons (Fig. 4.2b-d).

The greatest model spread is observed in the winter season, with several ensemble members suggesting a decrease in precipitation and some showing an increase of four or more inches at all selected locations (Fig. 4.2e). Model spread is much less in the drier seasons (on the order of a couple of inches for spring and fall), but there is still disagreement on whether precipitation will increase or decrease (Fig. 4.2f,h). The typically dry summer season sees no change from the historical period (Fig. 4.2g).

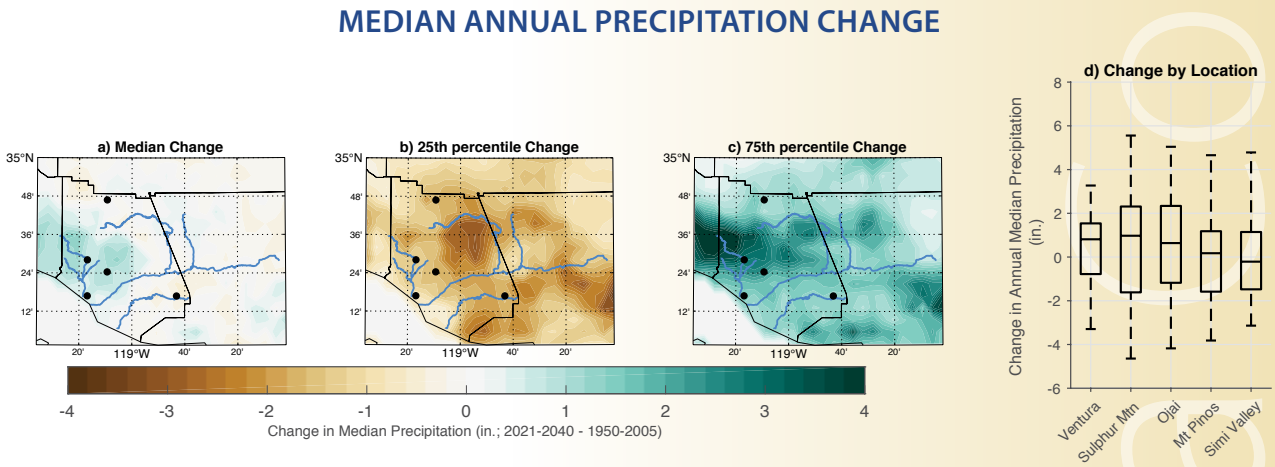

FIGURE 4.3: Changes in median annual precipitation (2021–2040 minus 1950–2005), shown as: a) The median change across all 32 models; b) The 25th percentile (driest quartile) in a distribution fit to the model range of values; c) The 75th percentile (wettest quartile) in a distribution fit to the model range of values; d) Spread in median annual precipitation change across all 32 CMIP5 models for five selected locations within Ventura County (black dots on map).

Due to high interannual variability and the role of extreme events, the precipitation distribution in southern California is non-normal and positively skewed (e.g., Oakley et al. 2018b). One characteristic of this distribution is that mean precipitation is higher than median precipitation. Therefore, we look at results associated with both the change in mean and median precipitation to provide both perspectives.

The median change (based on 32 models) of median annual precipitation (Fig. 4.3a) shows some increased precipitation in the western part of Ventura County, while little to no change or slight decreases are seen elsewhere. As the median is less than the mean, it would take a smaller change to have an increase. The model spread (Fig. 4.3d) demonstrates more spread in the inland mountainous locations than along the immediate coast, potentially reflecting how different global climate models simulate precipitation in areas with mountainous terrain.

CHANGE IN CONTRIBUTION TO TOTAL PRECIPITATION FROM TOP 5% OF WETTEST DAYS

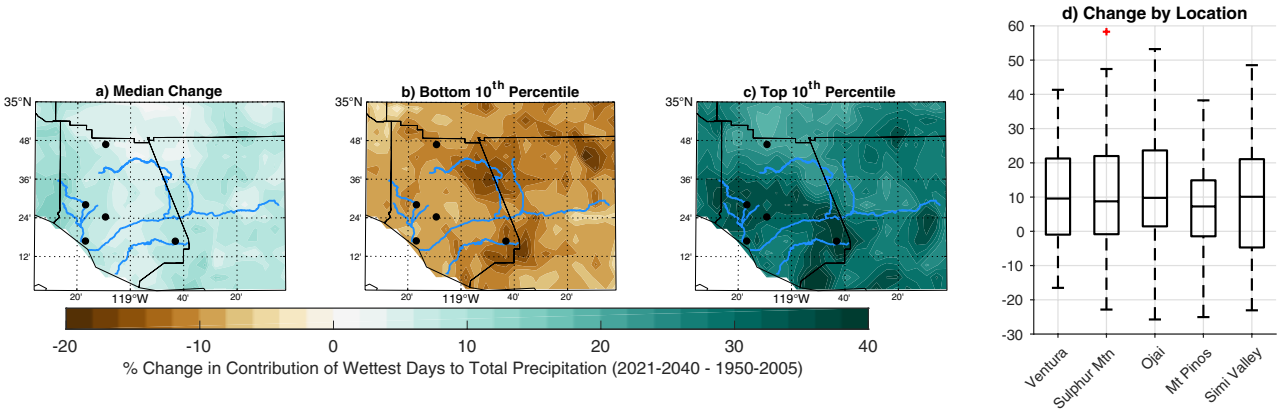

FIGURE 4.4: Changes in contribution of the top 5% of wettest days to total annual precipitation (2021–2040 minus 1950–2005) as: a) Median change in contribution across models; b) The bottom 10th percentile (decile with smallest or negative change in contribution) in a distribution fit to the model range of values; c) The top 10th percentile (decile with greatest positive changes in contribution) in a distribution fit to the model range of values; d) Spread in change in contribution across all 32 CMIP5 models for five selected locations within Ventura County (black dots on map).

Previous research has demonstrated a large fraction of historic precipitation, especially in Southern California, comes from just a few storms (or "wet days"; Dettinger et al. 2011; Oakley et al. 2018b). The contribution to total precipitation from the wettest 5% of days each year represents this phenomenon (Dettinger and Cayan 2014). The median change in contribution from the wettest 5% of wet days across all models (Fig. 4.4a) shows an increase of approximately 10%. This means that the wettest 5% of wettest days will contribute 10% more to total annual precipitation in the future period than during the historic period. This is one metric to suggest precipitation intensification.

There is model disagreement as to the sign and magnitude of the changes in contribution of the wettest 5% of days. There are some models that show a decrease in contribution from the wettest 5% of days, with the bottom 10th percentile showing a decrease of roughly 5–20% (Fig. 4.4b,d). In the top 10th percentile (Fig. 4.4c,d), increases of 10–50% are seen across the region. Given the model spread, such that the lower quartile of the boxplots lies close to zero across all locations shown (Fig. 4.4d), it is more likely to see the wetter outcome (intensification of precipitation on the top 5% of wettest days), as roughly 75% of models agree on this signal for all locations.

CHANGE IN AVERAGE ANNUAL NUMBER OF DRY DAYS

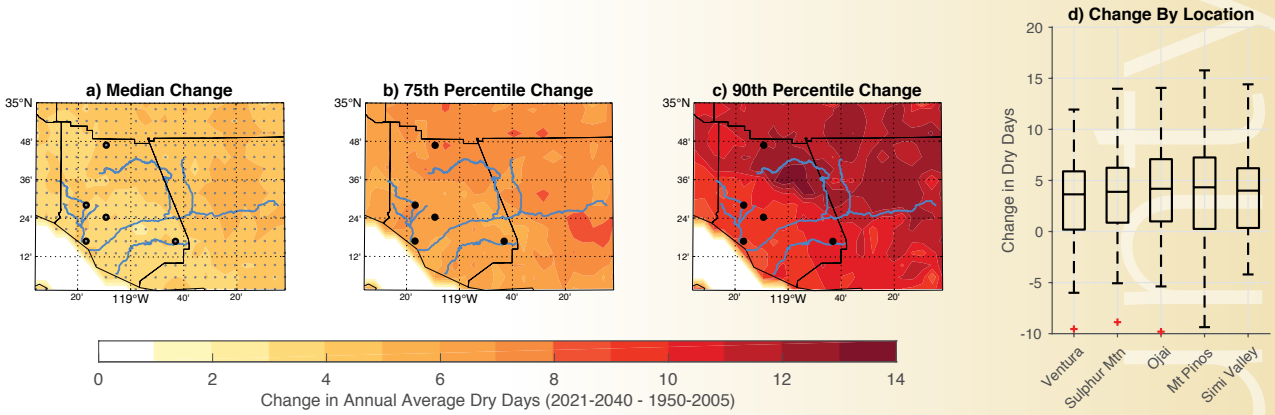

FIGURE 4.5: Change in average annual number of dry (zero precipitation) days, 2021–2040 minus 1950–2005 for: a) median change across all models as filled contours with grid cells where at least 75% (24 of 32) of models are in agreement on an increase in number of dry days shown as dots; b) The 75th percentile change in dry days (upper quartile) in a distribution fit to the model range of values; c) The 90th percentile change in dry days (uppermost decile) in a distribution fit to the model range of values; d) Spread in change in annual dry days across all 32 CMIP5 models for five selected locations within Ventura County (black dots on map).

The models suggest increases in the median average annual number by at least three days. There is good agreement across models on an increasing number of dry days. At nearly all grid points, over 75% of models depict a positive change (Fig. 4.5a). As there is good agreement in an increase, the 75th and 90th percentile changes in number of dry days are examined rather than the lowest quartile or decile. At the 75th percentile threshold, models suggest an increase of between four to eight dry days on average per year across the region (Fig. 4.5b). At the 90th percentile of model projections, increases are between eight to 14 days across the region (Fig. 4.5c).

A few models show a decrease in the number of dry days. It is likely that these models tend to be wetter on average. There is also notable spread across models, with ranges between 15–20 days for each location (Fig. 4.5d). With models tending towards an increased number of dry days and little change expected in average annual precipitation (Fig. 4.1), it follows that precipitation will intensify, with more rain falling on the remaining wet days. This is consistent with increases in contributions to total precipitation from the wettest 5% of days (Fig. 4.4) and more frequent days where precipitation exceeds the 85th percentile of daily precipitation (Fig. 4.7).

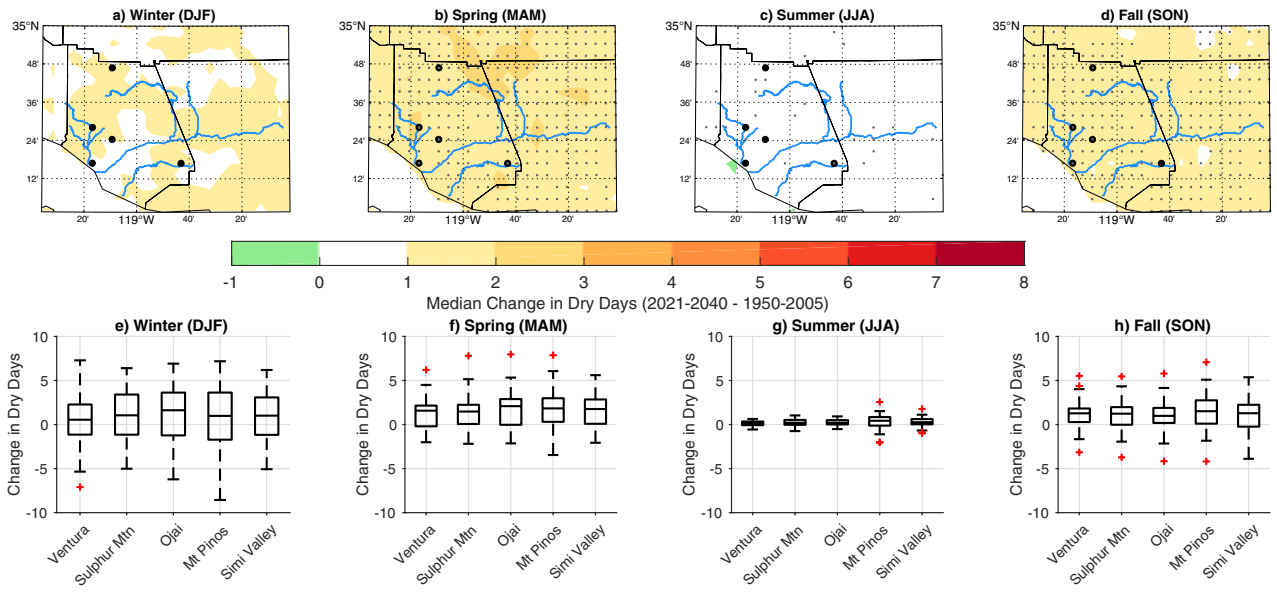

FIGURE 4.6: Change in median annual number of dry (zero precipitation days), 2021–2040 minus 1950–2005. a-d) By season, median change across all models as filled contours with grid cells where at least 75% (24 of 32) of models agree on an increase in dry days shown as dots; e-h) By season, the spread in change in annual dry days across all 32 CMIP5 models for five selected locations within Ventura County (black dots on map).

In both the spring and fall season, models are in good agreement (>75% agree) on an increase of *at least* one to two dry days (Fig. 4.6b,d). For these seasons, model spread is relatively small as compared to annual change (Fig 4.5d). As there is little change in average precipitation for the spring and fall seasons (Fig. 4.2), the increase in dry days in this season implies precipitation intensification.

For the winter season, more uncertainty exists. The model median change is one to two dry days across much of the region (Fig 4.6a,e) though model spread is large and there are no grid points where >75% of models are in agreement on this change. There is a spread of roughly 12–14 days across models for the winter season (4.6e), and at least a quarter of models depict a decrease in dry days for the winter season. Historically, this region experiences little to no summer season precipitation and this appears unlikely to change in a warming climate (Fig 4.6c,g).

To evaluate the relevance of changes in number of dry days to precipitation intensification, it is useful to determine how this relates to a decrease in wet (non-zero precipitation) days. For the winter season, there are on average between 25–35 wet days across the region (Fig. 4.7a). Using 30 wet days as representative for winter wet days and anticipating an increase of two dry days (Fig. 4.6a), all winter precipitation would now come in 28 days, or 7% fewer days than in the historic period.

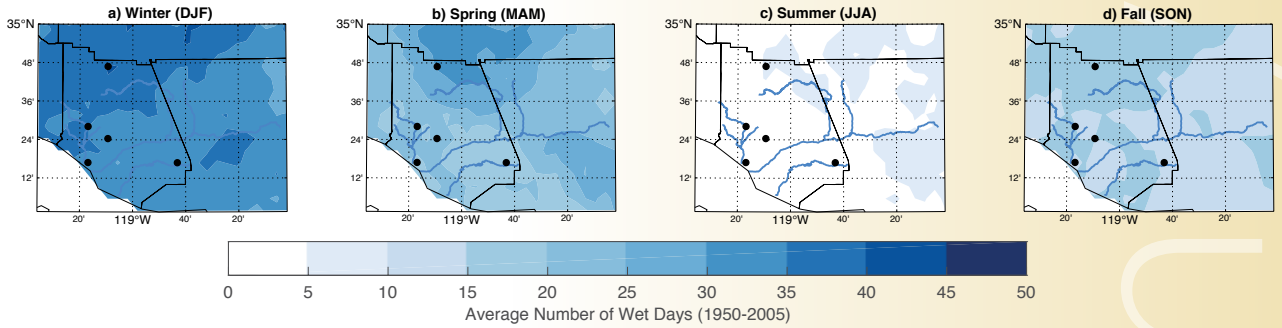

FIGURE 4.7: Average number of wet days (non-zero precipitation days) by season for the 1950–2005 period averaged across 32 CMIP5 models.

For the spring and fall season, precipitation falls on fewer days historically, so the change of a few dry days represents a greater percentage change. In spring, there are on average 15–25 precipitation days across the region (Fig. 4.7b). Using 20 wet days as a representative value for the region, an increase of two dry days (Fig. 4.6b) would mean all precipitation would arrive in 18 days, an 11% decrease in wet days. For fall, using 10 wet days as a representative number of wet days across the region (Fig. 4.7d), an increase of two dry days (Fig. 4.6d) is a 20% decrease in the number of days on which precipitation occurs on average in the 2021–2040 period. There are little to no anticipated changes in the dry summer season (Fig. 4.6c).

CHANGE IN FREQUENCY OF 85TH PERCENTILE DAILY PRECIPITATION EVENTS

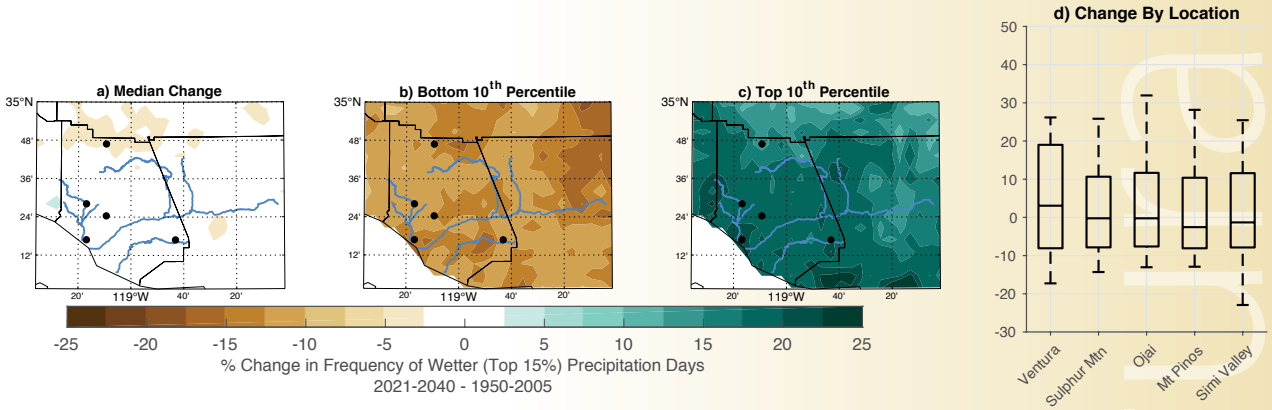

FIGURE 4.8: Percent change in frequency of 85th percentile (wettest 15%) precipitation days, based on historic 85th percentile and frequency during 2021–2040 minus 1950–2005. a) Median change; b) Bottom (least change) 10th percentile in a distribution fit to the model range of values; c) Top (greatest change) 10th percentile in a distribution fit to the model range of values; d) Spread in percent change in annual percent change of 85th percentile events across all 32 CMIP5 models for five selected locations within Ventura County (black dots on map).

Daily precipitation exceeding the historic 85th percentile is relevant to stormwater management (Ventura County, California 2010). Little change is seen in the model median (Fig. 4.8a) with regards to 85th percentile events. However, there is substantial disagreement among models. The bottom 10th percentile of the distribution suggests a roughly 7–20% decrease in occurrence of 85th percentile precipitation days, while the top 10th percentile depicts an increase of 10–30%. This greater spread of "wetter" potential outcomes is consistent with the distribution seen in the contribution from top 5% of wettest days (Fig. 4.5).

4.4 Changes in Hourly Precipitation Characteristics

A growing body of research provides evidence for an intensification of precipitation at the sub-daily timescale in a warmer climate (Westra et al. 2014). Here, we examine the change in precipitation distribution at hourly timescales as well as the change in frequency of precipitation exceeding certain thresholds. This is performed using hourly output from a numerical weather model at 4-km horizontal resolution from a pseudo-global warming simulation for the period October 2000–March 2013. The "control" simulation refers to output from dynamically downscaling the 0.75° ERA-INTERIM reanalysis product to 4 km, a scale capable of resolving both atmospheric convection and the interactions of terrain with atmospheric precipitation processes. The "perturbed" simulation represents the warmed scenario that considers the RCP 8.5 pathway. The images depicting "difference" show the difference between variables in the perturbed scenario minus the control scenario. See Data and Methods (Section 2) for more detail. Changes in summer hourly precipitation characteristics are not depicted here, as little to no precipitation falls in Ventura County in this season and changes in this characteristic are not anticipated in the future.

SHIFT IN HOURLY PRECIPITATION DISTRIBUTION

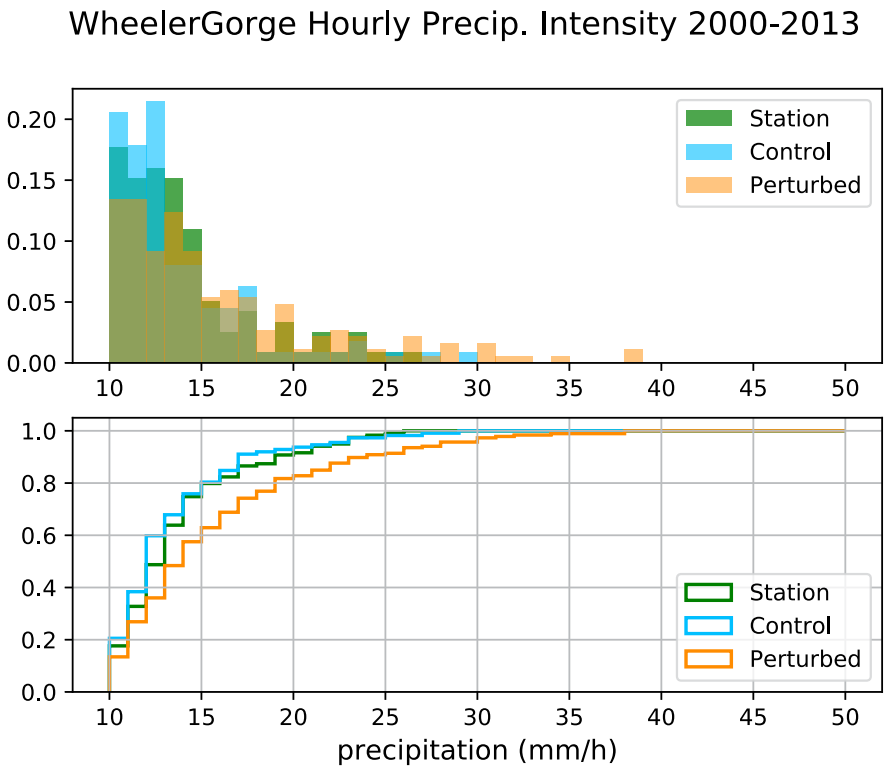

FIGURE 4.9: Top: Normalized frequency of hourly precipitation events greater than 10 mm h^{-1} for the period 2000–2013 for the Wheeler Gorge precipitation gauge (green), the control simulation (blue) and perturbed simulation (orange). Bottom: Cumulative distribution function for hourly precipitation events greater than 10 mm h^{-1} for the period 2000–2013 for the Wheeler Gorge precipitation gauge (green), the control simulation (blue) and perturbed simulation (orange).

The distribution of hourly precipitation intensities in the control simulation reasonably approximates the station data (Fig. 4.9). This provides confidence in the simulation results. There is an increase in the frequency of high intensity events (≥15 mm h^{-1}) in the perturbed simulation, as well as a lengthening of the tail of the distribution towards more extreme events (Fig. 4.9, top). The distribution of hourly precipitation intensities is shifted towards more intense events, especially above the 60th percentile (Fig. 4.9, bottom). This can be seen in the rightward shift of the orange line as compared to the blue and green lines. Other stations examined in this area reveal a similar shift towards increased frequencies of the heaviest precipitation.

Changes (control versus perturbed climate scenarios) in the frequency of precipitation events exceeding two thresholds are presented here: 10 mm (0.39 in.) in one hour, as a moderate intensity, and 25 mm (0.98 in.) in one hour, as a more extreme intensity. These are generalizations of thresholds discussed in scientific literature to be relevant to triggering post-wildfire debris flows and shallow landslides in this region. Based on observations following the 2003 Piru Fire, Cannon et al. (2008) derived an equation that suggests 12.5 mm (0.49 in.) in one hour is sufficient to trigger post-wildfire debris flows in Ventura County. This work also states that post-wildfire debris flows in Southern California were generally associated with storms that had recurrence intervals of two years or less. An hourly precipitation total of ~1 in. (~25 mm) roughly corresponds to the two-year average recurrence interval for elevations over ~1000 ft. exposed to southerly flow in Ventura County according to the NOAA Atlas 14 (https://hdsc.nws.noaa.gov/hdsc/pfds/pfds_map_cont.html). The U.S. Geological Survey uses an intensity of 24 mm h^{-1} for a 15-minute duration as a general guideline for post-wildfire debris flow initiation in the Transverse Ranges in the first year following a wildfire (USGS 2019). Though this multiplies out to 24 mm (0.94 in.) in one hour, the intensity needed to trigger debris flows for a 1-hour period used in practice is less than 24 mm. An hourly total exceeding 24 mm, as presented here, will generally well exceed post-fire debris flow thresholds and can be used as an example of an extreme case. Thresholds of 10 mm and 20 mm (0.79 in.) in one hour have been noted in the literature as capable of initiating shallow landslides in Southern California assuming sufficient antecedent rainfall and soil moisture (Oakley et al. 2018a and references therein).

CHANGES IN NUMBER OF >10 MM H^{-1} EVENTS

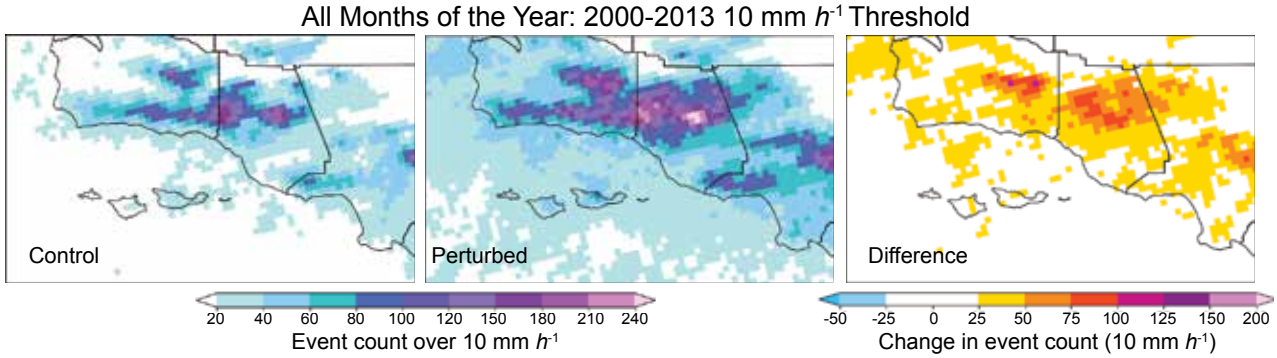

FIGURE 4.10: Number of >10 mm h^{-1} events summed over all months in the 2000–2013 period for a) control simulation and b) perturbed simulation and c) difference between b) and a) (perturbed minus control).

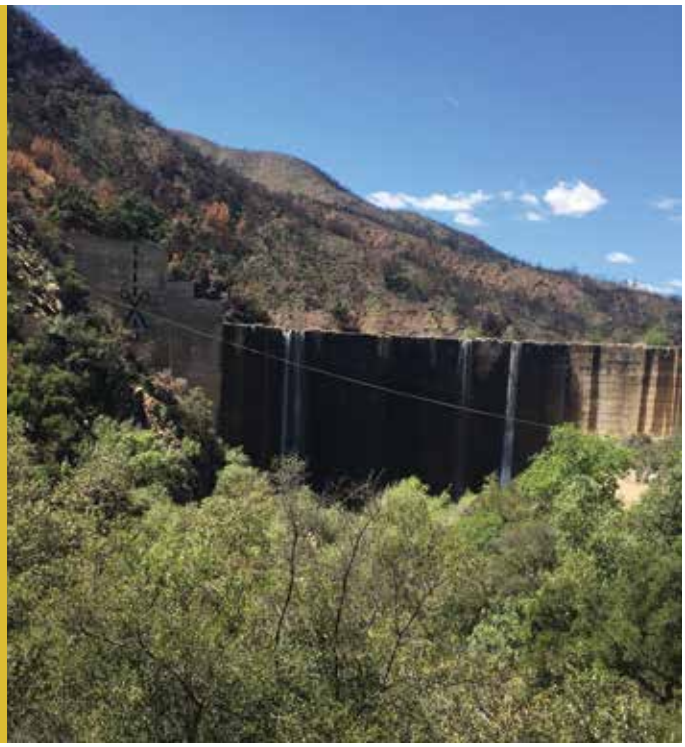

The greatest increase in instances of hourly precipitation >10 mm h^{-1} in the perturbed scenario are observed in areas of elevated terrain. Changes range from an increase of between 25–50 events at lower elevations to between 50–100 or more events in the mountainous terrain in the central part of the county (Fig. 4.10). This is consistent with the climatological tendency of mountainous areas to observe more frequent high intensity rainfall (Oakley et al. 2018a). Mountains provide an efficient atmospheric lifting mechanism, as rainfall is initiated when moist air is forced upward, cools and condenses. Mountains also facilitate moisture convergence in the lower atmosphere, enhancing precipitation by increasing moisture availability.

The winter season accounts for the majority of the increase of >10 mm h^{-1} events in the perturbed simulation (Fig. 4.11). At lower elevations, an increase of between 15–45 events is observed in this season, with changes of between 45–60+ events at the higher elevations. During the spring season changes are much smaller. Spring changes show between 15–30 more events at the moderate-to-high elevations of the region (Fig. 4.12). In the fall season, changes are relatively small with only a few grid points in the high terrain showing an increase of 15–30 events (Fig. 4.13). Several locations show a decrease of >10 mm h^{-1} events in the fall season, especially in Santa Barbara County. Due to the relatively small change it is difficult to discern whether this is a robust signal or model noise.

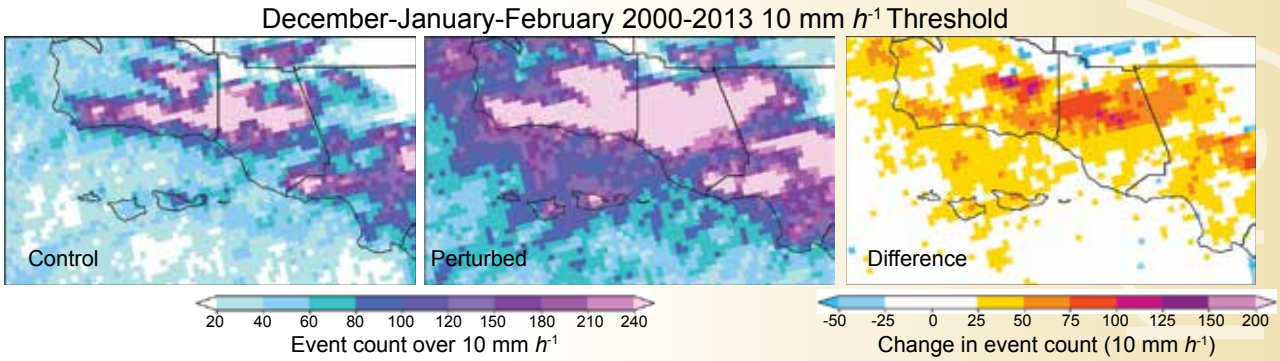

FIGURE 4.11: Number of >10 mm h^{-1} events summed over December–January–February periods in the 2000–2013 period for a) control simulation b) perturbed simulation and c) difference between b and a (perturbed minus control).

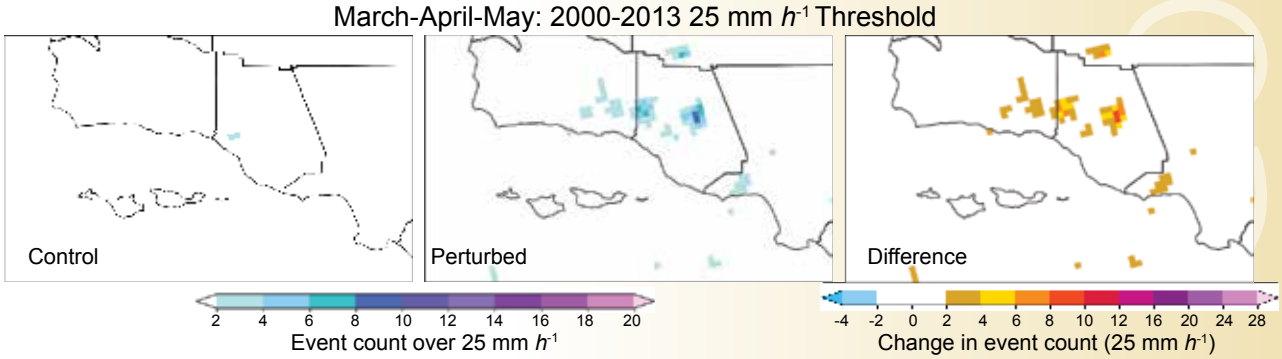

FIGURE 4.12: Number of >10 mm h^{-1} events summed over March–April–May periods in the 2000–2013 period for a) control simulation b) perturbed simulation and c) difference between b and a (perturbed minus control).

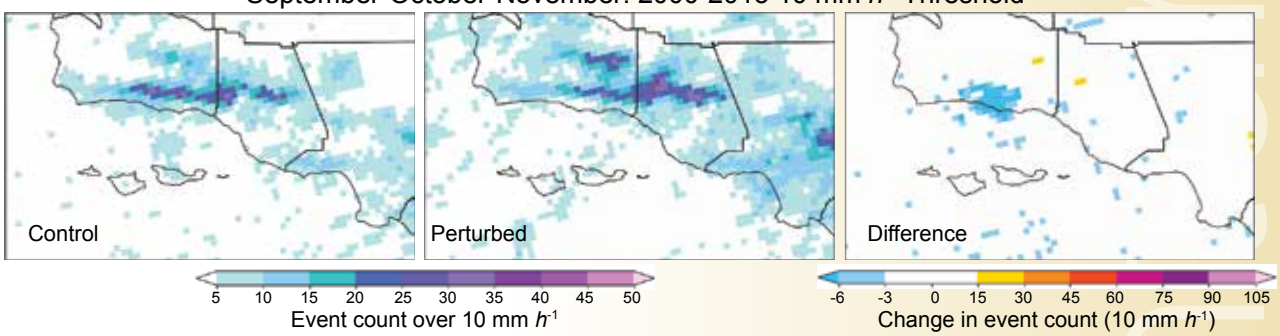

FIGURE 4.13: Number of >10 mm h^{-1} events summed over September–October–November periods in the 2000–2013 period for a) control simulation b) perturbed simulation and c) difference between b and a (perturbed minus control).

CHANGES IN NUMBER OF >25 MM H^{-1} EVENTS

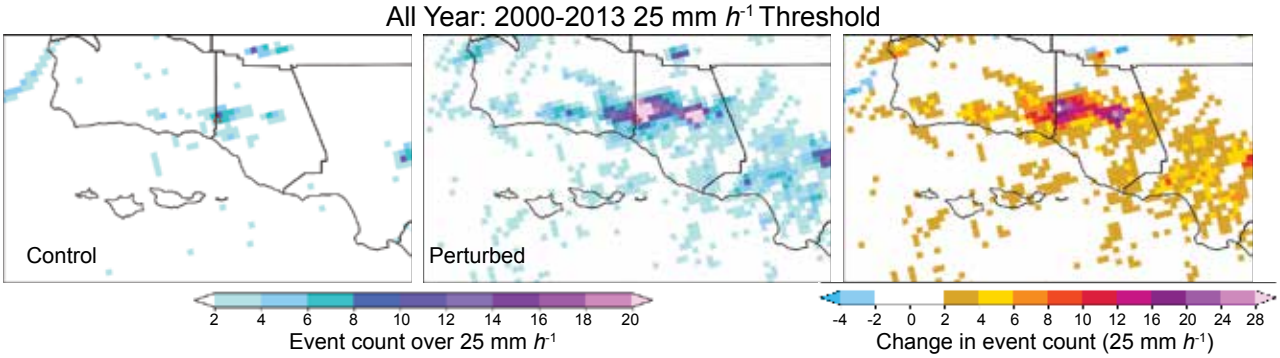

FIGURE 4.14: Number of >25 mm h^{-1} events summed over all months in the 2000–2013 period for a) control simulation and b) perturbed simulation and c) difference between b and a (perturbed minus control).

The greatest increase in instances of hourly precipitation >25 mm h^{-1} in the perturbed scenario occur in the areas of elevated terrain along the Ventura-Santa Barbara County line and in the central part of Ventura County. Increases between 6–20 events are simulated (Fig. 4.14). Although higher terrain lies to the north of this area, much of the moisture is "wrung out" of storms by the mountains to the south, resulting in less opportunity for high precipitation intensities in the more northerly ranges due to this rain-shadowing effect.

The winter season accounts for most of the increase in >25 mm h^{-1} in the perturbed simulation (Fig. 4.15). At lower elevations, an increase of between two to six events are observed in this season, with changes of roughly 8–16 events at higher elevations. During spring (Fig. 4.16), changes are much smaller, on the order of two to eight more events at the high elevations of the region. In the fall, changes are relatively small, between two and six events, and mostly confined to high terrain (Fig. 4.17).

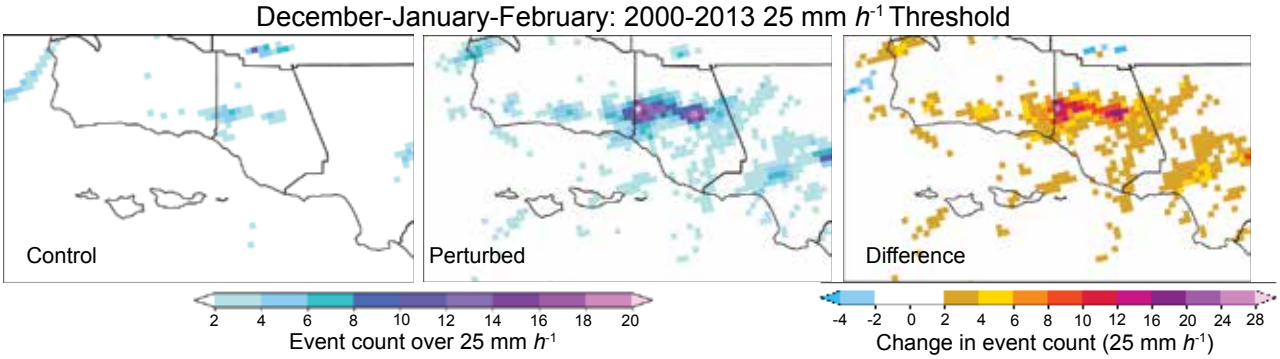

FIGURE 4.15: Number of >25 mm h^{-1} events summed over December–January–February periods in the 2000–2013 period for a) control simulation b) perturbed simulation and c) difference between b and a (perturbed minus control).

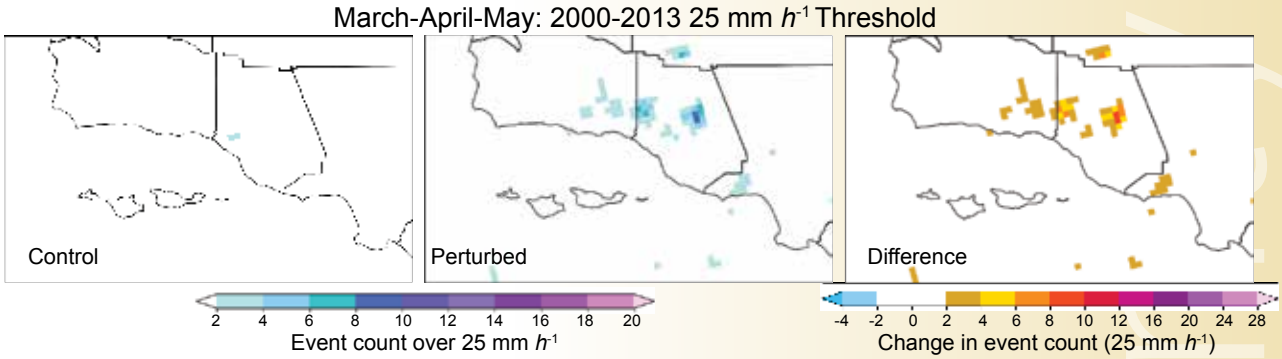

FIGURE 4.16: Number of >25 mm h^{-1} events summed over March–April–May periods in the 2000–2013 period for a) control simulation b) perturbed simulation and c) difference between b and a (perturbed minus control).

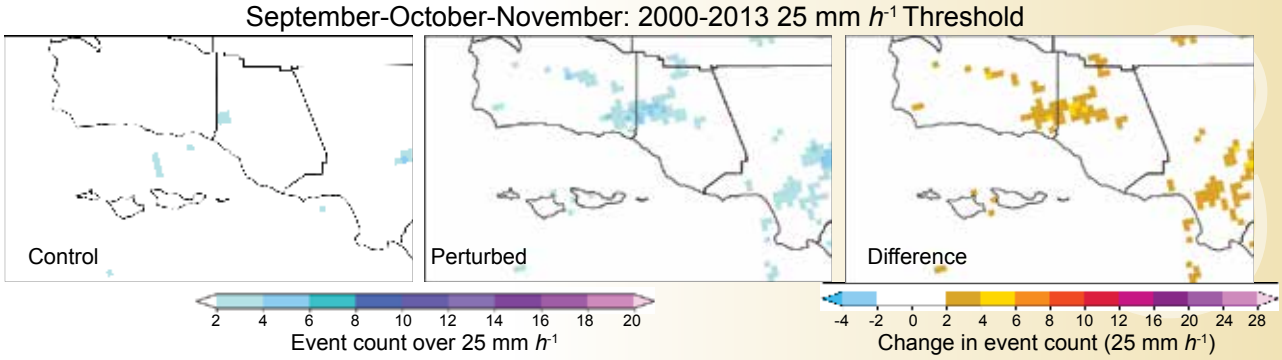

FIGURE 4.17: Number of >25 mm h^{-1} events summed over September–October–November periods in the 2000–2013 period for a) control simulation b) perturbed simulation and c) difference between b and a (perturbed minus control).

JANUARY 7–11 STORM EVENT COMPARISON

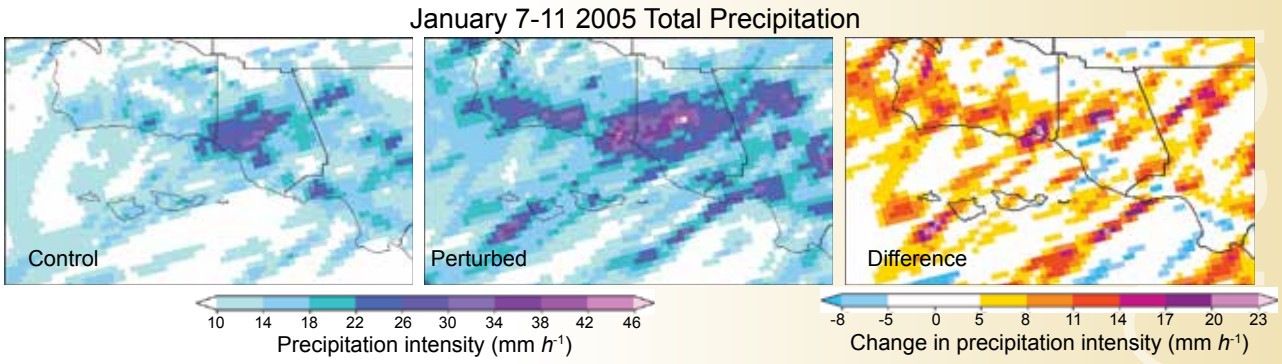

FIGURE 4.18: Total precipitation (sum of hourly model output) for the 5-day period January 7–11 for a) control simulation b) perturbed simulation and c) difference between b and a (perturbed minus control).

The storm event of January 7–11, 2005, caused millions of dollars of flood and storm-related damage in southern California as well as played a role in the deadly La Conchita landslide in western coastal Ventura County. This landslide killed ten people and damaged or destroyed 36 homes (CNRFC 2019; Jibson 2005). The pseudo-global warming experiment allows for the comparison of precipitation characteristics of a storm as it occurred (control simulation) and how it may have changed under a warmer climate (perturbed simulation).

Storm total precipitation increases substantially in the perturbed simulation. Increases of 4-5+ in. (100–125+ mm) in the higher elevations and 13 in. (25–75 mm) in lower elevation areas are observed (Fig. 4.18). The storm featured periods of high intensity rainfall not tied to orographic (terrain) forcing, most notably on January 10th. This supported higher storm totals at lower elevations. The banded features inthe figures may correspond with bands of precipitation within the storm system, though they may also be model noise.

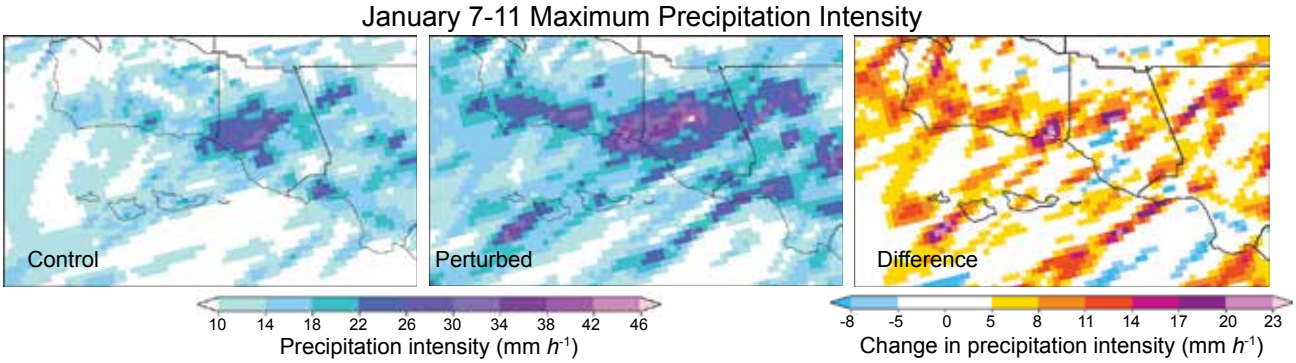

FIGURE 4.19: Maximum hourly precipitation at each grid cell for the 5-day period January 7–11 for a) control simulation b) perturbed simulation and c) difference between b and a (perturbed minus control).

The highest intensities during this storm appear to be associated with a period of intense post-frontal thunderstorms on the morning of January 10, 2005. As post-frontal convection is not necessarily driven by terrain, some of the most extreme intensities occur at lower elevations near the coast between Santa Barbara and Ventura Counties. The areas of highest intensity in the control simulation increase by roughly 10-20 mm h^{-1} in the perturbed simulation (Fig. 4.19).

SECTION 5

Evaporative Demand

5.1 Summary

Evapotranspiration represents the fluxes, or transfer, of moisture from open water and soil moisture (evaporation), and plant transpiration of water to the atmosphere under ambient conditions. Reference evapotranspiration (ET_0) represents a simplified estimation of evapotranspiration from a hypothetical reference crop. It can be considered the thirst of the atmosphere under the assumption of an unlimited supply of surface moisture (Hobbins and Huntington 2017). Simulated future ET_0 suggests consistent increases across the subset of seven CMIP5 models (Fig. 5.1). Because only seven models are used out of the original 32 models and because all models agree on the sign of change, we do not report model agreement of given minimum value, as was done for temperature. The greatest changes occur in inland terrain, particularly in the headwaters of the Santa Clara River (Los Angeles County). The lower quartile of ET_0 changes (Fig. 5.1b) can be interpreted as less severe increases in atmospheric water demand and drought, whereas the upper quartile (Fig. 5.1c) favors more rapid depletions of surface moisture and severe drought potential. In terms of total change, the projected increases in ET_0 are most pronounced during the spring season, followed by summer and then fall, with modest changes during winter (Fig. 5.2). The fall season demonstrates the largest percentage increases in ET_0 over the largest area while the greatest percentage increases during spring and summer occur in the Topa Mountains (Fig. 5.3).

ET_0 can be moderated by the presence or absence of marine stratus (coastal fog; Fischer et al. 2009). GCMs and the LOCA downscaling process do not accurately represent marine stratus, introducing uncertainty in projections of ET_0. Thus, results presented here for the summer season (during which marine stratus is most prevalent) and possibly other seasons are potentially biased low. Changes may be greater if a continued decrease in marine stratus is realized in the future. Marine stratus in a changing climate is discussed in more detail in Section 6.3.

5.2 Implications of Changes in ET_0

Historically, positive changes in ET_0 have been associated with increased water demand (Hobbins and Huntington 2017), increased wildfire activity (Abatzoglou and Williams 2016), and ecosystem impacts (Schwinning and Sala 2004). Thus, with projected ET_0 increases, the following impacts may be anticipated:

- All seven models project county-wide increases in annual ET_0, with minimum increases of at least 2 in. and maximum increases of approximately 6.5 in, which may impact water demand for crops (Hall et al. 2018), ecosystems, and municipal water use.
- The greater thirst of the atmosphere will deplete soil and plant moisture leading to faster rates of fuel moisture decline and longer periods of dry vegetation. This will increase the susceptibility of landscapes to wildfire and drought, as there is the potential for vegetation to dry more quickly and for longer periods of time.

- Reductions in soil moisture associated with increased ET_0 may reduce runoff production in some areas. The greatest increases in ET_0 (and thus reductions in soil moisture) are projected to occur in inland elevated terrain.
- Greater ET_0 over open water will hasten the drying of ephemeral and perennial landscapes with open water (e.g., marshes, wetlands) or more moist soils (e.g., riparian areas) through direct evaporation. This will occur in conjunction with faster drying of vegetation via enhanced evapotranspiration and the loss of water from wetlands into adjacent drier soils. The combination of these factors may have negative impacts on some ecosystems.

5.3 ET_0 Analyses

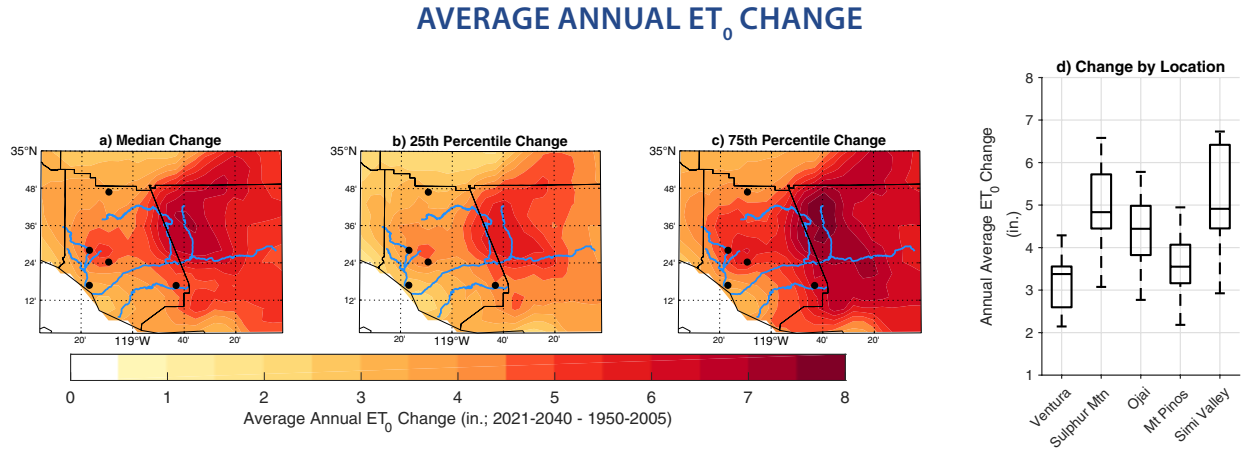

FIGURE 5.1: Change in average annual reference evapotranspiration (ET_0), 2021–2040 mean minus 1950–2005 mean for the a) median change in ET_0; b) 25th percentile (bottom quartile) change in ET_0; c) 75th percentile (upper quartile) change in ET_0; d) Spread in change of average annual ET_0 for five selected locations within Ventura County (black dots on map).

The greatest projected increases in ET_0 occur in the inland regions, especially the headwaters of the Santa Clara River in Los Angeles County (Fig. 5.1a-c). This is consistent with the region of greatest temperature increases shown in Section 3. In Ventura County the inland regions such as Ojai, Sulphur Mountain and Simi Valley are projected to experience the greatest increases with lower changes in the highest terrain and immediately along the coast (Fig. 5.1d).

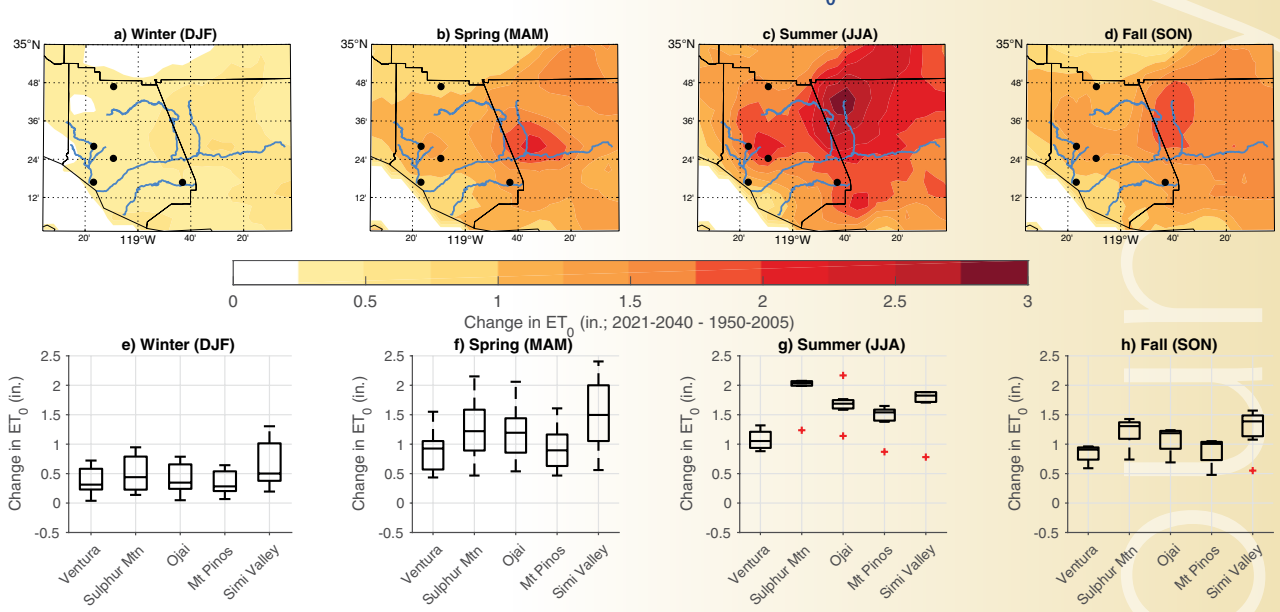

FIGURE 5.2: Change in seasonal average reference evapotranspiration (ET_0), 2021–2040 minus 1950–2005 for winter (a), spring (b), summer (c) and fall (d). Spread in change in seasonal ET_0 across all seven CMIP5 models for five selected locations within Ventura County (black dots on map) for winter (e), spring (f), summer (g) and fall (h).

Seasonally, winter (the season with the climatologically lowest ET_0 rates) is projected to have the smallest increases in ET_0 (Fig. 5.2a) with changes on the order of less than 1 in. Exceptions occur along the eastern margin of Ventura County. In Simi Valley (Fig. 5.2e) and the headwaters of the Santa Clara River (Fig. 5.2a), ET_0 increases exceed 1 in. The greatest increases in ET_0 are projected to occur during summer (Fig. 5.2c,g) with increases between 1–2 in. Increases in ET_0 during spring (Fig. 5.2b) are of slightly greater magnitude (>0.5 in.) compared to fall (Fig. 5.2d), however the model spread is much larger for the spring season (ranging from 0.5 to over 2 in.; Fig. 5.2f) as compared to fall (Fig. 5.2h). It should be noted that the whiskers of the spring ET_0 projections exceed 1.5 times the upper limit of the interquartile range for summer, with the exception of one outlier model (Fig. 5.2g). This implies that there is a chance that the greatest absolute increases in ET_0 will occur during spring.

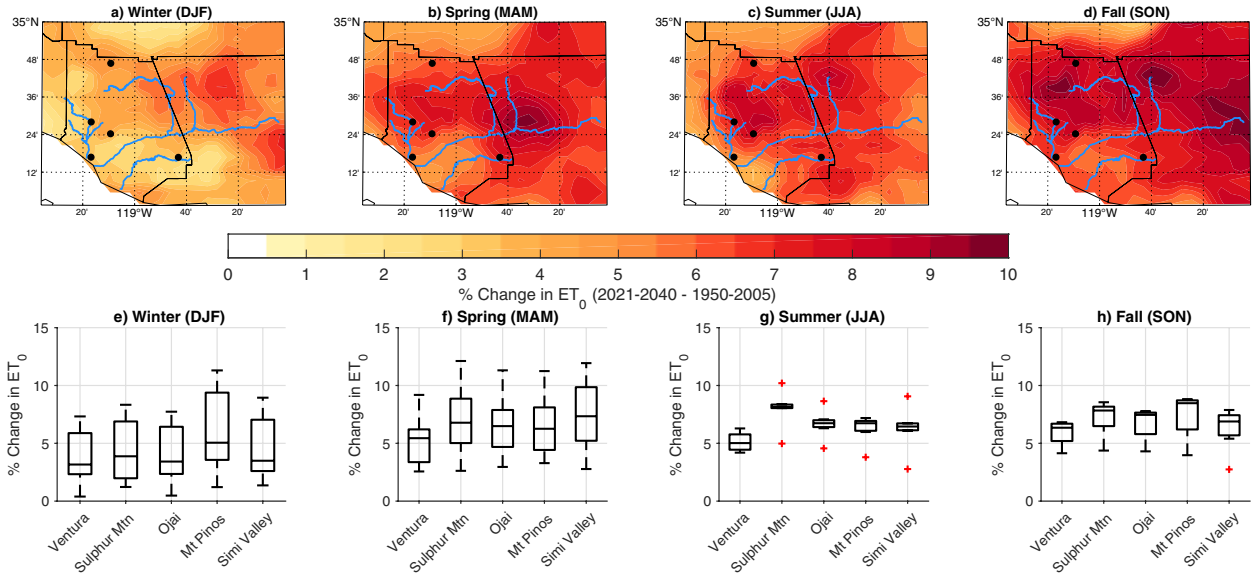

FIGURE 5.3: Percentage change in seasonal average reference evapotranspiration (ET_0), 2021–2040 minus 1950–2005 for winter (a), spring (b), summer (c) and fall (d). Spread in percentage change in seasonal ET_0 across all seven 32 CMIP5 models for five selected locations within Ventura County (black dots on map) for winter (e), spring (f), summer (g) and fall (h).

Although the greatest changes in absolute ET_0 occur during summer (Fig. 5.2c), percentage-wise, the largest increases (between 4–8%) are observed during fall in terms of spatial extent and magnitude (Fig. 5.3d). This will add stress to vegetation, decrease fuel moisture, and increase fire risk. Dry conditions extending into the late fall and early winter have a greater chance to coincide with Santa Ana winds. These conditions can lead to destructive wildfires such as the December 2017 Thomas Fire (Nauslar et al. 2018) and the November 2018 Woolsey Fire. Spring and summer show similar magnitudes of change and are consistent in the locations of change, though the core regions of greatest percentage increases shift westward from the Santa Clara River watershed (Fig. 5.3b) to the Ventura River watershed (Fig. 5.3c) during summer. The spring season shows the greatest model spread and increase in ET_0, with the highest projections indicating more than 10% increase (Fig. 5.3f). The winter season also exhibits large model spread, with a greater interquartile range than spring. Winter projections suggest ET_0 changes may increase by less than 2% or exceed 8% (Fig. 5.3a). Summer projections demonstrate the least model spread (Fig. 5.3g) followed by fall (Fig. 5.3h).

SECTION 6

Other Considerations

6.1 Atmospheric Rivers

A large fraction of southern California's annual precipitation is tied to atmospheric rivers (ARs; Rutz et al. 2014). Though ARs are not explicitly analyzed in this report, this brief statement describes current knowledge on this topic.

Climate model projections evaluated by Dettinger (2011) indicate that the average number of ARs impacting California each year is not projected to change substantially from the historic period. However, there is an increase in individual years with more ARs later in the mid-to-late 21st Century. Five of seven models evaluated in this study also showed an increase in AR days in both the winter and spring seasons. More recent work by Espinoza et al. (2018) demonstrates that, following the RCP 8.5 pathway, the number of time steps with AR conditions along the California Coast (31-41°N) increases from 7% (for 1979–2002) to 10% (for 2073–2096). This represents a 43% increase. Espinoza et al. (2018) also demonstrate an intensification of ARs with integrated vapor transport (IVT; a measure of how much moisture is being transported by the winds in a vertical column of the atmosphere) increasing by 30%. While there is spread across models in this study with respect to IVT and frequency changes, models agree on an increase in these variables for California. The Los Angeles chapter of the California 4th Climate Change Assessment (Hall et al. 2018, and references therein) suggests a nearly 40% increase in precipitation from ARs by the late 21st century following RCP 8.5. This is consistent with evidence for precipitation intensification provided in this report (Section 4).

6.2 Sierra Nevada Snowpack Changes

A study by the University of California, Los Angeles suggests a 64% decrease in Sierra Nevada April 1 snow water equivalent (SWE) by the end of the 21st Century as compared to the 1981–2000 baseline following the RCP 8.5 scenario (Fig. 6.1; Reich et al. 2018). The study also indicates earlier snowmelt runoff in the spring season associated with increased temperatures (Reich et al. 2018). Ventura County depends, at least partially, on water from the State Water Project (SWP), whose resources are derived mainly from the Sierra snowpack. The reduction in snowpack and earlier snowmelt are likely to impact the availability of SWP. For example, the California Department of Water Resources projects a slight decrease in Article 21 water availability in the 2025 "Early Long Term" scenario as compared to 2015 (California Department of Water Resources 2015).

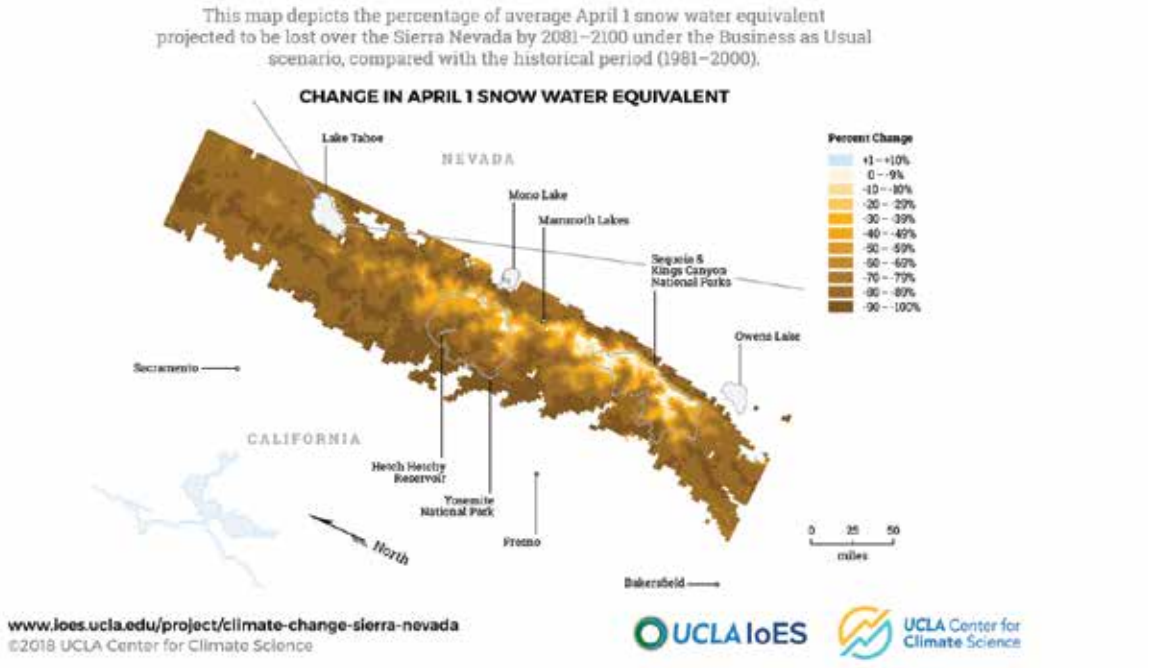

FIGURE 6.1: Business-as-usual snowpack, 2081–2100. This map depicts the percentage of April 1 snow water equivalent projected to be lost over the Sierra Nevada by 2081–2100 under the RCP 8.5 (business-as-usual) scenario compared with the historical period 1981–2000. Source: Reich et al. (2018).

6.3 Marine Stratus (Coastal Fog)

Low elevation marine stratus and stratocumulus (often referred to as coastal fog) is prevalent along the California Coast throughout the year. Marine stratus peaks in summer months. It plays an important role in moderating coastal temperatures (Iacobellis and Cayan 2013; Hall et al. 2018) and provides water resources for ecological function in coastal ecosystems (Fischer et al. 2016). Marine stratus lowers atmospheric evaporative demand, which can reduce drought stress for some species by 22–40% along the coast (Fischer et al. 2009) as well as influences irrigation demand for crops (Baguskas et al. 2018). Marine stratus has also been demonstrated to moderate coastal heat waves in southern California (Gershunov et al. 2011; Clemesha et al. 2016).

Marine stratus has been in decline over southern California over the observed historic record (Williams et al. 2015a). There is some evidence of reduction in marine stratus in Global Climate Models, though large uncertainty remains in these projections (Klein et al. 2017; Hall et al. 2018). Global and regional climate models have difficulty simulating coastal fog, onshore advection of the marine boundary layer, and offshore flow moving dry and warm inland air to coastal areas. This is due to the complex interplay between the atmosphere, ocean, and terrestrial systems that are subject to appreciable variability over broad scales of time and space (Torregrosa et al. 2014). Because the global climate models and the LOCA downscaling approach cannot account for dynamical changes influencing fog formation such as advection of the marine layer, sea surface temperature gradients, and microphysical processes important to fog formation, model projections may underestimate future temperature changes in

coastal areas. The uncertainty associated specifically with marine stratus and onshore/offshore flow cannot be quantified within the scope of this analysis, thus the reader should consider that the range of temperature projections presented herein (Section 3) likely represent a minimum estimate; large declines in marine stratus in a future climate may lead to greater changes. The same limitation applies to estimates of evaporative demand along the coast (Section 5) as evaporative demand depends on incident solar radiation, temperature, relative humidity, and wind. All of these factors are influenced by the presence or absence of marine stratus.

6.4 Drought

The negative impacts of drought on human society and ecosystems spans time scales ranging from weeks to years. Drought can be considered as insufficient water to meet ones' needs. Yet these needs likely vary dramatically in time and space, as a river basin is different from a backyard garden. Fundamentally, drought is an extended imbalance between the supply and demand of water, in favor of demand and relative to the long-term average conditions for the time period of interest (Hobbins et al. 2016). There are three classic measures of drought that represent the deficits in moisture stocks and flows at varying time scales. These include: precipitation in meteorological drought; streamflow or runoff and surface water storage depletion in hydrologic drought, and evapotranspiration and soil moisture in agricultural drought (Hobbins et al. 2016). While drought is often conceived through a deficit in precipitation resulting from lack of storminess, a surplus in atmospheric evaporative demand (or potential evaporation) can also contribute to drought conditions. Increases in atmospheric evaporative demand result from increases in temperature, wind, and radiation, and/or decreases in relative humidity (Allen et al. 2005). Depending on the atmospheric conditions, all of these factors can occur in tandem or can offset one another.

By virtue of its Mediterranean climate and location along the periphery of the Pacific subtropical high, California experiences warm and dry summers with wet winters. During the wet winter months, which in Southern California typically begin in November and terminate in March, the bulk of precipitation arrives in a few, large storms (Dettinger et al. 2011; Oakley et al. 2018b). Should these storms not arrive due to the presence of a persistent blocking ridge of high pressure in the North Pacific Ocean, precipitation deficits will be large (Cook et al. 2018). These deficits will be superimposed with climatologically high evaporative demands and may be exacerbated by above-normal winter season temperatures. Such dry years occur commonly in California, and multi-year periods of severe drought are not uncommon. However, evidence from various locations in California and throughout the southwestern United States indicates that extreme droughts lasting decades to several centuries have occurred numerous times since the end of the last ice age (e.g., Stine 1994; Benson et al. 2002; Woodhouse et al. 2010; Dingemans et al. 2014). The most recent extreme and persistent droughts occurred during the Medieval period, approximately 800-1000 years ago, with locally warm and dry conditions inferred from paleoproxy evidence provided by sedimentary cores taken from Zaca Lake in the San Rafael Mountains of Santa Barbara County (Dingemans et al. 2014). These droughts indicate that such extreme periods of aridity can occur under natural conditions (i.e., independent of human-driven changes in greenhouse gas concentrations) implying consideration of extended drought is prudent to sustainable water resource management, especially if projected warming increases drought risk (Cook et

al. 2015; Hatchett et al. 2015). Modeling studies of the Central Sierra Nevada have shown these droughts to be of comparable precipitation deficits to the most recent California Statewide drought that began in winter 2012 and ended in January of 2017 (Hatchett et al. 2015). The severity of the recent drought was exacerbated by anomalously warm temperatures driving a surplus in atmospheric evaporative demand and reducing the fraction of precipitation falling as snow in mountain regions (Williams et al. 2015b; Hatchett et al. 2017). The duration and severity of the recent drought varied statewide, with Ventura County being one of the first regions to go into drought conditions and one of the last to emerge (U.S. Drought Monitor 2019).

California has long experienced drought conditions (Stine 1994; MacDonald 2007, Woodhouse et al. 2010). As a result of changing atmospheric composition and land surface conditions, loss of sea ice, and the resultant changes in atmospheric and oceanic circulations, climate models project increased temperatures, more frequent dry days, and greater chances of persistent mid-winter high pressure suppressing storminess for California (Polade et al. 2015, 2017; Cvijanovic et al. 2017). Anthropogenic warming, and the circulation changes it induces, will increase the probability that low precipitation years will coincide with above-average temperature years (Diffenbaugh et al. 2015; Cook et al. 2015). This elevates drought risk via both decreased supply of moisture and an increased atmospheric demand for moisture. Water availability may decline through changes in rainfall-runoff generation processes; as soil moisture declines due to greater evaporation from bare soil and increased plant evapotranspiration, more precipitation will be required to generate the same volume of runoff. GCMs project significantly drier soils in the future over the Southwest (including California), with more than an 80% chance of a multidecadal drought during 2050–2099 under RCP 8.5 ("business as usual" climate change scenario; Cook et al. 2015).

The specific types of drought, their magnitude and duration, and the hydroclimatic patterns that end drought in Ventura County will require additional research that integrates modeling approaches to evaluate water availability changes on both the supply and demand sides as well as examines the dynamical circulation mechanisms. Based upon the analysis provided in this document, clear evidence for increases in drought severity is provided, but evidence for occasional wet years is also demonstrated. Because precipitation remains variable, some years will be less drought prone than others due to more frequent and possibly stronger storms. Yet the ubiquitous projected increases in evaporative demand imply that more water will be lost to the atmosphere and the increases in projected dry days provides additional opportunities for evaporative losses.

6.5: Wildfire

Wildfire is a common feature on the Southern California landscape. For the period 1959–2009, 130,000 acres burned per year on average, though there has been considerable inter-annual variability in the number and size of wildfires each year over the observed record (Jin et al. 2014). Historically, Southern California shrublands are "ignition limited". This means that in most years, the dry summer and autumn climates are conducive to significant fire events; an ignition is the limiting factor to wildfire activity (Keeley and Syphard 2017). As this area rarely experiences lightning, human activity is the main driver of ignitions (Balch et al. 2017). This ignition-limited system is likely to persist in the future, though climate and anthropogenic factors will affect the size, frequency, and behavior of wildfires.

For Mediterranean regions of central and southern California, no significant trend in large wildfires is observed from 1984–2011 (Dennison et al. 2014). Similarly, there is no discernible trend in area burned in the South Coast region of California from 1920–2010 on USFS or CalFire protected lands (Keeley and Syphard 2017). Climate projections suggest Santa Ana wind activity will decrease in the spring and fall seasons, with Santa Ana wind events becoming more focused in the November–December–January period (Guzman-Morales and Gershunov 2019). As Santa Ana and Sundowner winds often drive large and destructive wildfires in Southern California (e.g., Hatchett et al. 2018; Nauslar et al. 2018), these changes will play into the complexities of understanding future fire activity. Projections from wildfire models suggest an increase in the number of wildfires and area burned by the mid 21st century following RCP 8.5 (Jin et al. 2015; Westerling et al. 2018). However, there is currently high uncertainty in wildfire models and further research is needed (Hall et al. 2018). Given this uncertainty, some of the factors contributing to changes in wildfire characteristics are presented below.

WILDFIRE FREQUENCY: Model projections presented here indicate an increased number of dry days in the spring and fall (Fig. 4.6) as well as increased evapotranspiration, with the greatest changes in the spring, summer, and fall (Fig. 5.3). While changes are relatively small for the 2021–2040 period examined, they are more pronounced in mid-century analyses (Appendix A) and noted in other studies (Pierce et al. 2013; Swain et al. 2018). The drying of spring and fall, either in total precipitation, number of dry days, or increased evapotranspiration, suggests a lengthening of the period each year during which the area is susceptible to wildfires due to drier conditions.

Another factor contributing to wildfire frequency is the conversion from chaparral to grasslands on Southern California landscapes. This transition is caused by urban sprawl that removes and fragments chaparral ecosystems, as well as increased fire frequency associated with grasslands that out-compete chaparral, which is not accustomed to such return frequencies. These newly established grasslands dry out quickly, are very flammable, and are susceptible to fire for a longer duration of the year than chaparral (Syphard et al. 2018). This longer fire season and more flammable fuels, combined with population increase, especially in the wildland-urban interface (Radeloff et al. 2018; Syphard et al. 2018), and greater public access to wildlands increases the likelihood of wildfire ignitions.

WILDFIRE SIZE: Increased evapotranspiration (Fig. 5.1) contributes to the drying of fuels. Fuel moisture influences the intensity at which fires burn and fire behavior. Firefighters often gain ground on wildfires at night when temperatures decrease, allowing relative humidity to increase. With rising minimum temperatures (typically overnight lows; Fig. 3.2), there is potential for lack of nighttime recovery of relative humidity (assuming constant atmospheric moisture). This may make fires more difficult to suppress in a future climate and potentially contribute to larger and more destructive wildfires. However, fire size is extremely hard to predict as it depends on a number of factors, including when and where a fire starts and the weather conditions present during and following ignition.

SECTION 7

Limitations and Future Work

7.1 Challenges and Limitations

The CMIP5 suite of Global Climate Models (GCMs) performs simulations at a spatial scale that is too coarse for climate change impact studies (Wilby and Wigley 1997). As a result, they do not accurately represent fine-scale processes (such as convection in the atmosphere) important to the overall atmospheric circulation and localized outcomes. To make coarse GCM data useful at a local scale, the process of downscaling must be done to bring the data to a finer resolution. The LOCA dataset used in this work is a statistical downscaling approach using historic analogs derived from weather stations (Pierce et al. 2014). The LOCA method is computationally efficient, but does not account for dynamic processes at small scales in the atmosphere. To address these fine-scale processes, the best approach is to dynamically downscale GCMs using a mesoscale atmospheric model or a variable resolution Earth system model. However, this process is very computationally intensive and not a reasonable approach within the scope of this work. This process may be more viable as high-performance computing becomes cheaper and more accessible.

Due to these limitations, there is uncertainty in the output from both the GCMs and the downscaled LOCA product, especially for the precipitation projections. The range of possible outcomes should be considered. To help demonstrate uncertainty and potential outcomes, box plots illustrate the model spread for five locations within Ventura County for each analysis. Additionally, depending on the variable, different thresholds are examined, such as model median, minimum change agreed upon by 75% of models, top 90th and bottom 10th percentile change. This helps to demonstrate the variability across model projections. Despite these limitations, this is currently the most appropriate dataset available for the task of climate change adaptation planning. As additional climate model projection output becomes available, it is recommended to incorporate this information into ongoing studies and planning efforts.

While we focus on 2021–2040 in this analysis, it is important to note that some commonly discussed changes in climate conditions may not emerge until mid-21st Century (Appendix A) or later. For example, for the 2021–2040 period, the median across LOCA data for 32 CMIP5 models indicates a slight increase in winter season precipitation (0.25 to 1.5 in. across the county, Fig. 4.2). In all other seasons, little to no change is projected, with median changes ranging from -0.5 in to +0.25 in. However, in the mid-21st Century (2041–2070; Appendix A, Fig. A.16), analyses demonstrate a greater decrease in precipitation in the spring (-0.25 to -1.5 in.) and fall (-0.25 to 0.5 in.) seasons. This change is in agreement with other studies that arrive at a similar conclusion of spring and fall drying using different datasets for the mid-to-late 21st Century (Pierce et al. 2013; Swain et al. 2018), which helps to build confidence in this projected change.

7.2 Future Work

This report covers a broad range of climate model projections and potential impacts for Ventura County and surrounding areas. There are several topics of interest to stakeholders that could not be adequately addressed in a robust manner within the scope of this project (e.g., sea level rise). Generally, the data and methods exist to address these topics; investments will be needed to support additional research and analysis. These topics were identified at two stakeholder meetings organized by the Watersheds Council of Ventura County in the fall of 2018 and spring of 2019:

- **Storm sequencing:** The sequencing of storms and length of dry periods between precipitation events is important to water resource and flood management. Future work can investigate changes in storm sequencing to determine if large storms in close succession become more or less likely in a changing climate. Criteria will need to be developed for what constitutes "consecutive" storms, the sensitivity of watersheds to spacing of dry days between storms, and what precipitation total or duration denotes a storm of interest. Approaching the question of storm sequencing in a reasonable manner will require a combination of atmospheric model output and hydrologic modeling.
- **Drought characteristics:** There is great interest in the changes in both drought frequency and duration in Ventura County. Drought definition varies by application (e.g., agricultural, hydrologic, ecologic, or meteorological drought) thus it is difficult to provide a "one-size-fits-all" metric for drought changes in a future climate. Future work can investigate various types of drought to quantify their changes in a warming climate in Ventura County.
- **Wildfire size, intensity, and frequency:** Modeling wildfire characteristics in a future climate remains challenging and current methods have large uncertainties (Hall et al. 2018). Human activities play a large part in driving wildfire in Southern California, contributing to the uncertainty. Because the topic is of great interest to numerous stakeholders and to the landscapes themselves, it should be prioritized for additional research.
- **Surface/Groundwater changes:** A calibrated, coupled surface and groundwater model would provide insight to changes in runoff and recharge in the watersheds providing water resources for Ventura County. Modeling using sub-monthly timescales may be useful for understanding responses to increasing precipitation intensities, evaluating potential mitigation strategies and the effectiveness of expanded managed aquifer recharge efforts. Such work could also identify what changes in temperature, precipitation, evaporative demand, or other climate variables are required to have notable impacts on the hydrology of Ventura County.
- **Changes in the availability of Article 21 water resources:** In some years, additional water may be available for purchase by State Water Project contractors, referred to as "Article 21" water. These resources are typically available in wetter-than-average years and may be related to the amount of water contained in the snowpack as well as the timing of spring snowmelt runoff.
- **Impacts of temperature on water quality:** Warming temperatures can have impacts on water quality for drinking water sources such as Lake Casitas. In preparation of this report, no air temperature thresholds or patterns were noted that determine reduced mixing or water quality impacts for the lake. Research can be done to determine air temperature thresholds or patterns that impact water quality in lakes and other surface waters in the area. Changes in these characteristics can then be examined in climate model projections.

- **Temperature and precipitation impacts on southern steelhead:** An inventory currently suitable habitat for southern steelhead and identification of the impacts of projected temperature change on available habitat could be performed. The role of projected precipitation intensification and changes in wildfire frequency in reduction of suitable habitat should also be determined.
- **Temperature and precipitation impacts on agriculture and native plant species:** Precipitation and temperature thresholds pertinent to native plants and agriculture (whether in the existing body of research or acquired through new research) can be examined in climate projections. This can aid in the determination of which plants to use in restoration projects that will be resilient to the changing climate and what crops might be most viable.
- **Overlay projected climate changes with crop, vegetation, or habitat type:** Precipitation, temperature, or evapotranspiration could be overlain on maps of a specific crop, vegetation, or habitat type. This could aid in determining the spatial extent to which the particular topic of interest is impacted by climate change. However, the 6 km scale of LOCA is likely too coarse to yield meaningful results, and additional downscaling techniques would need to be utilized as well as climate envelope modeling.
- **Assessment of model skill:** A model is deemed skillful if it produces better results than a simpler alternative. There is interest in understanding at the local level of how well climate model projections have performed compared to observations, for the time period during which there is overlap. Have projected trends been captured in observations?
- **Outreach and education:** Education on climate change and its potential impacts to the community and resources can empower people to be informed voters and to participate in the decision making process. Some recommendations for outreach and engagement are described in Hall et al. (2018).

SECTION 8

Concluding Remarks

Analyses presented herein for the 2021–2040 period demonstrate increases in both maximum and minimum temperatures and heat extremes, more intense precipitation focused during the winter season, and increased evapotranspiration. Increased drought risk, potential for a longer wildfire season with more ignitions as population growth continues, reduced marine stratus, reduction in Sierra Nevada snowpack, and longer duration and more intense atmospheric rivers are also noted as concerns for the region. This report covers the 2021–2040 period, thus some climate projections commonly discussed in the popular media and associated with mid-to-late century change may not be represented here (e.g., see Section 4.1). There is generally an intensification/augmentation/increase in magnitude of changes across all variables in the mid-to-late century (see Appendix A).

This report addresses some of the wide range of impacts potentially associated with changes in temperature (Section 3.2), precipitation (Section 4.2), evaporative demand (Section 5.2) and other variables (Section 6). The findings of this report may be used for the prioritization of adaptation strategies aimed at addressing vulnerabilities related to climate in order to support the Integrated Regional Water Management planning process. This will ultimately improve the resiliency of Ventura County to future weather and climate extremes.

SECTION 9

References

Abatzoglou, J. T., & Williams, A. P. (2016). Impact of anthropogenic climate change on wildfire across western US forests. *Proceedings of the National Academy of Sciences*, *113*(42), 11770-11775. doi: 10.1073/pnas.1607171113

Allen, R. G., Walter, I. A., Elliott, R., Howell, T., Itenfisu, D., & Jensen, M. (Eds.). (2005). The ASCE standardized reference evapotranspiration equation. Reston, VA: American Society of Civil Engineers.

Baguskas, S. A., Clemesha, R. E., & Loik, M. E. (2018). Coastal low cloudiness and fog enhance crop water use efficiency in a California agricultural system. *Agricultural and Forest Meteorology*, *252*, 109-120. doi: 10.1016/j.agrformet.2018.01.015

Balch, J. K., Bradley, B. A., Abatzoglou, J. T., Nagy, R. C., Fusco, E. J., & Mahood, A. L. (2017). Human-started wildfires expand the fire niche across the United States. *Proceedings of the National Academy of Sciences*, *114*(11), 2946-2951. doi: 10.1073/pnas.1617394114

Behl, R. J. and Kennet, J. P. (1996). Brief interstadial events in the Santa Barbara Basin, NE Pacific, during the past 60 kyr. *Nature*, 379, 243-246.

Benson, L., Kashgarian, M., Rye, R., Lund, S., Paillet, F., Smoot, J., . . . Lindström, S. (2002). Holocene multidecadal and multicentennial droughts affecting Northern California and Nevada. *Quaternary Science Reviews*, *21*(4-6), 659-682. doi: 10.1016/S0277-3791(01)00048-8

California Department of Water Resources (2015). Delivery capability report and studies 2015. Retrieved from https://water.ca.gov/Library/Modeling-and-Analysis/Central-Valley-models-and-tools/CalSim-2/DCR2015

California-Nevada River Forecast Center (CNRFC), National Oceanic and Atmospheric Administration (n.d.). Heavy precipitation event, Southern California, January 7-11, 2005. Retrieved from: https://www.cnrfc.noaa.gov/storm_summaries/jan2005storms.php

Cal/OSHA. (n.d.) Heat Illness Prevention. California Code of Regulations, Subchapter 7, Group 2, Article 10, §3395. Retrieved from: https://www.dir.ca.gov/title8/3395.html

Cannon, S. H., Gartner, J. E., Wilson, R. C., Bowers, J. C., & Laber, J. L. (2008). Storm rainfall conditions for floods and debris flows from recently burned areas in southwestern Colorado and southern California. *Geomorphology*, *96*(3-4), 250-269.

Campbell, R. H. (1975). Soil slips, debris flows, and rainstorms in the Santa Monica Mountains and vicinity, southern California (U.S. Geological Survey Professional Paper 851). Washington, DC: U.S. Government Printing Office. Retrieved from https://pubs.usgs.gov/pp/0851/report.pdf.

CAL FIRE (2012). Ventura County FHSZ map 2007. Retrieved from http://www.fire.ca.gov/fire_prevention/fhsz_maps_ventura

Cook, B. I., Ault, T. R., & Smerdon, J. E. (2015). Unprecedented 21st century drought risk in the American Southwest and Central Plains. *Science Advances*, *1*(1), e1400082. doi: 10.1126/sciadv.1400082

Cook, B. I., Williams, A. P., Mankin, J. S., Seager, R., Smerdon, J. E., & Singh, D. (2018). Revisiting the leading drivers of Pacific coastal drought variability in the contiguous United States. *J. Climate, 31*, 25-43. doi: 10.1175/JCLI-D-17-0172.1

California Geological Survey. (2018). Landslides. Retrieved from https://www.conservation.ca.gov/cgs/geohazards/landslides

Clemesha, R. E., Gershunov, A., Iacobellis, S. F., Williams, A. P. and Cayan, D. R. (2016). The northward march of summer low cloudiness along the California coast. *Geophysical Research Letters*, *43*(3), 1287-1295. doi: 10.1002/2015GL067081

Cvijanovic, I., Santer, B. D., Bonfils, C., Lucas, D. D., Chiang, J. C. H., & Zimmerman, S. (2017). Future loss of Arctic sea-ice cover could drive a substantial decrease in California's rainfall. *Nature Communications*, *8*, 1947. doi: 10.1038/s41467-017-01907-4

Dennison, P. E., Brewer, S. C., Arnold, J. D., & Moritz, M. A. (2014). Large wildfire trends in the western United States, 1984-2011. *Geophysical Research Letters 41*(8): 2928-2933. doi: 10.1002/2014GL059576

Dettinger, M. (2011). Climate change, atmospheric rivers, and floods in California–A multimodel analysis of storm frequency and magnitude changes. *JAWRA Journal of the American Water Resources Association 47*(3), 514-523. doi: 10.1111/j.1752-1688.2011.00546.x

Dettinger, M. and Cayan, D.R. (2014). Drought and the California delta—A matter of extremes. San Francisco Estuary and Watershed Science, *12*(2). doi: http://escholarship.org/ojs/index.php/jmie_sfews/editor/viewMetadata/dx.doi.org/10.15447/sfews.2014v12iss2art4

Dettinger, M. D., & Earman, S. (2007). Western ground water and climate change - Pivotal to supply sustainability or vulnerable in its own right?: Ground Water News and Views, *Association of Ground Water Scientists and Engineers Newsletter*, *4*(1), 4-5. Retrieved from: http://tenaya.ucsd.edu/%7edettinge/agwse07.pdf

Dettinger, M. D., Ralph, F. M., Das, T., Neiman, P. J., & Cayan, D. R. (2011). Atmospheric rivers, floods and the water resources of California. *Water*, *3*(2), 445-478. Retrieved from: https://www.mdpi.com/2073-4441/3/2/445/htm

Diffenbaugh, N. S., Swain, D. L., & Touma, D. (2015). Anthropogenic warming has increased drought risk in California. *Proceedings of the National Academy of Sciences*, *112*(13), 3931-3936. doi: 10.1073/pnas.1422385112

Dingemans, T., Mensing, S. A., Feakins, S. J., Kirby, M. E., & Zimmerman, S. R. (2014). 3000 years of environmental change at Zaca Lake, California, USA. *Frontiers in Ecology and Evolution*, *2*, 34. doi: 10.3389/fevo.2014.00034

Espinoza, V., Waliser, D. E., Guan, B., Lavers, D. A., & Ralph, F. M. (2018). Global analysis of climate change projection effects on atmospheric rivers. *Geophysical Research Letters*, *45*(9), 4299-4308. doi: 10.1029/2017GL076968

Farm Bureau of Ventura County. (2016). Frequently asked questions about Ventura County agriculture. Retrieved from http://www.farmbureauvc.com/new/assets/pdf-forms/Farm%20Bureau%20VC%20Crop%20Data%20FAQs.pdf

Fischer, D. T., Still, C. J., & Williams, A. P. (2009). Significance of summer fog and overcast for drought stress and ecological functioning of coastal California endemic plant species. *Journal of Biogeography*, *36*(4), 783-799. doi: 10.1111/j.1365-2699.2008.02025.x

Fischer, D. T., Still, C. J., Ebert, C. M., Baguskas, S. A., and Williams, A. P. (2016). Fog drip maintains dry season ecological function in a California coastal pine forest. *Ecosphere 7*(6): e01364. doi: 10.1002/ecs2.1364

Gershunov, A., et al. (2011). The California heat wave 2006 with impacts on statewide medical emergency: A space-time analysis. *Geogr. Res. Forum, 31*, 6-31.

Greene, H.G., Murai, L.Y., Watts, P., Maher, N.A., Fisher, M.A., Paull, C.E. and Eichhubl, P. (2006). Submarine landslides in the Santa Barbara Channel as potential tsunami sources. *Natural Hazards and Earth System Science*, *6*(1), pp. 63-88.

Gruntfest, E. and Taft, V. (1992). What we can learn from the February 1992 Floods in Ventura County, California. Retrieved from https://hazards.colorado.edu/uploads/basicpage/QR50.pdf

Guzman-Morales, J., and Gershunov, A. (2019). Climate change suppresses Santa Ana winds of Southern California and sharpens their seasonality. *Geophysical Research Letters*, 46, 2772-2780. https://doi.org/10.1029/2018GL080261

Hall, A., Berg, N., Reich, K. (2018). California's Fourth Climate Change Assessment, Los Angeles Summary Report (Report No. SUM-CCCA4-2018-007). Sacramento: State of California. Retrieved fromhttp://climateassessment.ca.gov/regions/docs/20180928-LosAngeles.pdf

Hatchett, B. J., Boyle, D. P., Putnam, A. E., & Bassett, S. D. (2015). Placing the 2012-2015 California-Nevada drought into a paleoclimatic context: Insights from Walker Lake, California-Nevada, USA. *Geophysical Research Letters*, *42*(20), 8632-8640. doi: 10.1002/2015GL065841

Hatchett, B. J., Daudert, B., Oakley, N. S., Garner, C. B., Putnam, A. E., White, A. B. (2017). Recent winter snow level rise in the Sierra Nevada, California, 2008-2017. *Water*, *9*(11), 899. doi:10.3390/w9110899.

Hatchett, B. J., Smith, C. M., Nauslar, N. J. and Kaplan, M. L. (2018). Brief communication: Synoptic-scale differences between Sundowner and Santa Ana wind regimes in the Santa Ynez Mountains, California. *Natural Hazards and Earth System Sciences*, *18*(2), 419-427. doi: 10.5194/nhess-18-419-2018

Hendershott, M. C. and Winant, C. D. (1996). Surface circulation in the Santa Barbara Channel, *Oceanography*, *9*(2), 114-121. Retrieved from http://www.jstor.org/stable/43925554

Hobbins, M. & Huntington, J. (2017). Evapotranspiration and evaporative demand. In V. P. Singh (Ed.). *Handbook of Applied Hydrology* (2nd ed., pp. xxx-xxx). New York, NY: McGraw-Hill Education.

Hobbins, M. T., Wood, A., McEvoy, D. J., Huntington, J. L., Morton, C., Anderson, M., & Hain, C. (2016). The Evaporative Demand Drought Index. Part I: Linking drought evolution to variations in evaporative demand. *J. Hydrometeor., 17*, 1745-1761. doi: 10.1175/JHM-D-15-0121.1

Iacobellis, S. F., & Cayan, D. R. (2013). The variability of California summertime marine stratus: Impacts on surface air temperatures. *Journal of Geophysical Research: Atmospheres*, *118*(16), 9105-9122. doi: 10.1002/jgrd.50652

Jibson, R. W. (2005). Landslide hazards at La Conchita CA (U.S. Geological Survey Open-File Report 2005-1067). Retrieved from U.S. Geological Survey website: https://pubs.usgs.gov/of/2005/1067/508of05-1067.html

Jin, Y., Randerson, J. T., Faivre, N., Capps, S., Hall, A., & Goulden, M. L. 2014. Contrasting controls on wildland fires in southern California during periods with and without Santa Ana winds. *Journal of Geophysical Research: Biogeosciences, 119*(3), 432-450. doi: 10.1002/2013JG002541

Jin, Y., Goulden, M. L., Faivre, N., Veraverbeke, S., Sun, F., Hall, A., . . . Randerson, J. T. (2015). Identification of two distinct fire regimes in southern California: Implications for economic impact and future change. *Environmental Research Letters, 10*(9), 094005. doi: 10.1088/1748-9326/10/9/094005

Keeley, J. E., & Syphard, A. D. (2017). Different historical fire-climate patterns in California. *International Journal of Wildland Fire*, *26*(4), 253-268. doi: 10.1071/WF16102

Keller, E. A., Valentine, D. W., & Gibbs, D. R. (1997). Hydrological response of small watersheds following the Southern California Painted Cave Fire of June 1990. *Hydrological Processes*, *11*(4), 401-414. doi: 10.1002/(SICI)1099-1085(19970330)11:4<401::AID-HYP447>3.0.CO;2-P

Klein, S. A., Hall, A., Norris, J. R., & Pincus, R. (2017). Low-cloud feedbacks from cloud-controlling factors: A review. *Surveys in Geophysics, 38*(6): 1307-1329. doi: 10.1007/s10712-017-9433-3

Liu, X., Mickelbart, M. V., Robinson, P. W., Hofshi, R., & Arpaia, M. L. (2002). Photosynthetic characteristics of avocado leaves. *Acta. Hortic.*, *575*, 865-874. doi: 10.17660/ActaHortic.2002.575.103

Livneh, B., Bohn, T. J., Pierce, D. W., Munoz-Arriola, F., Nijssen, B., Vose, R., . . . Brekke, L. (2015). A spatially comprehensive, hydrometeorological data set for Mexico, the U.S., and southern Canada 1950-2013. *Scientific Data*, *2*, 150042. doi: 10.1038/sdata.2015.42

Loarie, S. R., Carter, B. E., Hayhoe, K., McMahon, S., Moe, R., Knight, C. A., & Ackerly, D. D. (2008). Climate change and the future of California's endemic flora. *PloS One*, *3*(6), e2502. doi: 10.1371/journal.pone.0002502
Lobell, D. B., Cahill, K. N., & Field, C. B. (2007). Historical effects of temperature and precipitation on California crop yields. *Climatic Change*, *81*(2), 187-203. doi: 10.1007/s10584-006-9141-3

MacDonald, G. M. (2007). Severe and sustained drought in southern California and the West: Present conditions and insights from the past on causes and impacts. *Quaternary International*, *173*, 87-100. doi: 10.1016/j.quaint.2007.03.012

Meinshausen, M., Smith, S. J., Calvin, K., Daniel, J. S., Kainuma, M. L. T., Lamarque, J-F., … van Vuuren, D. P. P. (2011). The RCP greenhouse gas concentrations and their extensions from 1765 to 2300. *Climatic Change*, *109*: 213. https://doi.org/10.1007/s10584-011-0156-z

Modrick, T. M., & Georgakakos, K. P. (2015). The character and causes of flash flood occurrence changes in mountainous small basins of Southern California under projected climatic change. *Journal of Hydrology: Regional Studies*, *3*, 312-336. doi: 10.1016/j.ejrh.2015.02.003

National Weather Service. (2018). WFO Non-precipitation weather products specification 10-515. Retrieved from https://www.nws.noaa.gov/directives/sym/pd01005015curr.pdf

Nauslar, N. J.; Abatzoglou, J. T.; Marsh, P. T. (2018). The 2017 North Bay and Southern California Fires: A Case Study. Fire, *1*, 18, https://doi.org/10.3390/fire1010018.

Niraula, R., Meixner, T., Dominguez, F., Bhattarai, N., Rodell, M., Ajami, H. . . . Castro, C.. (2017). How might recharge change under projected climate change in the western U.S.? *Geophysical Research Letters*, *44*(20), 10-407-10, 418. doi: 10.1002/2017GL075421

Oakley, N. S., Lancaster, J. T., Kaplan, M. L., & Ralph, F. M. (2017). Synoptic conditions associated with cool season post-fire debris flows in the Transverse Ranges of southern California. *Natural Hazards*, *88*(1), 327-354. doi: 10.1007/s11069-017-2867-6

Oakley, N. S., Lancaster, J. T., Hatchett, B. J., Stock, J., Ralph, F. M., Roj, S., & Lukashov, S. (2018a). A 22-Year Climatology of Cool Season Hourly Precipitation Thresholds Conducive to Shallow Landslides in California. *Earth Interactions*, *22*(14), 1-35. doi: 10.1175/EI-D-17-0029.1

Oakley, N. S., Cannon, F., Boldt, E., Dumas, J., & Ralph, F. M. (2018b). Origins and variability of extreme precipitation in the Santa Ynez River Basin of Southern California. *Journal of Hydrology: Regional Studies*, *19*, 164-176. Retrieved from https://www.sciencedirect.com/science/article/pii/S2214581818300624

Pierce, D. W., Cayan, D. R., Das, T., Maurer, E. P., Miller, N. L., Bao, Y., . . . & Franco, G. (2013). The key role of heavy precipitation events in climate model disagreements of future annual precipitation changes in California. *Journal of Climate*, *26*(16), 5879-5896. doi: 10.1175/JCLI-D-12-00766.1

Pierce, D. W., Cayan, D. R., and Thrasher, B. L. (2014). Statistical downscaling using Localized Constructed Analogs (LOCA). *Journal of Hydrometeorology*, *15*, 2558-2585. doi: 10.1175/JHM-D-14-0082.1

Pierce, D. W., Cayan D. R., Dehaan, L. (2016). Creating climate projections to support the 4th California Climate Assessment. Retrieved from http://loca.ucsd.edu/~pierce/IEPR_Clim_proj_using_LOCA_and_VIC_2016-06-13b.pdf

Polade, S. D., Pierce, D. W., Cayan, D. R., Gershunov, A., & Dettinger, M. D. (2014). The key role of dry days in changing regional climate and precipitation regimes. *Scientific Reports*, *4*, 4364. doi: 10.1038/srep04364

Polade, S. D., Gershunov, A., Cayan, D. R., Dettinger, M. D., & Pierce, D. W. (2017). Precipitation in a warming world: Assessing projected hydro-climate changes in California and other Mediterranean climate regions. *Scientific Reports*, *7*(1), 10783. doi: 10.1038/s41598-017-11285-y

Prein, A. F., Rasmussen, R. M., Ikeda, K., Liu, C., Clark, M. P., & Holland, G. J. (2017). The future intensification of hourly precipitation extremes. *Nature Climate Change*, *7*(1), 48. doi: http://dx.doi.org/10.1038/nclimate3168

Radeloff, V. C., Helmers, D. P., Kramer, H. A., Mockrin, M. H., Alexandre, P. M., Bar-Massada, A., . . . & Stewart, S. I. (2018). Rapid growth of the US wildland-urban interface raises wildfire risk. *Proceedings of the National Academy of Sciences*, *115*(13), 3314-3319. doi: 10.1073/pnas.1718850115

Reich, K. D., Berg, N., Walton, D. B., Schwartz, M., Sun, F., Huang, X., & Hall, A. (2018). Climate change in the Sierra Nevada: California's water future. Retrieved from UCLA Center for Climate Science website https://www.ioes.ucla.edu/wp-content/uploads/UCLA-CCS-Climate-Change-Sierra-Nevada.pdf

Rutz, J. J., Steenburgh, W. J., & Ralph, F. M. (2014). Climatological characteristics of atmospheric rivers and their inland penetration over the western United States. *Monthly Weather Review*, *142*(2), 905-921. doi: 10.1175/MWR-D-13-00168.1

Schwinning, S., & Sala, O. E. (2004). Hierarchy of responses to resource pulses in arid and semi-arid ecosystems. *Oecologia*, *141*(2), 211-220. doi: 10.1007/s00442-004-1520-8

South Coast Wildlands (2006). Wildlands of the Santa Clara River watershed: Restoring and maintaining the integrity and health of the river and its watershed. Retrieved from: http://www.scwildlands.org/reports/WildlandsoftheSCRWatershed.pdf

Spina, A. P. (2007). Thermal ecology of juvenile steelhead in a warm-water environment. *Environmental Biology of Fishes*, *80*(1), 23-34. doi: 10.1007/s10641-006-9103-7

Sterle, K., Hatchett, B. J., Singletary, L. and Pohll, G. (2019). Hydroclimate variability in snow-fed river systems: Local water managers' perspectives on adapting to the new normal. *Bulletin of the American Meteorological Society*. doi:10.1175/BAMS-D-18-0031.1, in press.

Stine, S. (1994). Extreme and persistent drought in California and Patagonia during mediaeval time. *Nature*, *369*(6481), 546.

Stock, J. D. & Bellugi, D. (2011). An empirical method to forecast the effect of storm intensity on shallow landslide abundance. *Italian Journal of Engineering Geology and Environment*, special issue on 5th International Conference on Debris-Flow Hazards "Mitigation, Mechanics, Prediction and Assessment," 1013-1022. doi: 10.4408/IJEGE.2011-03.B-110

Swain, D. L., Langenbrunner, B., Neelin, J. D., & Hall, A. (2018). Increasing precipitation volatility in twenty-first-century California. *Nature Climate Change*, *8*(5), 427. doi: 10.1038/s41558-018-0140-y

Syphard, A. D., Brennan, T. J., & Keeley, J. E. (2018). Chaparral landscape conversion in Southern California. In E. C. Underwood, H. D. Safford, N. A. Molinari & J. E. Keeley (Eds.) *Valuing Chaparral* (pp. 323-346). Cham, Switzerland: Springer.

Taha, H. and Freed, T. 2015. Creating and mapping an urban heat island index for California. Final report prepared for the California Environmental Protection Agency. 100 pp. [Available at: https://calepa.ca.gov/wp-content/uploads/sites/6/2016/10/UrbanHeat-Report-Report.pdf]

Torregrosa, A., O'Brien, T., & Faloon, I. (2014). Coastal fog, climate change, and the environment, *Eos Trans. AGU, 95*(50), 473-474. doi: 10.1002/2014EO500001.

U.S. Census Bureau (1995). California: Population of counties by decennial census: 1900 to 1990. Retrieved from https://www.census.gov/population/cencounts/ca190090.txt

U.S. Census Bureau (2019). Quick Facts, Ventura County, California. Retrieved from https://www.census.gov/quickfacts/venturacountycalifornia

United States Drought Monitor. (2019). Map Archive. Retrieved from https://droughtmonitor.unl.edu/Maps/MapArchive.aspx

U.S. Geological Survey (USGS). (2005). Southern California: Wildfires and debris flows (Fact Sheet 2005-3106). Retrieved from https://pubs.usgs.gov/fs/2005/3106/pdf/FS-3106.pdf

U.S. Geological Survey (USGS). (2019). Emergency assessment of post-fire debris-flow hazards. Retrieved from https://landslides.usgs.gov/hazards/postfire_debrisflow/

Ventura County Agricultural Commission. (2017). Ventura County's 2017 Crop & Livestock Report. Retrieved from https://cdn.ventura.org/wp-content/uploads/2018/07/Ag-Comm-2017-Annual-Crop-Report-final-lr-07-30-18.pdf

Ventura County Flood Info (2019). Flooding history. Retrieved from Ventura County Flood Info Community Rating System website: http://www.vcfloodinfo.com/programs/flooding-and-flood-risk/vc-flood-history

Ventura County, California. (2018). Ventura County 2040 General Plan Update Draft. Retrieved from Ventura County 2040 General Plan website: https://vc2040.org/review/documents

Ventura County, California. (2010). Ventura County Technical Guidance Manual for Stormwater Quality Control Measures. Retrieved from http://www.vcstormwater.org/images/stories/NPDES_Documents/TGM/TGM_2010/TGM_Manual_9-27-10.pdf

Westerling, A. L.. (University of California, Merced). (2018). *Wildfire Simulations for the Fourth California Climate Assessment: Projecting Changes in Extreme Wildfire Events with a Warming Climate* (technical report for California's Fourth Climate Change Assessment, *Publication No. CCCA4-CEC-2018-014)*. Sacramento, CA: California Energy Commission.

Westra, S., Fowler, H. J., Evans, J. P., Alexander, L. V., Berg, P., Johnson, F., ... & Roberts, N. M. (2014). Future changes to the intensity and frequency of short-duration extreme rainfall. *Reviews of Geophysics*, *52*(3), 522-555. doi: 10.1002/2014RG000464

Wilby, R. L., & Wigley, T. M. L. (1997). Downscaling general circulation model output: A review of methods and limitations. *Progress in Physical Geography*, *21*(4), 530-548. doi: 10.1177/030913339702100403

Williams, A. P., Schwartz, R. E., Iacobellis, S., Seager, R., Cook, B. I., Still, C. J., Husak, G. and Michaelsen, J. (2015a). Urbanization causes increased cloud base height and decreased fog in coastal Southern California. *Geophysical Research Letters*, *42*(5), 1527-1536. doi: 10.1002/2015GL063266

Williams, A. P., Seager, R., Abatzoglou, J. T., Cook, B. I., Smerdon, J. E., & Cook, E. R. (2015b). Contribution of anthropogenic warming to California drought during 2012-2014. *Geophysical Research Letters*, *42*(16), 6819-6828. doi: 10.1002/2015GL064924

Wills, C. J., Roth, N. E., McCrink, T. P., & Short, W. R. (2017). The California landslide inventory database. In *Proceedings, Third North American Symposium on Landslides* (pp. 666-674). Roanoke, VA: Association of Environmental and Engineering Geologists.

Woodhouse, C. A., Meko, D. M., MacDonald, G. M., Stahle, D. W., & Cook, E. R. (2010). A 1,200-year perspective of 21st century drought in southwestern North America. *Proceedings of the National Academy of Sciences*, *107*(50), 21283-21288. doi: 10.1073/pnas.0911197107

Appendix A

Analyses for 2041–2070 Period (Mid-21st Century)

TEMPERATURE ANALYSES

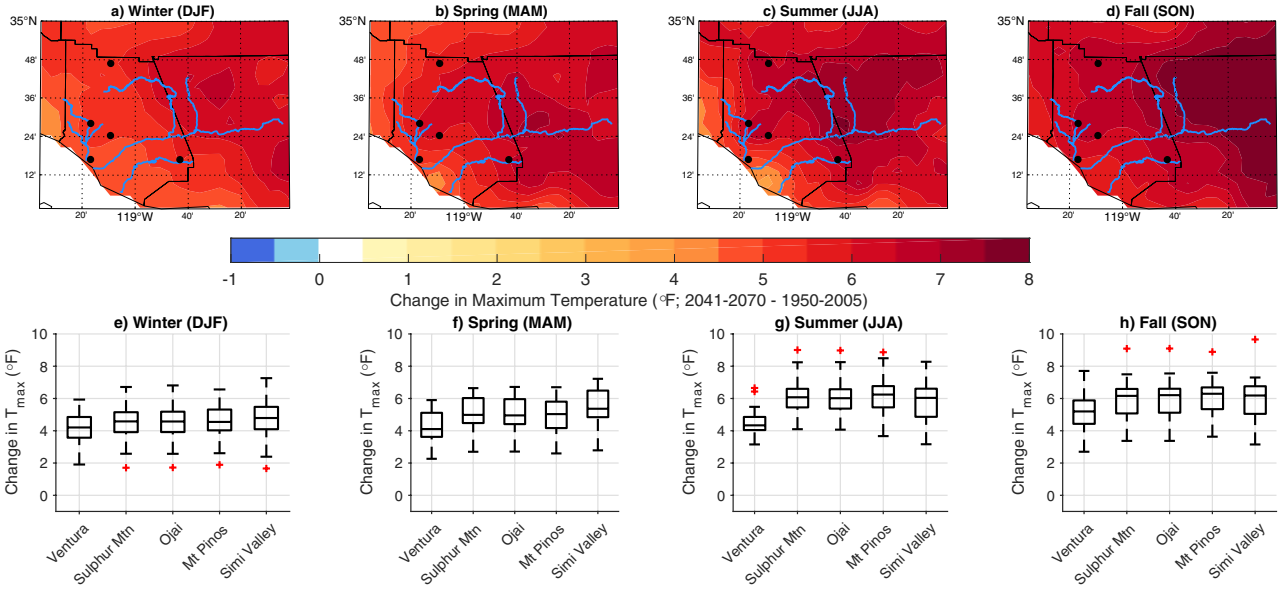

FIGURE A.1: **Change in maximum temperature by season, 2041–2070 mean minus 1950–2005 mean. The top row shows the minimum change that ≥75% of models (≥24 of 32) agree on. Bottom row depicts spread of average change in maximum temperatures across all 32 CMIP5 models for five selected locations within Ventura County (black dots on map). Rivers and creeks are shown as blue lines.**

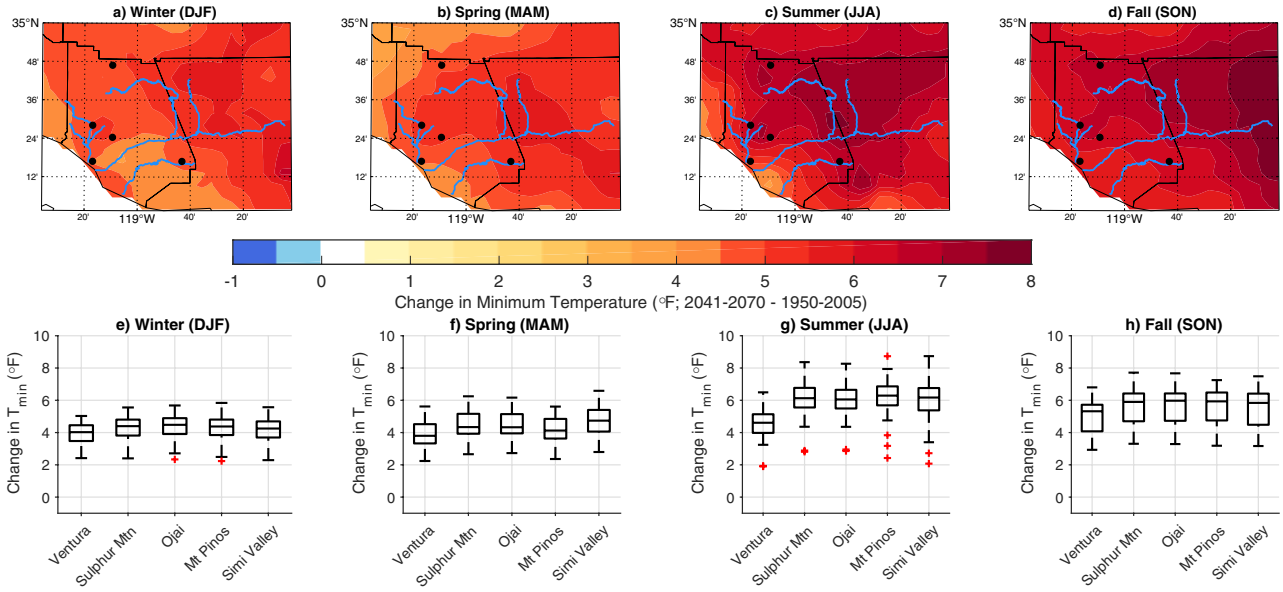

FIGURE A.2: **Change in minimum temperature by season, 2041–2070 mean minus 1950–2005 mean. The top row shows the minimum change that ≥75% of models (≥24 of 32) agree on. Bottom row depicts spread of average change in minimum temperatures across all 32 CMIP5 models for five selected locations within Ventura County (black dots on map).**

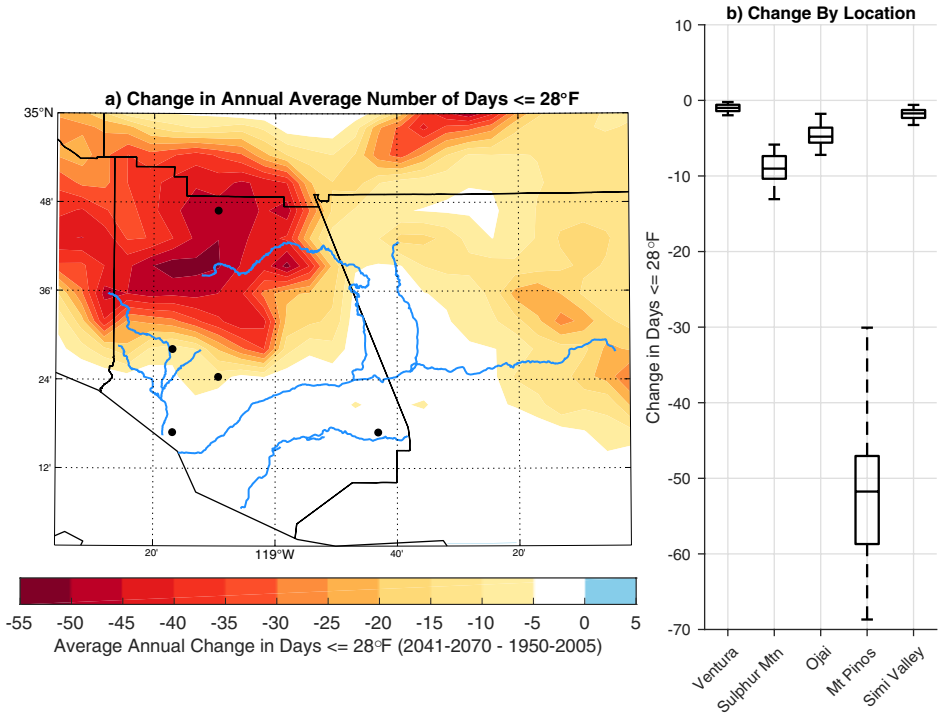

FIGURE A.3: Change in average annual number of days with minimum temperature ≤28°F, 2041–2070 mean minus 1950–2005 mean. Left panel shows minimum change that ≥75% of models (≥24 of 32) agree on. Right panel depicts spread of change in average annual number of days with minimum temperature ≤28°F across all 32 CMIP5 models for five selected locations within Ventura County (black dots on map).

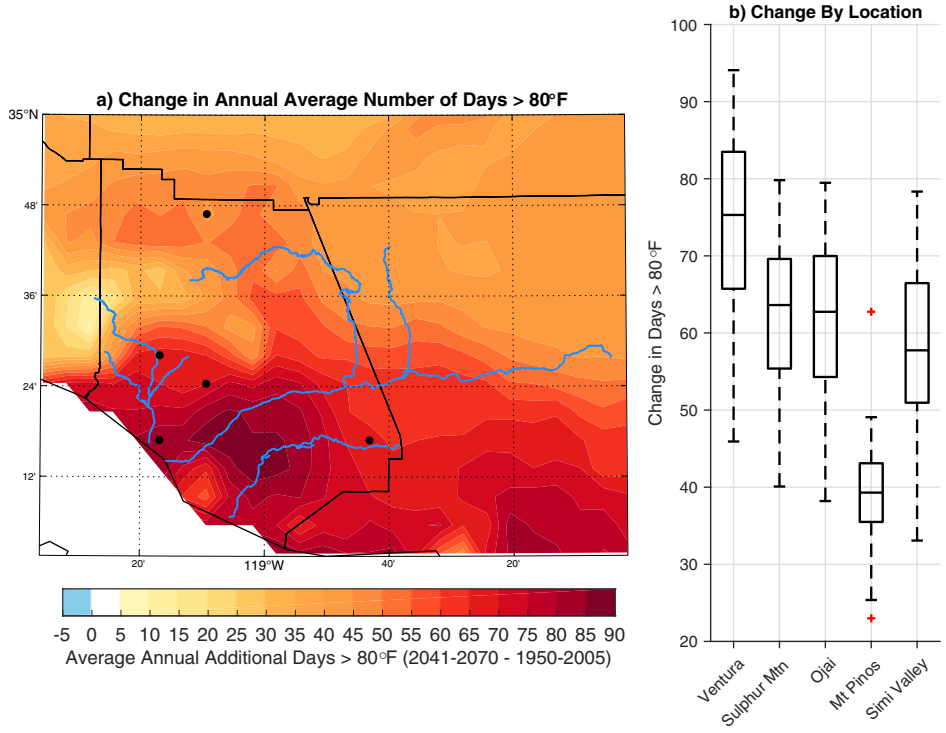

FIGURE A.4: Change in average annual number of days with maximum temperature >80°F, 2041–2070 mean minus 1950–2005 mean. Left panel shows minimum change that ≥75% of models (≥24 of 32) agree on. Right panel depicts spread of change in average annual number of days with maximum temperature >80°F across all 32 CMIP5 models for five selected locations within Ventura County (black dots on map).

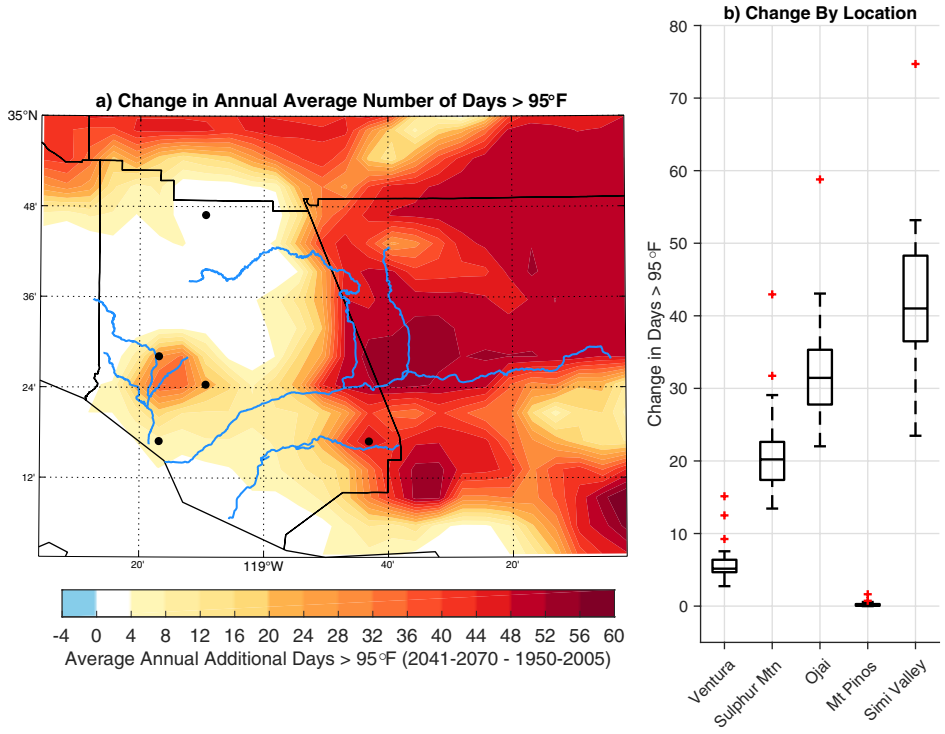

FIGURE A.5: **Change in average annual number of days with maximum temperature >95°F, 2041–2070 mean minus 1950–2005 mean. Left panel shows minimum change that ≥75% of models (≥24 of 32) agree on. Right panel depicts spread of change in average annual number of days with maximum temperature >95°F across all 32 CMIP5 models for five selected locations within Ventura County (black dots on map).**

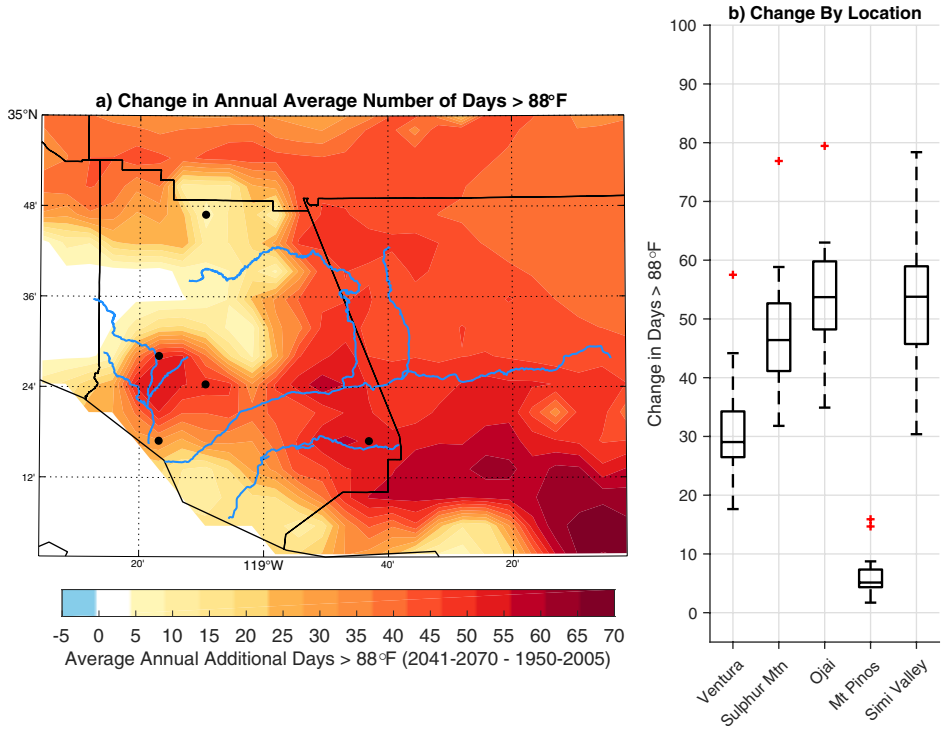

FIGURE A.6: **Change in average annual number of days with maximum temperature >88°F, 2041–2070 mean minus 1950–2005 mean. Left panel shows minimum change that ≥75% of models (≥24 of 32) agree on. Right panel depicts spread of change in average annual number of days with maximum temperature >88°F across all 32 CMIP5 models for five selected locations within Ventura County (black dots on map).**

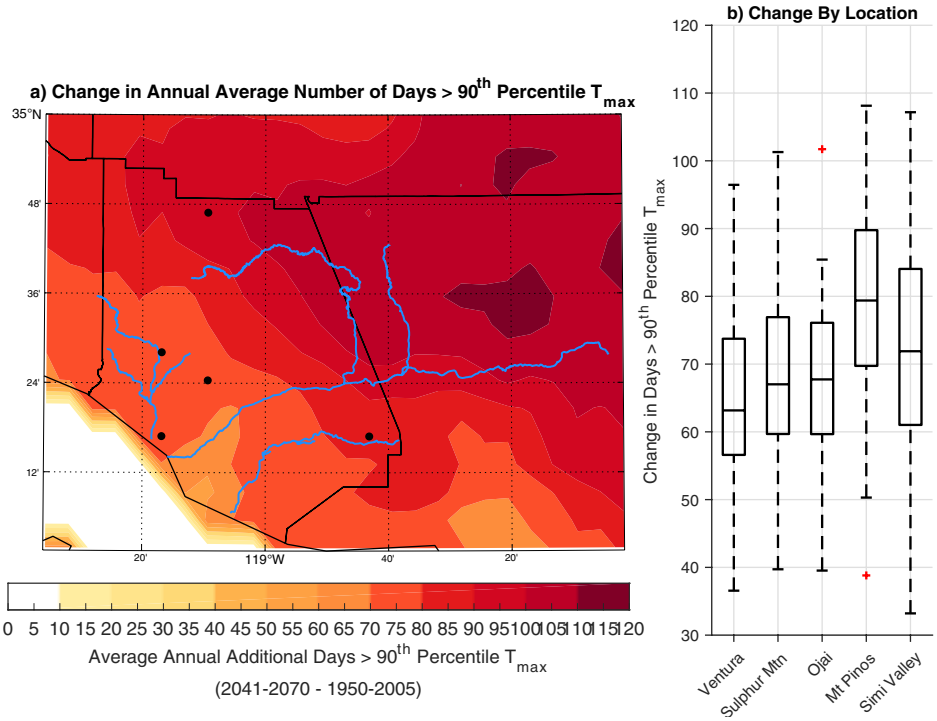

FIGURE A.7: Change in average annual number of days with maximum temperature exceeding the historic 90th percentile maximum temperature. Left panel shows minimum change that ≥75% of models (≥24 of 32) agree on. Right panel depicts spread of change in average annual number of days with maximum temperature >90th percentile across all 32 CMIP5 models for five selected locations within Ventura County (black dots on map).

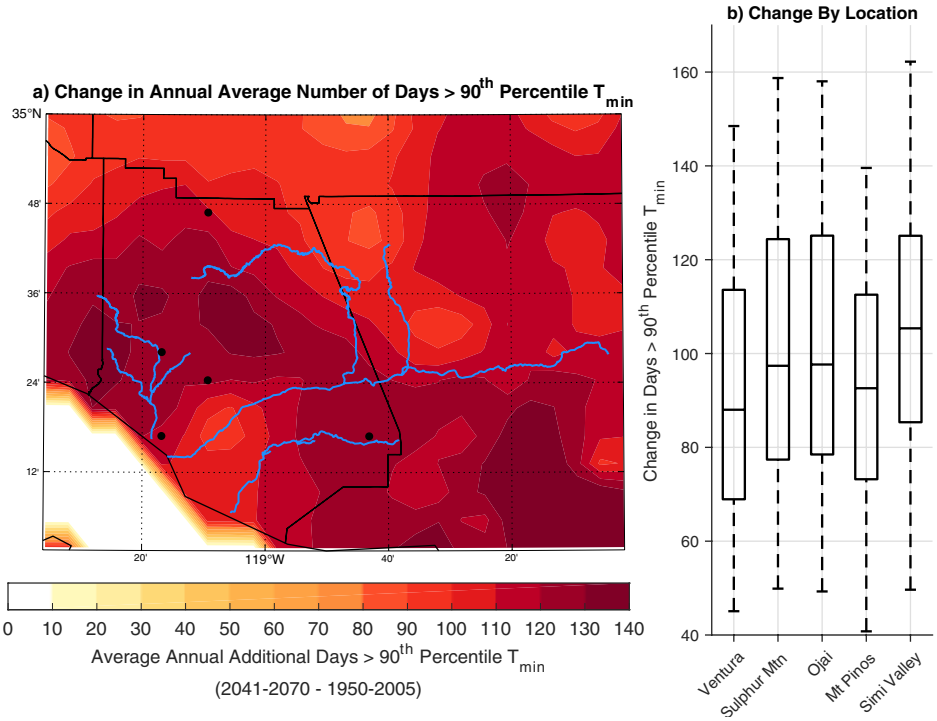

FIGURE A.8: Change in average annual number of days with minimum temperature exceeding the historic 90th percentile minimum temperature. Left panel shows minimum change that ≥75% of models (≥24 of 32) agree on. Right panel depicts spread of change in average annual number of days with minimum temperature >90th percentile across 32 CMIP5 models for five selected locations within Ventura County (black dots on map).

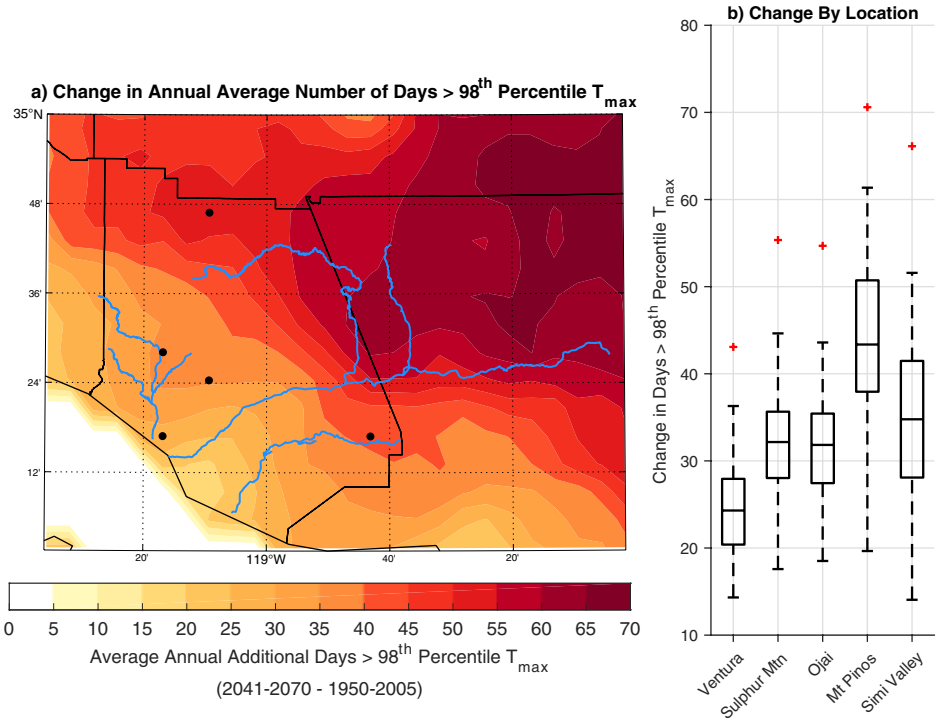

FIGURE A.9: Change in average annual number of days with maximum temperature exceeding the historic 98th percentile maximum temperature. Left panel shows minimum change that ≥75% of models (≥24 of 32) agree on. Right panel depicts spread of change in average annual number of days with maximum temperature >98th percentile across all 32 CMIP5 models for five selected locations within Ventura County (black dots on map)

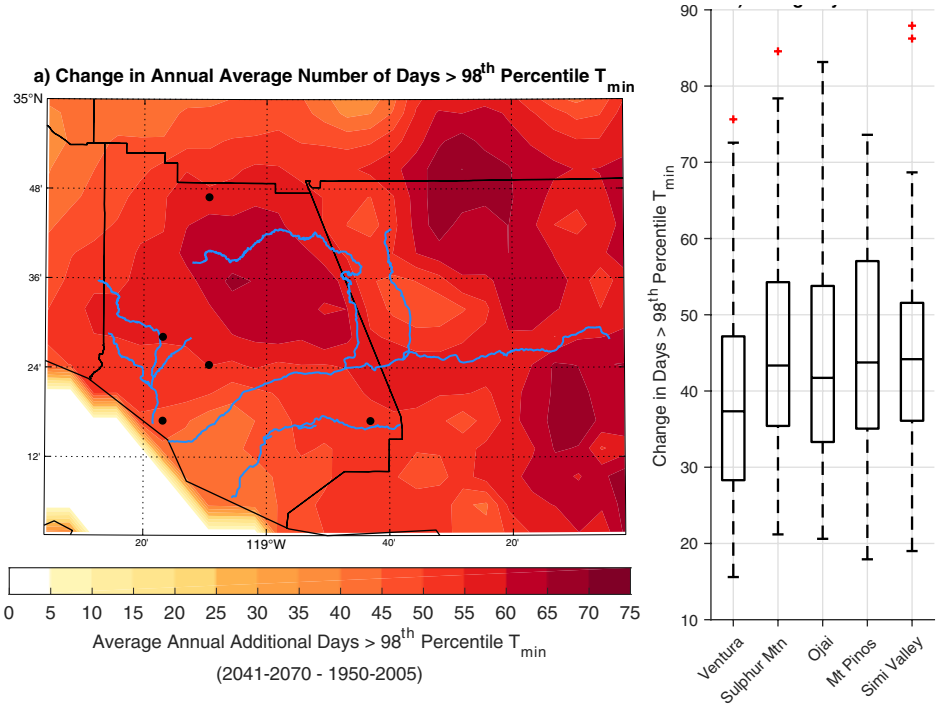

FIGURE A.10: Change in average annual number of days with minimum temperature exceeding the historic 98th percentile minimum temperature. Left panel shows minimum change that ≥75% of models (≥24 of 32) agree on. Right panel depicts spread of change in average annual number of days with minimum temperature >98th percentile across all 32 CMIP5 models for five selected locations within Ventura County (black dots on map).

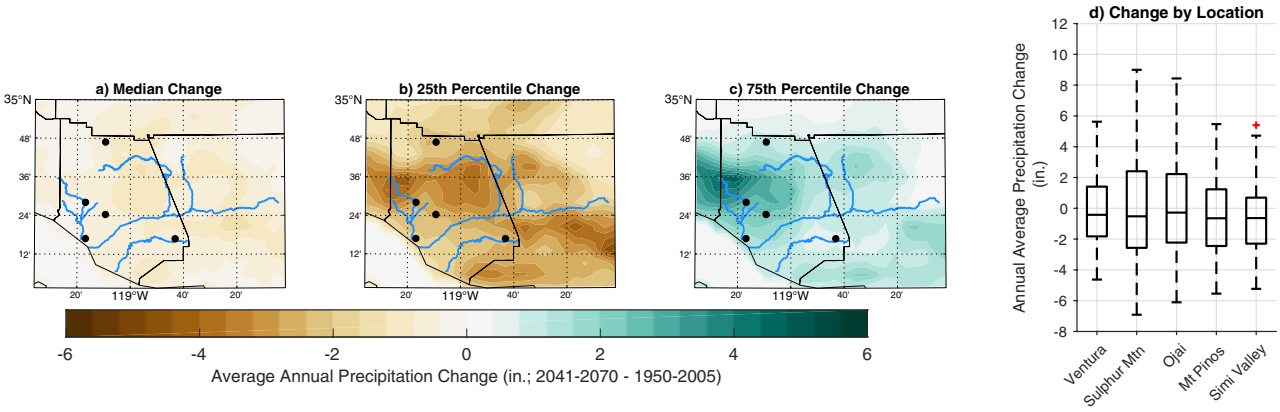

FIGURE A.11: Changes in average annual precipitation (2041–2070 minus 1950–2005), shown as: a) The median change across all 32 models; b) The 25th percentile (driest quartile) change in a distribution fit to the model range of values; c) The 75th percentile (wettest quartile) change in a distribution fit to the model range of values; d) Spread in average annual precipitation change across all 32 CMIP5 models for five selected locations within Ventura County (black dots on map).

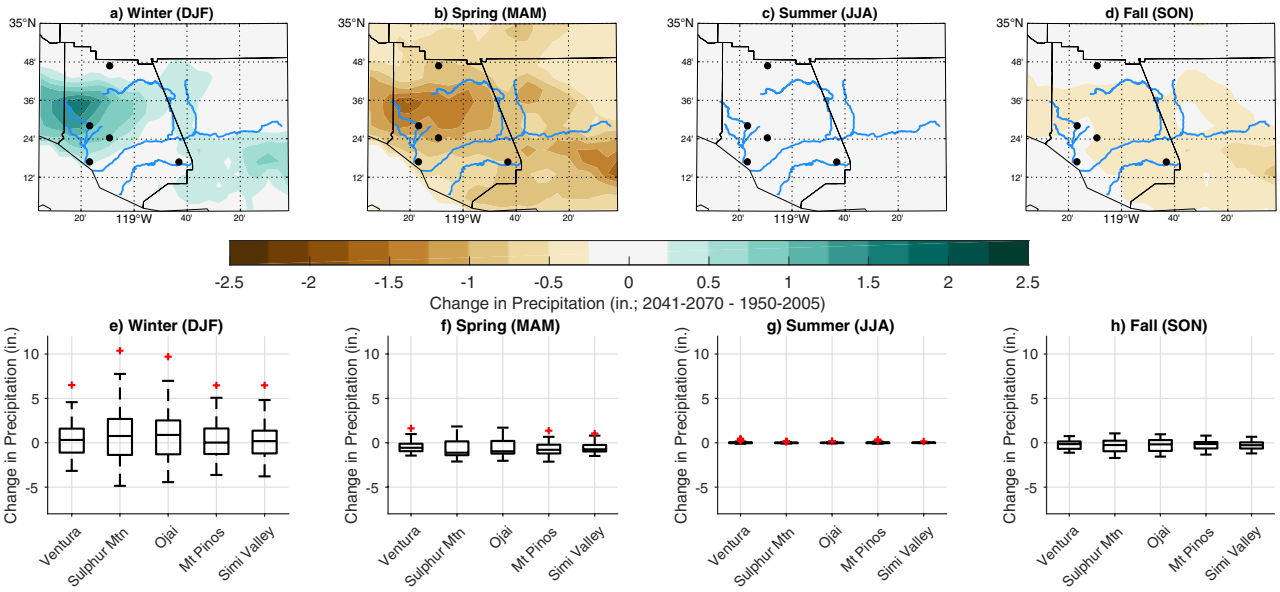

FIGURE A.12: Changes in average seasonal precipitation (2041–2070 minus 1950–2005), shown as: a-d) Median average precipitation change across models for each season; e-h) Spread in average seasonal precipitation change across all 32 CMIP5 models for five selected locations within Ventura County (black dots on map).

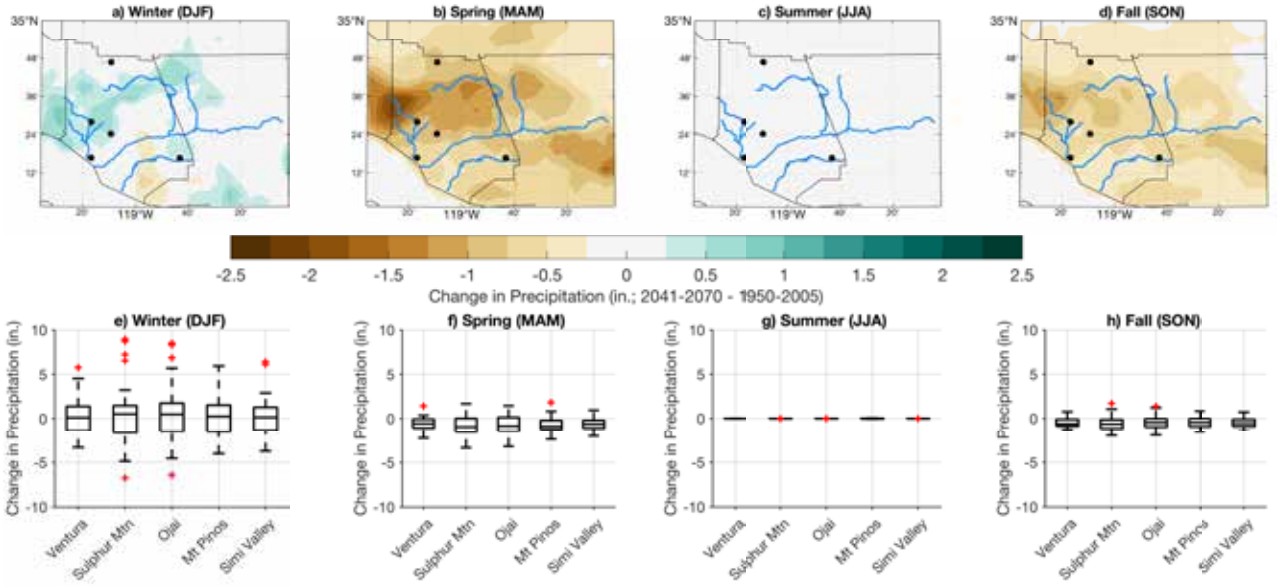

FIGURE A.13: **Changes in median annual precipitation (2041–2070 minus 1950–2005), shown as: a) The median change across all 32 models; b) The 25th percentile (driest quartile) in a distribution fit to the model range of values; c) The 75th percentile (wettest quartile) in a distribution fit to the model range of values; d) Spread in median annual precipitation change across all 32 CMIP5 models for five selected locations within Ventura County (black dots on map).**

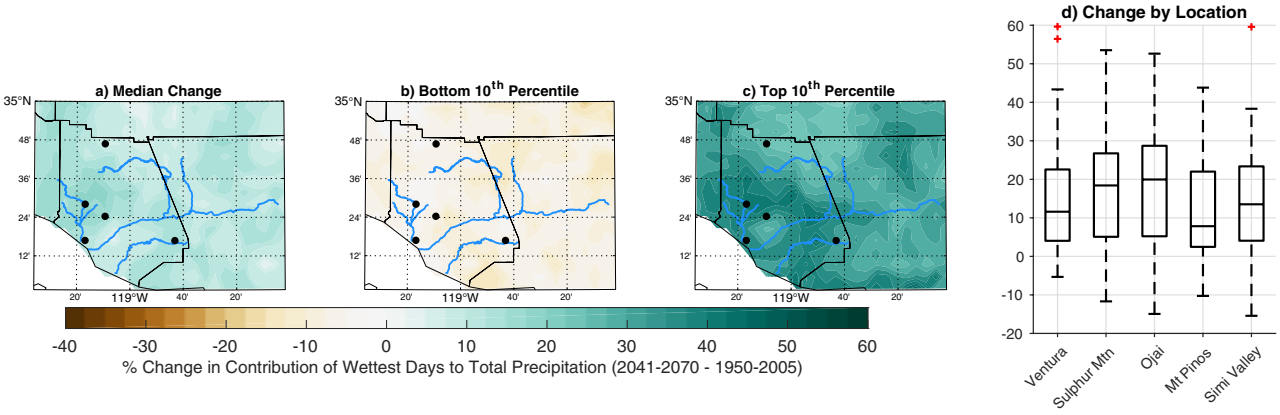

FIGURE A.14: **Changes in contribution of the top 5% of wettest days to total annual precipitation (2041–2070 minus 1950–2005) as: a) Median change in contribution across models; b) The bottom 10th percentile (decile with smallest or negative change in contribution) in a distribution fit to the model range of values; c) The top 10th percentile (decile with greatest positive changes in contribution) in a distribution fit to the model range of values; d) Spread in change in contribution across all 32 CMIP5 models for five selected locations within Ventura County (black dots on map).**

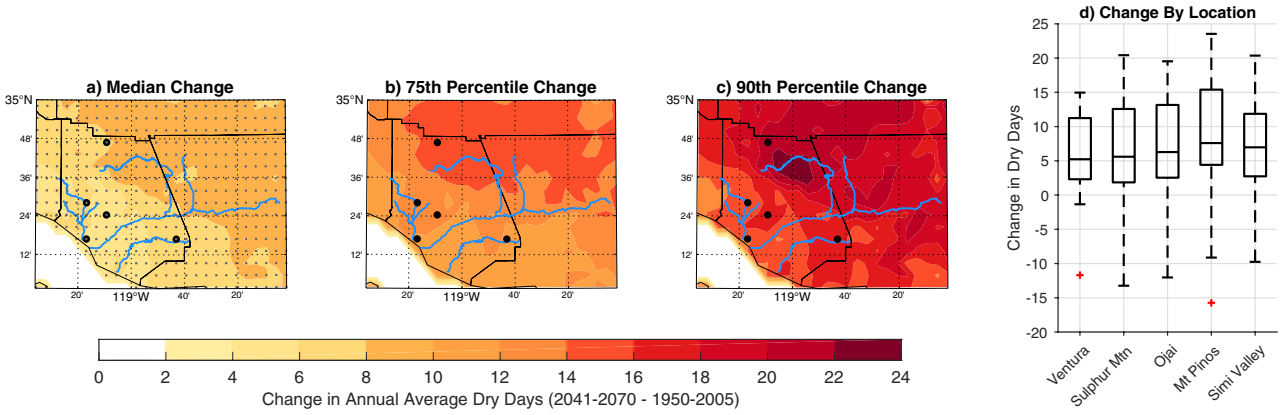

FIGURE A.15: **Change in average annual number of dry (zero precipitation days), 2041–2070 minus 1950–2005 for: a) median change across all models as filled contours with grid cells where at least 75% (24 of 32) of models are in agreement on an increase in number of dry days shown as dots; b) The 75th percentile change in dry days (upper quartile) in a distribution fit to the model range of values; c) The 90th percentile change in dry days (uppermost decile) in a distribution fit to the model range of values; d) Spread in change in annual dry days across all 32 CMIP5 models for five selected locations within Ventura County (black dots on map).**

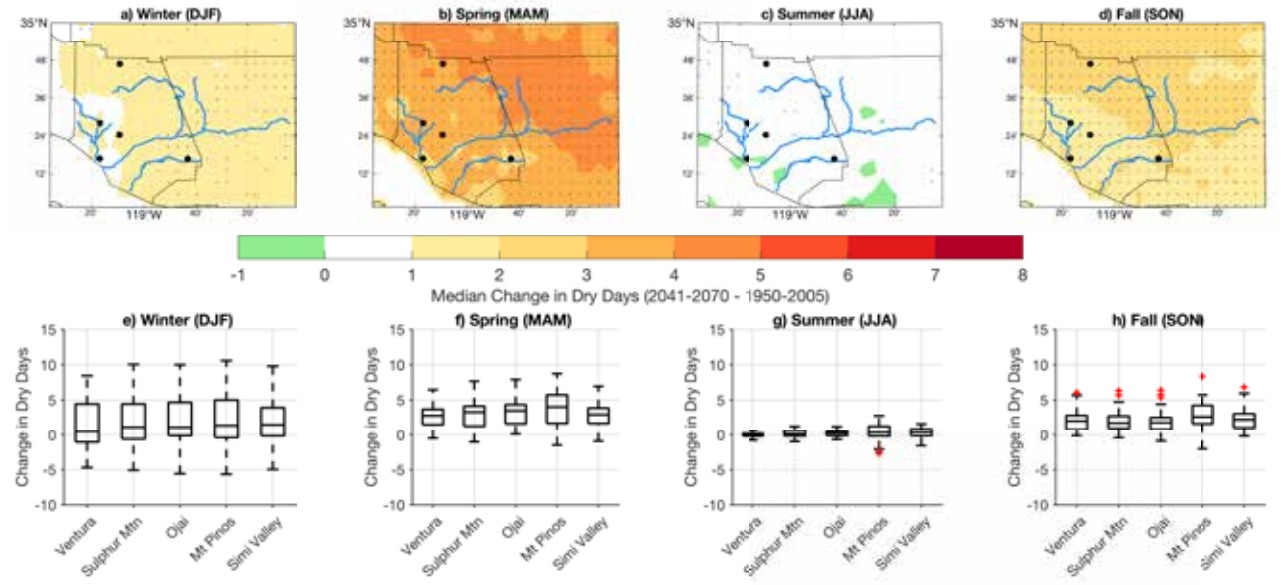

FIGURE A.16: **Change in median annual number of dry (zero precipitation days), 2041–2070 minus 1950–2005. a-d) By season, median change across all models as filled contours with grid cells where at least 75% (24 of 32) of models agree on an increase in dry days shown as dots; e-h) By season, the spread in change in annual dry days across all 32 CMIP5 models for five selected locations within Ventura County (black dots on map).**

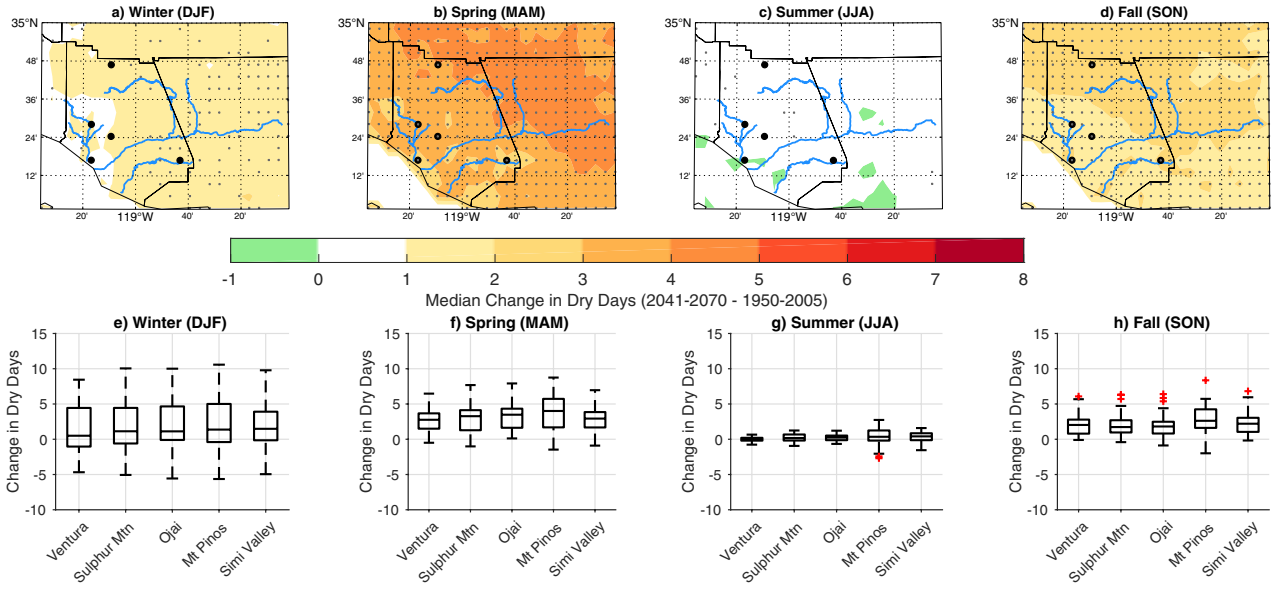

FIGURE A.17: **Percent change in frequency of 85th percentile (wettest 15%) precipitation days, based on historic 85th percentile and frequency during 2041–2070 minus 1950–2005. a) Median change; b) Bottom (least change) 10th percentile in a distribution fit to the model range of values; c) Top (greatest change) 10th percentile in a distribution fit to the model range of values; d) Spread in percent change in annual percent change of 85th percentile events across all 32 CMIP5 models for five selected locations within Ventura County (black dots on map).**

EVAPORATIVE DEMAND ANALYSES

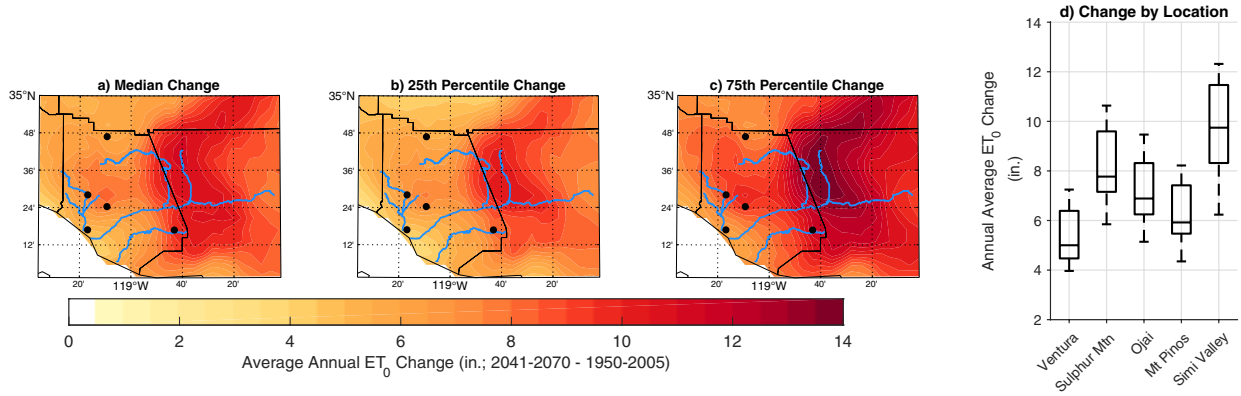

FIGURE A.18: **Change in average annual reference evapotranspiration (ET_0), 2041–2070 mean minus 1950–2005 mean for the a) median change in ET_0; b) 25th percentile (bottom quartile) change in ET_0; c) 75th percentile (upper quartile) change in ET_0; Spread in change of average annual ET_0 for five selected locations within Ventura County (black dots on map).**

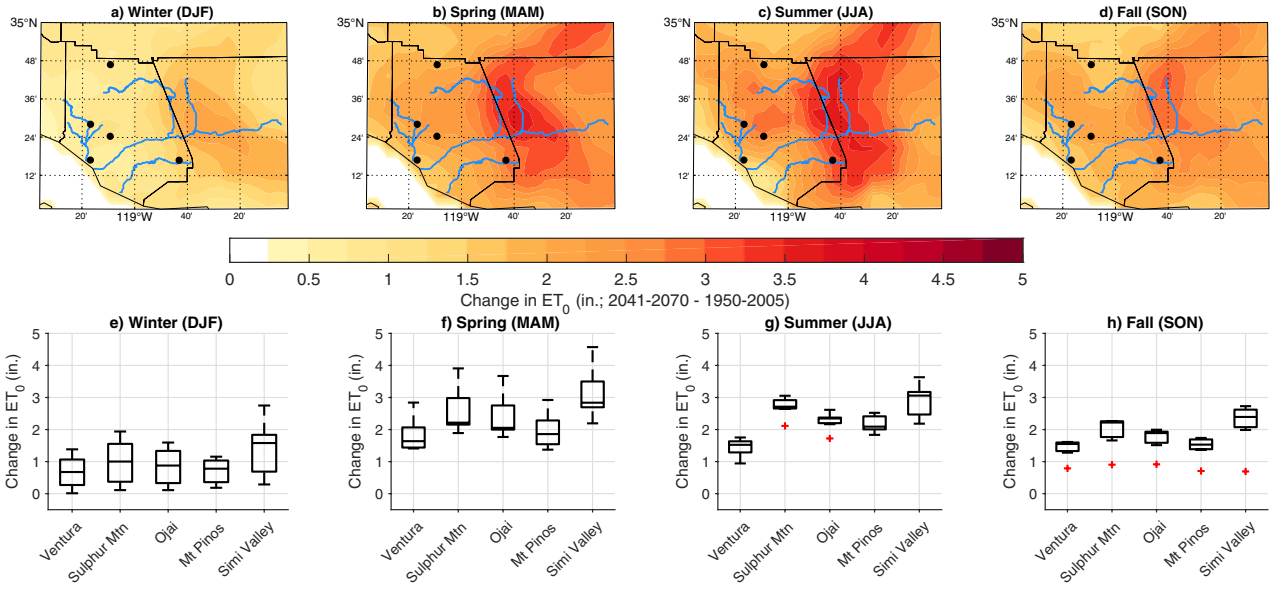

FIGURE A.19: **Change in seasonal average reference evapotranspiration (ET_0), 2041–2070 minus 1950–2005 for winter (a), spring (b), summer (c) and fall (d). Spread in change in seasonal ET_0 across all seven CMIP5 models for five selected locations within Ventura County (black dots on map) for winter (e), spring (f), summer (g) and fall (h).**

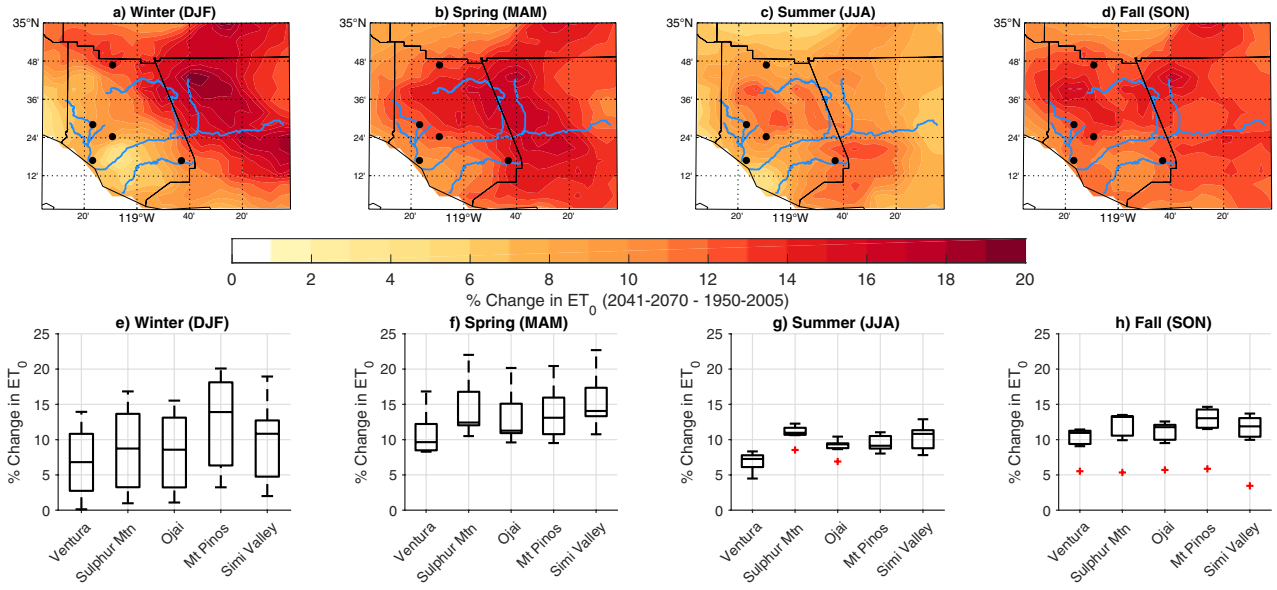

FIGURE A.20: **Percentage change in seasonal average reference evapotranspiration (ET_0), 2041–2070 minus 1950–2005 for winter (a), spring (b), summer (c) and fall (d). Spread in percentage change in seasonal ET_0 across all seven 32 CMIP5 models for five selected locations within Ventura County (black dots on map) for winter (e), spring (f), summer (g) and fall (h).**

RESOURCES LEGACY FUND®
CREATIVE SOLUTIONS. LASTING RESULTS.

DRI
Desert Research Institute

CNAP
California-Nevada Climate Applications Program
A NOAA RISA team

OJAI VALLEY LAND CONSERVANCY

Watersheds Coalition of Ventura County

June 2019